

**Effect of genotoxic and non-genotoxic nephrotoxins
on differentiation and dedifferentiation processes of
renal proximal tubular epithelial cells**

Inaugural dissertation

for the attainment of the title of doctor
in the Faculty of Mathematics and Natural Sciences
at the Heinrich Heine University Düsseldorf

Presented by

Isaac Musong Mboni Johnston

From Konye (Cameroon)

Düsseldorf, August 2024

From the Institute of Toxicology
of Heinrich Heine University Düsseldorf

Published by permission of the
Faculty of Mathematics and Natural Sciences at
Heinrich Heine University Düsseldorf

Supervisor: Prof. Dr. Nicole Schupp
Co-supervisor: Prof. Dr. Rainer Kalscheuer

Date of the oral examination: 09/12/2024

Table of Contents

Table of Contents	2
List of Abbreviations.....	4
1. Introduction	7
1.1 The kidneys	7
1.1.1 Structure and physiology of the human kidneys	7
1.1.2 Role of nephron in excretion	8
1.1.3 Role of proximal tubule in excretion.....	9
1.2 Kidney and proximal tubular cell toxicity.....	11
1.3 Compounds that cause acute/chronic renal tubular damage	12
1.3.1 Cisplatin and DNA damage response in cisplatin-induced renal injury	12
1.3.2 Cyclosporin A.....	15
1.3.3 Role of oxidative stress in kidney damage	15
1.4 Regeneration in the kidney.....	18
1.4.1 Dedifferentiation and tubular epithelial regeneration	18
1.5 Induced pluripotent stem cells (iPSC)	23
1.5.1 Somatic cell types and reprogramming methods used to generate iPSC.....	25
1.6 <i>In vitro</i> differentiation of iPSC into proximal tubular epithelial-like Cells	26
2. Aim of the study	28
2. Published data (international journal of molecular sciences, 25, 81, 2023) ...	30
2.1. Sensitivity of human induced pluripotent stem cells and thereof.....	30
differentiated proximal tubular cells towards selected nephrotoxins	30
2.1.1. Introduction	30
2.1.2. Materials and Methods	32
2.1.3. Results	36
2.1.4. Discussion.....	43
3. Unpublished data	48
3.1. Increased DNA damage response and decreased expression	48
of genes associated with the maintenance of genome integrity.....	48
during differentiation.....	48
3.2. Impact of nephrotoxins and oxidants on survival and function of renal	50
proximal tubular epithelial cells differentiated out of hiPSC.....	50
3.2.1. Introduction	50
3.2.2. Materials and Methods	53

3.2.3. Results	58
3.2.4. Discussion	70
3.3. Influence of nephrotoxins on the efficacy of hiPSC differentiation into proximal tubular epithelial-like cells.....	76
3.3.1. Introduction	76
3.3.2. Materials and Methods.....	77
3.3.3. Results.....	78
3.3.4. Discussion.....	81
3.4. Influence of nephrotoxins on the dedifferentiation process of hiPSC-derived proximal tubular epithelial cells	83
3.4.1. Introduction	83
3.4.2. Materials and Methods.....	84
3.4.3. Results.....	85
3.4.4. Discussion.....	89
4. Overall discussion	91
4.1. Differentiation of hiPSC generates cellular structures expressing markers of proximal tubular epithelial cells (PTELCs).....	91
4.2. PTELCs Express PTEC transporters and recapitulate PTEC-specific transporters properties.....	93
4.3. Sensitivity of hiPSC, hiPSC differentiating, and hiPSC differentiated into PTELCs towards known genotoxic and non-genotoxic nephrotoxins.....	94
4.4. Sensitivity of hiPSC, hiPSC differentiating, and hiPSC differentiated into PTELCs towards known oxidative stress inducing agents.....	97
4.5. Differentiated PTELC dedifferentiated by acquiring an EMT phenotype and this phenotype is impaired by nephrotoxic substances	99
5. Limitations and Outlook	101
6. Summary	103
7. References.....	105
8. Appendix.....	119
Curriculum vitae	142
Publications and conference paper	143
Acknowledgements.....	145
Declaration on oath.....	146

List of Abbreviations

·g	Force of gravity
°C	Degree Celsius
μ	Micro
μg	Microgram
μl	Microliter
μM	Micromolar
ADMET	Absorption Distribution Metabolism Excretion
AKI	Acute Kidney Injury
ALDH	Aldehyde dehydrogenase
ASC	Adult Stem Cells
ATM	Ataxia Telangiectasis Mutated
ATP	Adenosine Triphosphate
ATR	ATM and Rad-related
BRCA2	Breast Cancer 2
BMP7	Bone Morphogenetic Protein 7
BSA	Bovine Serum Albumin
CON	Control
cDNA	Complementary Deoxyribonucleic Acid
CKD	Chronic Kidney Disease
Ct	Cycle threshold
CTR1	Copper Transporter 1
CsA	Cyclosporin A
DAPI	4',6-diamidino-2-phenylindole
d	Day(s)
diffD3	Differentiation day 3
diffD9	Differentiation day 9

DNA	Deoxyribonucleic Acid
DDR	DNA Damage Response
DMEM	Dulbecco's Modified Eagle Medium
DMSO	Dimethyl Sulfoxide
DPBS	Dulbecco's Phosphate Buffered Saline
DSBs	DNA Double Strand Breaks
ECM	Extracellular Matrix
EGFR	Epithelial Growth Factor Receptor
EMT	Epithelial-Mesenchymal Transition
ESRD	End Stage Renal Disease
F4hiPSC	Foreskin-4-human Induced Pluripotent Stem Cells
FDA	Food and Drug Administration
FITC	Fluorescein Isothiocyanate
g	Gram
GAPDH	Glycerinaldehyde-3-phosphate Dehydrogenase
GGT	Gamma Glutamyl Transferase
GSH	Glutathione
GSSG	Glutathione Disulfide
h	Hour(s)
hESC	Human Embryonic Stem Cell
hiPSC	Human Induced Pluripotent Stem Cells
H ₂ O ₂	Hydrogen Peroxide
IF	Immunofluorescence
IL	Interleukin
iPSC	Induced Pluripotent Stem Cells
IRI	Ischemia Reperfusion Injury
kDa	Kilo Dalton
L	Liter
MACS	Magnetic Activated Cell Sorting
MET	Mesenchymal-Epithelial Transition
Min	Minute(s)
ml	Milliliter

MACS	Magnetic Activated Cell Sorting
MET	Mesenchymal-Epithelial Transition
Min	Minute(s)
ml	Milliliter
mM	Millimolar
MMP	Matrix Metalloproteinase
mRNA	Messenger Ribonucleic Acid
NADPH	Nicotinamide Adenine Dinucleotide Phosphate
NFAT	Nuclear Factor of Activated T Cells
NOS	Reactive Nitrogen Species
NOX	NADPH Oxidase
Nrf2	Nuclear Factor Erythroid 2-related Factor 2
OAT	Organic Anion Transporter
OCT	Organic Cation Transporter
OS	Oxidative Stress
8OH-dG	8-hydroxy-2-deoxyguanosine
PT	Proximal Tubule
PTEC	Proximal Tubular Epithelial Cells
PTELCs	Proximal Tubular Epithelial-like Cells
P-gp	P-glycoprotein
QVD	Pan-Caspase Inhibitor
RNA	Ribonucleic Acid
RT-qPCR	Quantitative Real-time Polymerase Chain Reaction
ROS	Reactive Oxygen Species
RSC	Resident Stem Cells
REGM	Renal Epithelial Growth Medium
SOD	Superoxide Dismutase
TBHQ	Tert Butylhydroquinone
XO	Xanthine Oxidase

1. Introduction

1.1 The kidneys

1.1.1 Structure and physiology of the human kidneys

The human kidney is a remarkable and complex epithelial organ composed of various cell types that work together seamlessly to maintain the body's internal equilibrium [1]. Its multifaceted functions include the regulation of fluid, electrolyte, and acid-base levels, controlling blood pressure through the renin-angiotensin-aldosterone system, supporting erythrocyte production through erythropoietin secretion, and regulating calcium levels through the activation of the vitamin D3 metabolite calcitriol (as reviewed by [2]). However, its primary and indispensable task is the reabsorption of vital substances such as water, minerals, amino acids and sugars, as well as the filtration and active excretion of metabolic end products such as urea, creatinine, and foreign substances from the bloodstream, and the biotransformation of xenobiotics. These critical functions, which depend almost entirely on the kidney's nephrons, its basic structural, functional and filtration units, make renal epithelial cells particularly susceptible to damage by xenobiotics and their metabolites and emphasise the paramount importance of stable renal function for maintaining homeostasis not only in the kidneys but throughout the body [2-5].

The kidney is a bean-shaped organ that lies in pairs on either end of the spine in between the twelfth thoracic and third lumbar vertebrae. It is protected by a sturdy fibrous capsule and can be divided macroscopically into three main parts - the outer renal cortex, the inner renal medulla, and the renal pelvis (**Fig. 1A**). The renal cortex is cup-shaped and surrounds the renal medulla, which resembles a pyramid and protrudes into the renal pelvis. The renal pelvis is situated in the renal sinus and opens through the renal hilum to the kidney surface. The human kidney contains about one million nephrons, each of which comprises a distinct set of components, including the glomerulus, proximal tubule, loop of Henle, distal tubule, and collecting duct system (**Fig. 1B**). These work together to perform the excretory functions of the kidney, which involve glomerular filtration, tubular reabsorption, and tubular secretion [2, 6].

The kidney is an incredible organ that operates with remarkable efficiency. Despite its small size, it receives approximately 25 % of the cardiac outflow through the renal arteries. It filters 180 litres of blood daily, with only one to two litres excreted. The filtration process initiates in the glomeruli, where the filtrate is passively purified, followed by selective reabsorption of essential nutrients, including small

molecules such as glucose, amino acids, and electrolytes, which are pushed into the interior of Bowman's capsule, forming the primary urine. The resulting primary urine is then pressed into the tubule system, where valuable substances are recovered actively and passively. In this way, the kidneys function as the ultimate detoxification system by selectively eliminating unwanted or harmful substances while reabsorbing vital nutrients, including water, with the help of the antidiuretic hormone (ADH) and aldosterone. Thus, underlining the importance of this organ in maintaining a constant internal environment.

1.1.2 Role of nephron in excretion

One of the many functions of the human kidneys is blood filtration, a function performed by the nephron. The renal nephron comprises a renal corpuscle and a downstream tubule system, as shown in **Fig. 1B** [2, 6, 7]. Filtration begins when blood from the circulation enters the glomerular capillaries through the vas afferens and passes through the glomerular filtration barrier, which consists of fenestrated endothelial cells, the glomerular basement membrane, and specialized glomerular epithelial cells, the podocytes. The blood plasma is forced through this barrier, and components larger than 15 kDa are retained, forming the primary urine, which is then passed into the tubular system and further modified. Thus, the filtration barrier must withstand significant hydrostatic pressure, and its integrity depends on all three barrier components [8, 9]. In healthy individuals, the barrier is almost impermeable to macromolecules such as proteins. However, in diseases that affect the glomerular filters, proteins leak out of the barrier and into the urine, which is associated with the progression of renal failure, a global health burden [10].

The renal tubular system consists of three main components: the proximal tubule, the loop of Henle, and the distal tubule, which can be further subdivided based on molecular and morphologic criteria. All three major segments have specialized roles in the physiological activity of the kidney by reabsorbing important solutes and altering the composition of the filtrate through various membrane channels and transporters in the different segments of the nephron [2]. This ensures that the water, salt, and pH levels in the tissue fluid are maintained, waste products, drugs, and other toxic substances are excreted in the urine, and vital components are returned to the bloodstream. In addition, the filtrate flows through a connecting segment into the collecting duct and then through the ureter into the bladder, where the urine is stored before excretion.

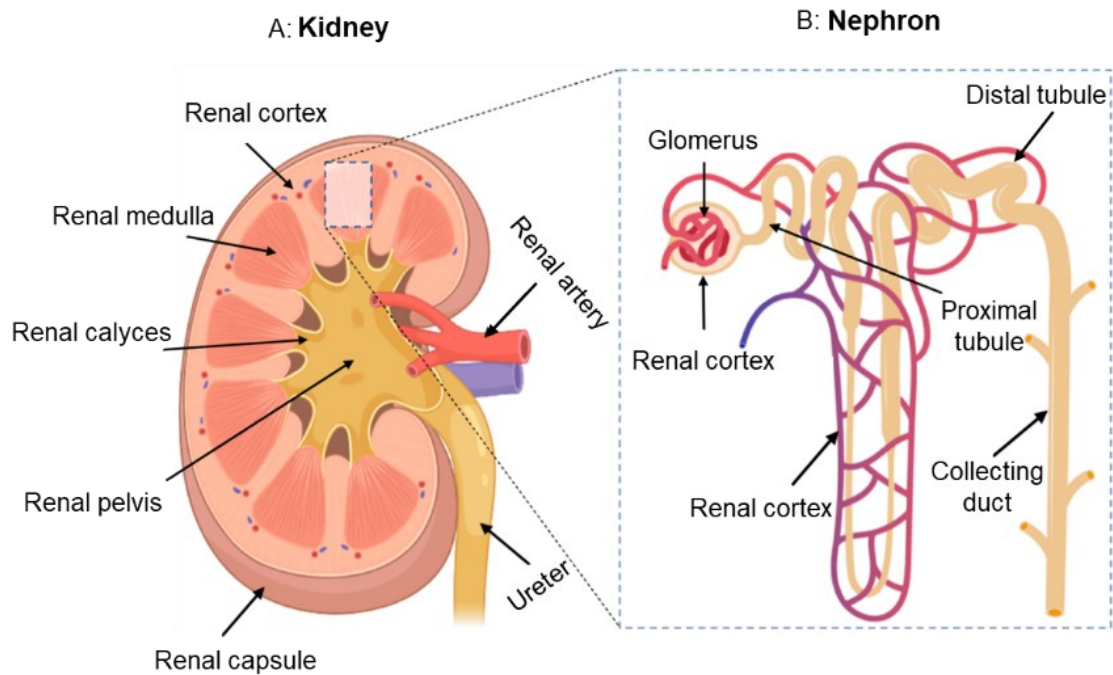


Figure 1: Anatomy of the essential components of the urinary system. (A) The kidney is anatomically divided into three areas: the outer renal cortex, the inner renal medulla, and the renal pelvis. The renal capsule encloses the kidney, and it is macroscopically divided into the outer renal cortex and the pyramid-shaped renal medulla. The renal pyramids flow into the renal calyces, forming the renal pelvis together. The ureter links the kidneys to the urinary bladder, enabling the elimination of waste products from the body. (B) The nephron is the functional component of the kidney and produces urine. Bowman's capsule surrounds the glomerulus, followed by the tubule system. The tubule system starts with the proximal tubule, followed by the loop of Henle, which merges into the distal tubule. The final part of the tubule system is the collecting tube. Modified from Faria et al. [2] and Adhipandito et al. [7].

1.1.3 Role of proximal tubule in excretion

The proximal tubule (PT) is the first part of the tubular system and comprises three segments: S1, S2, and S3. S1 and S2 are in the outer cortex of the kidney, while S3 is situated in the outer medullary region [11]. The processes of tubular reabsorption and secretion are carried out by the proximal tubular epithelial cells (PTEC) of the proximal tubules in all the segments of the proximal tubule [12]. This is a well-coordinated process involving active tubular secretion of protein-bound molecules, including drugs, from the glomerular filtrate and systemic circulation into the tubule lumen. PTEC are square mononuclear cells with apical-basal polarization and brush borders densely covered with microvilli on the apical side. This unique morphological feature distinguishes PTEC from distal tubular cells (**Fig. 2A**). PTEC expresses various types of membrane transporters in their apical and basolateral compartments, belonging to two prominent families: the solute carrier family (SLC) and the adenosine triphosphate (ATP)-binding cassette (ABC) transporter family (**Fig. 2B**) [13-15]. The SLC family comprises organic cation transporters (OCTs) and organic anion transporters (OATs), which are responsible

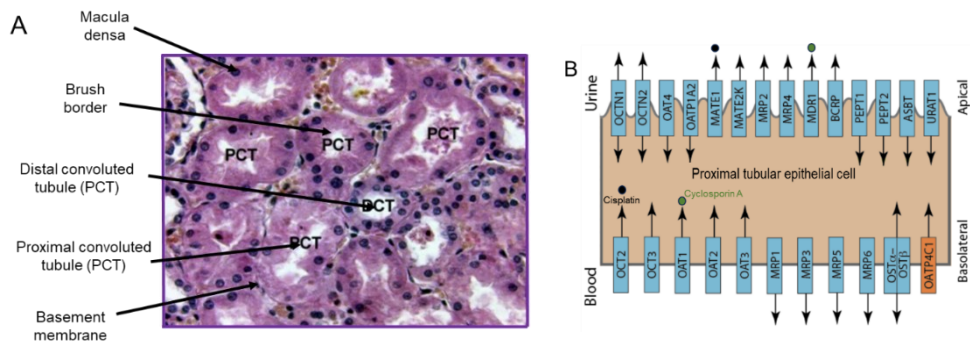


Figure 2: Photomicrographs showing vital morphological features and drug transporters of the proximal tubules. (A) The micrograph of the PTC highlights the unique morphological feature of the apical cell membrane with brush borders densely covered with microvilli, which maximize the reabsorption and secretory function of the proximal tubule and differentiate it from the distal tubule cells. (B) In addition to the above morphological features, the epithelial cells of the PTC also express several drug transporters, including OAT1, OAT3, OCT2, MRP1, MATE1 and MATE2-k, which play an essential role in nephrotoxicity as they are involved in the uptake, secretion and export of various drugs, including immunosuppressants and chemotherapeutic agents such as cyclosporine A and cisplatin, respectively. The information presented in this figure was modified from the following sources: <http://www.vetfolio.com/internalmedicine/renal-tubular-acidosis> and <http://bts.ucsf.edu/fda-transportal/organs/kidney/>.

for drug uptake. In contrast, the ABC family consists of breast cancer resistance protein (BCRP), multidrug resistance proteins (MRP2 and 4), multidrug and toxin extrusion protein (MATE), and P-glycoprotein (P-gp) responsible for the exportation of drugs from cells into the tubular lumen, from where they are excreted in the urine. These ABC exporters transport substrates out of the cells using ATP as an energy currency, thus significantly influencing excretion [13-15].

Moreover, the membrane transporters of PTEC play a crucial role in the retrieval and reabsorption of vital substances from the primary urine in a process known as tubular reabsorption. This process begins as soon as the ultrafiltrate enters the lumen of the proximal tubule and involves the reabsorption of organic nutrients such as glucose, amino acids, and minerals in conjunction with passive water reabsorption. Aquaporins, integral membrane channel proteins responsible for the passive transport of water and small, uncharged solute molecules through the cell membrane against their concentration gradient, are responsible for water reabsorption. Aquaporin 1, expressed in all proximal tubule segments, is the predominant aquaporin in the proximal tubule and an excellent marker for PTEC [16, 17]. In addition, peptides such as albumin are reabsorbed from the ultrafiltrate back into the cell by endocytosis involving the albumin transporters megalin and cubilin, which are localized in the apical membrane of the PTEC [18]. Due to the enhanced energy-dependent transport processes that mediate tubular absorption and secretion in the proximal tubule, PTEC contains many mitochondria to meet

the high energy demand. However, these cells are susceptible to mitochondrial damage, which reduces ATP production, increases oxidative stress, and leads to cell damage [19].

1.2 Kidney and proximal tubular cell toxicity

The segments of the nephron exhibit a high degree of morphological, physiological, and biochemical heterogeneity, and the cells of the individual segments display site-specific sensitivities to xenobiotics. Among these regions, the proximal tubules are the most frequently affected by xenobiotics and their cells are thus extensively studied in the context of drug safety assessment [20-23]. The proximal tubular epithelial cells (PTEC) detoxify and secrete exogenous substances, such as drugs and xenobiotics, into the urine. This critical role renders them particularly susceptible to damage caused by these substances and their toxic metabolites. Their sensitivity to various metabolic waste products could also result from the high amount of blood and with it, a lot of solutes, filtered through the kidney in relation to its own mass as well as from the high number of biotransformation and active transport processes in the kidney, which the various tubular transporters may facilitate [24, 25]. In addition, the primary urine filtrated in the glomeruli, which is about 170 L during a 24-h period, is concentrated to about 1 L, almost a 200-fold before its excretion, which could lead to a further increase in local exposure to toxic substances and toxic metabolites found in the blood by accumulation [26].

Due to this high exposure, these toxic compounds and their harmful metabolites may disrupt tubular cell polarity, which, along with the expression of apical and basolateral-transporters, is crucial for tubular cell function. The dislocation of apical and basolateral transporters resulting in a leaky epithelium and the subsequent increase in intracellular calcium disrupts ion homeostasis, leading to nephrotoxicity, cell death or, in severe cases, necrosis, thus compromising renal function and leading to acute kidney injury (AKI) [19, 27]. It has already been estimated that more than 20 % of AKI cases in the hospital are attributed to drug toxicity in the PTEC, which is correlated with increased morbidity and mortality [3, 20, 28]. AKI commonly leads to chronic kidney disease (CKD), with AKI survivors at approximately 9-fold increased risk of CKD, 3-fold increased risk of end-stage renal disease (ESRD), and 2-fold increased risk of mortality, compared with patients without AKI [29-31]. Currently, there are no definite therapies to prevent or treat established AKI, with dialysis and organ transplantation being the only viable options [32]. However, understanding the sensitivity of individual nephron

segments to xenobiotics is crucial for drug safety assessment and the prevention of nephrotoxicity-induced AKI.

1.3 Compounds that cause acute/chronic renal tubular damage

During the excretory function, PTEC absorbs and concentrates compounds from the glomerular filtrate and systemic circulation. Consequently, PTEC is prone to nephrotoxic compounds and their toxic metabolites found in the filtrate. Various known drugs, chemicals and some food additives have been reported to cause renal tubular damage when present at high doses [2, 5, 20]. Several possibilities have been described by which these toxins can damage PTEC. Firstly, it is known that xenobiotics enter renal cells directly and lead to tissue damage without having been metabolized beforehand. Other foreign substances may lead indirectly to PTEC damage without prior metabolization, mainly through the generation of reactive oxygen species (ROS), interacting with cellular macromolecules and leading to oxidative stress [27]. However, on the other hand, foreign substances are taken up into renal cells, where they are metabolized into their active form and interact with cellular components. Moreover, they could also be metabolized externally (in the liver or lungs) to stable metabolites, which enter the renal tissue via the bloodstream or intrarenal, where they are converted into their active form or detoxified by further biotransformation [33]. The most frequently cited PTEC toxic compounds include chemotherapeutics (such as cisplatin), immunosuppressants (such as cyclosporin A), oxidizing agents (e.g., hydrogen peroxide, tert-butylhydroquinone), radiocontrast agents, antimicrobials, bisphosphonates, and also environmental agents are associated with tubular injury [2, 3, 5, 20].

1.3.1 Cisplatin and DNA damage response in cisplatin-induced renal injury

The chemotherapeutic cisplatin is a highly effective cytostatic drug commonly used in anticancer therapy to treat malignant tumors, including those of the lung, bladder, breast, ovary, head, neck, and cervix. With its ability to damage the DNA of rapidly proliferating cancer cells, it is considered one of the most effective cancer medications available today [34-37]. However, despite its numerous benefits, cisplatin has limitations that must be considered. It can cause side effects, even in non-proliferating normal cells, such as ototoxicity, gastrointestinal toxicity, myelosuppression, and allergic reactions, with the most important dose-limiting side effect of cisplatin being nephrotoxicity [38, 39]. The nephrotoxicity of cisplatin, particularly in the proximal tubular cells of the kidney, is a major concern and limits its clinical use in 25-30 % of patients in whom even the first dose leads to AKI [39-

43]. The molecular mechanism by which cisplatin kills these non-proliferating proximal tubule cells is not well understood. It is known for its propensity to accumulate in the renal PTEC, damaging the nuclear and mitochondrial DNA through transporter-mediated uptake. This results in a profound inflammatory response, the build-up of reactive oxygen species (ROS), and cell death, leading to AKI [43-46]. In cells, several research groups have shown that following aquation, cisplatin is converted into a highly reactive and positively charged metabolite that binds to DNA and forms cross-links between strands and within strands. The cross-linking unwinds the DNA double helix and disrupts DNA replication and transcription, leading to replication stress and DNA damage with subsequent activation of the DNA damage response and DNA repair mechanisms, cell cycle arrest, and cell death [34-36, 47] (shown in **Fig. 3** for a PTEC).

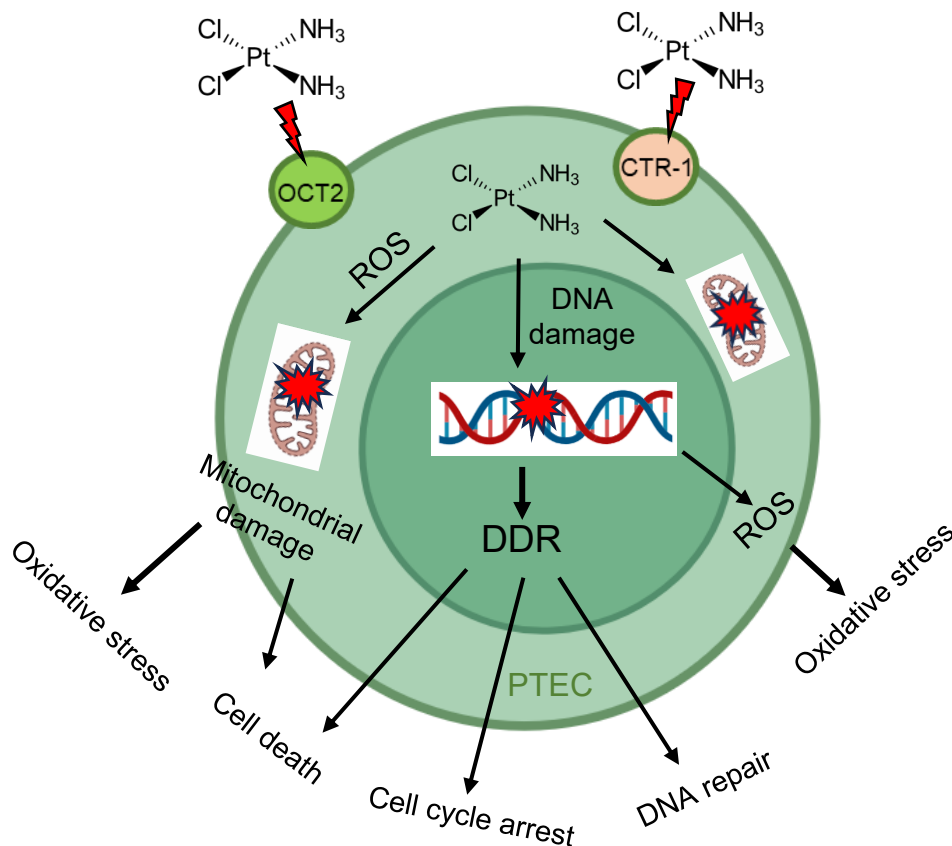


Figure 3: Illustration of the fate of PTEC during cisplatin-induced nephrotoxicity (CIN) in AKI. Cisplatin enters the renal epithelial cells via the transporters OCT2 and Ctr1, causing mitochondrial DNA damage that activates the formation of reactive oxygen species (ROS). The ROS, in turn, damage the mitochondria, leading to cell death. Additionally, cisplatin can damage nuclear DNA, activating the DNA Damage Response (DDR). Depending on the extent of damage, DDR can cause cell cycle arrest and DNA repair for cell survival or trigger cell death signaling pathways. This information is based on extensive research by Tiong et al. [5] and Pabla & Dong [42] and was created using BioRender.com. OCT2 (Organic Cation Transporter 2), CTR1 (Copper Transporter), PTEC (Proximal Tubular Epithelial Cell), and AKI (Acute Kidney Injury).

Recent studies have revealed that DNA damage and DNA damage response

(DDR) are critical pathogenic mechanisms of cisplatin-induced AKI in kidneys [48, 49]. DDR is an exquisite and elaborate network that cells commonly employ to protect genome integrity and stability, and it involves three major phases: DNA lesion recognition, delay of cell cycle progression, and promotion of DNA repair [50]. In concert, these complex phases of DDR can regulate cell cycle progression, cell death pathways, and DNA repair, determining the balance between survival and death [51]. DDR is mainly regulated by the PI3-like protein kinases Ataxia telangiectasia mutated (ATM) and ATM and Rad3-related (ATR), and prototypical activators of DDR are DNA double-strand breaks (DSBs) or DNA replication blocking lesions [52, 53]. The tumour suppressor p53 is a pivotal player in cellular DDR and is often considered a master regulator of cell fate because it plays a prominent role following DNA damage by enabling a plethora of cellular reactions, such as cell cycle arrest, apoptosis, and DNA repair, to determine the fate of affected cells [54, 55]. Therefore, it is unsurprising that the first detection of DDR in cisplatin-AKI was the involvement of p53 in cisplatin-induced apoptosis of renal tubule cells [48]. Interestingly, several DDR signalling pathways have now been shown to be altered in cisplatin-induced AKI. Pabla et al. [42] showed that during treating renal tubule cells with cisplatin, ATR was rapidly activated but not ATM or DNA-PK. More specifically, suppression of ATR, which is mainly mediated by mismatch repair proteins such as MSH2, resulted in attenuation of p53 activation and apoptosis, arguing for a specific role of ATR in cisplatin nephrotoxicity. Furthermore, this study demonstrated that Chk2 was subsequently activated ATR-dependent to induce p53 activation, which triggers renal cell apoptosis [42, 56]. These results indicate that the ATR/Chk2/p53 signalling pathway mediates the early DDR during cisplatin-induced renal injury.

On the other hand, ATM and its related DDR may play a more cytoprotective role in cisplatin-induced renal injury. This hypothesis is supported by ATM-deficient cells being more vulnerable to cisplatin-induced nephrotoxicity. Moreover, ATM was proteolytically cleaved from renal tubular cells and inactivated by caspases in the late phase of cisplatin treatment, suggesting a mechanism for blocking ATM-mediated cytoprotection from apoptosis [57]. Interestingly, Kim et al. [58] showed that cisplatin treatment inhibited the MRN (Mre11, Rad50, and Nbs1) complex in the kidneys, essential for ATM recognition and binding to DNA lesions [58]. Therefore, in the early phase of cisplatin treatment, ATM may be activated for DNA repair and cell survival. However, in the late phase, caspases are cleaved and deactivated to promote apoptosis.

1.3.2 Cyclosporin A

Cyclosporin A (CsA) is a highly potent immunosuppressant first isolated from the fungus *Tolypocladium inflatum*. It has been authorized by the United States Food and Drug Administration since the 1980s for prophylactic anti-rejection therapy in patients receiving allogeneic transplants in the liver, kidney, and heart and for the control of several autoimmune disorders such as psoriasis and rheumatoid arthritis [59-61]. CsA's immunosuppressive effect is based on its intracellular interaction with calcineurin phosphatase via a drug-receptor complex involving cyclophilins [62]. This interaction reduces the production of interleukin-2 (IL-2), a cytokine supporting T and B cell growth and proliferation. By inhibiting the activation of calcineurin phosphatase, an enzyme that plays a central role in the activation of NF-AT (nuclear factor of activated T-cells), CsA stops the proliferation and activation of helper and cytotoxic T-cells by indirectly inhibiting the production of the NF-AT-regulated gene IL-2. Therefore, the inhibition of IL-2 production by CsA is a crucial mechanism for its ability to suppress the immune system [63]. CsA has also been proposed to treat resistant tumours as it can reverse the multidrug resistance phenotype, which is usually overexpressed in tumour cells [64].

Despite its numerous benefits, treatment with CsA is limited due to its nephrotoxicity, and the multiple mechanisms underlying this deleterious effect are not yet fully understood. However, long-term therapy with CsA is known to cause kidney damage in more than 30 % of patients [65, 66]. It induces preglomerular vasoconstriction, reducing the glomerular filtration rate [67]. In addition, it causes both systemic and renal vasoconstriction by activating the renin-angiotensin system, one of the most critical blood pressures regulating systems [68]. Oxidative stress, mitochondrial damage, and cell membrane lipid peroxidation are also probable causes of CsA's nephrotoxicity [61]. Furthermore, it induces epithelial-mesenchymal transition (see 1.4.1.1) in the renal tubular cells, which may lead to renal fibrosis [69].

1.3.3 Role of oxidative stress in kidney damage

Kidney disorders such as AKI and CKD are global health problems with a prevalence in Europe of 3 to 17 % [70]. AKI describes a rapid decline in kidney function due to damage to kidney cells caused by various conditions, such as sepsis and nephrotoxicity, which can often progress to CKD [30, 71]. In addition, recent findings have demonstrated that oxidative stress is a recognised factor in the pathophysiology and progression of kidney diseases [72, 73]. It results from

the accumulation of highly reactive intermediates, including reactive oxygen species (ROS) and reactive nitrogen species (NOS), which are generated within cells during aerobic metabolism or the metabolism of xenobiotics [73-75]. ROS can either be classified as free radicals such as superoxide anion radical ($O_2^{\cdot-}$), peroxy (ROO^{\cdot}), nitric oxide (NO^{\cdot}), alkoxy (RO^{\cdot}), and hydroxyl radical (OH^{\cdot}) or non-radical species such as peroxynitrite ($ONOO^-$), hydrogen peroxide (H_2O_2), and hypochlorous acid ($HOCl$) [76]. ROS can be produced endogenously and exogenously. Endogenous sources include several cellular enzymes such as NADPH oxidase (Nox), superoxide dismutase (SOD), mitochondrial oxidases, xanthine oxidase (XO), lipoxygenase, cyclooxygenase, myeloperoxidase, amino acid oxidase, and peroxisomes [74]. Exogenous sources of ROS include ionizing radiation, cigarette smoke, heavy metal ions, and hyperoxia. While they have beneficial effects on the cell in low to moderate concentrations, such as in cell signalling and the maintenance of "redox homeostasis", higher concentrations can cause damage to molecular components such as DNA, proteins, and lipids, and can also activate various stress-induced transcription factors and trigger the production of pro-inflammatory and anti-inflammatory cytokines [77, 78].

To counteract the effects of oxidants, the human body has enzymatic and non-enzymatic antioxidant defence mechanisms. These mechanisms include various antioxidant enzymes and non-enzymatic antioxidants such as SOD, catalase, thioredoxin, peroxiredoxin, glutathione peroxidase, glutathione transferase, as well as vitamins C and E, glutathione, and carotenoids, which are released in response to the intracellular increase in ROS following activation of the transcription factor Nrf2 (nuclear factor erythroid 2-related factor 2). However, when an imbalance occurs between oxidants and scavenger defence systems, oxidative stress occurs, which can be particularly dangerous for nucleic acids (**Fig. 4**), leading to base changes, covalent cross-linking, and single- and double-strand breaks, producing the oxidation products 8-hydroxy-2'-deoxyguanosine (8-OH-dG), one of the most common oxidation products of DNA, which is known to play a role in several diseases, including renal failure [79, 80].

Recent reports have shown that oxidative stress in renal disease triggers apoptosis, senescence, fibrosis, and reduced cell regeneration capacity in renal cells, leading to the accumulation of extracellular matrix proteins, podocyte damage, mesangial dilation, renal hypertrophy, endothelial dysfunction, tubulointerstitial fibrosis and glomerulosclerosis, thus contributing to the deterioration of renal function and disease progression [76, 81]. Although various

cellular processes can cause ROS generation, mitochondrial damage is the main contributor to ROS formation in patients with kidney disease. Accordingly, impaired mitochondrial function, increased mitochondrial ROS and upregulation of various genes involved in oxidative phosphorylation have been implicated as causes of increased oxidative stress in renal failure [82].

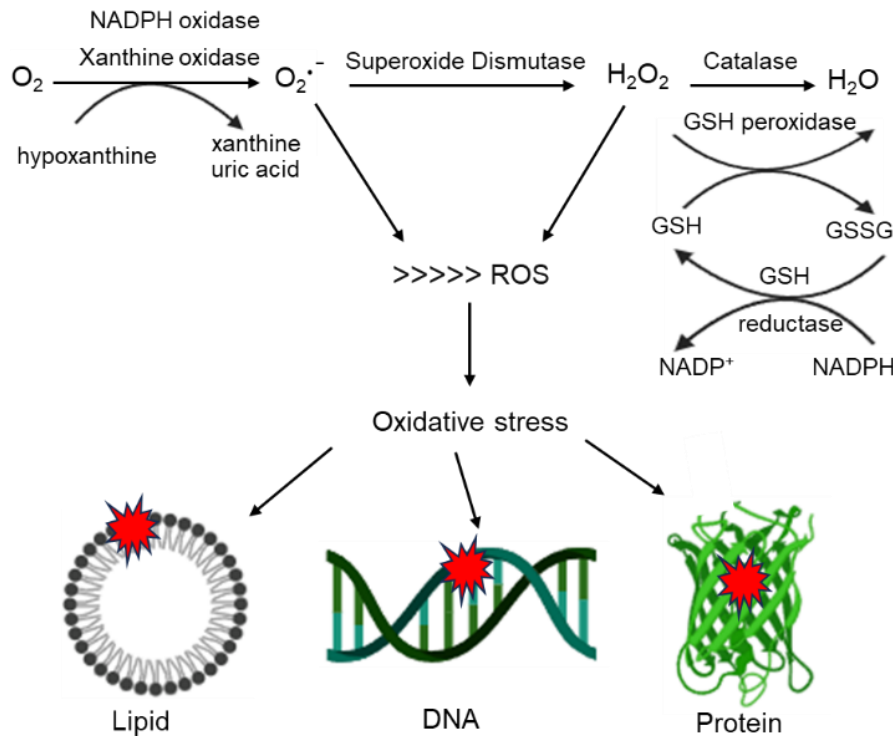


Figure 4: Pathways of ROS production and removal. The production pathways of ROS can be attributed to enzymes such as NADPH oxidase, superoxide dismutase, and xanthine oxidase, while the removal pathway of ROS is mediated by catalase and glutathione peroxidase. Superoxide dismutase facilitates the conversion of the superoxide radical into hydrogen peroxide, which can be further transformed into H_2O by the enzymes catalase or glutathione peroxidase. The glutathione peroxidase reaction oxidizes glutathione (GSH) to glutathione disulfide (GSSG), which can be converted back to glutathione by the glutathione reductase in a further NADPH-consuming reaction. Enhanced exposure to ROS contributes to oxidative damage to lipids, deoxyribonucleic acids (DNA), and proteins. GSH and GSSG, superoxide anion ($O_2^{\cdot-}$), and hydrogen peroxide (H_2O_2) are the key players in this process. The illustration was modified based on research by Dröge [77] and with the aid of Biorender.com.

Moreover, exposure of PTEC to nephrotoxic substances can trigger oxidative stress by either mitochondrial damage or activation of NADPH oxidase [83]. For instance, oxidizing agents like H_2O_2 and tert-butylhydroquinone can induce apoptosis in cultured PTEC through either the JNK or the MEK1-ERK1/2 pathway [84, 85]. At the same time, the nephrotoxicity of gentamicin, cephalosporin, and aristolochic acid is associated with tubular cell death and oxidative stress due to mitochondrial damage or depletion of cytochrome c in the mitochondrial respiratory chain [86-89]. Similarly, cisplatin-induced PTEC damage is associated with oxidative stress through the activation of NADPH oxidase or upregulation of NOX4

expression [90, 91], suggesting that the damaging effects of oxidative stress on kidney function and disease progression cannot be ignored, and the potential antioxidant approaches to prevent ROS induced AKI should be designed differently depending on the source of oxidative stress.

1.4 Regeneration in the kidney

When the kidney, and PTEC in particular, are exposed to nephrotoxic drugs or ROS, AKI may occur with a concomitant loss of renal function. Depending on the extent of damage, recovery of renal function after xenobiotic- or ROS-induced AKI depends on renal regeneration, which occurs primarily through maintenance regeneration and injury-induced regeneration [92-95]. Contrary to the whole functional units of the kidney, the nephrons, which are only formed during nephrogenesis and do not regenerate after kidney injury or postnatally during ageing, likely due to depletion of the nephrogenic progenitor cell population, the renal tubule epithelium, however, can undergo a regeneration process to repair the damaged areas [92, 96, 97]. In uninjured adult kidneys, tubular epithelial cells show a low baseline rate of maintenance regeneration, as demonstrated by Nadasdy et al. [98] using PCNA and Ki-67 mitotic staining. Nevertheless, in the case of nephrotoxicity or other damage to the kidney, the regeneration process exceeds the baseline cell turnover to repair the damaged areas [93]. Evidence for the existence of renal epithelial cell regeneration after injury was first illustrated by Bonventre [99] using a standard model of ischemia-reperfusion injury (IRI). Under these conditions, tubular epithelial cells die and detach from their basement membrane but are rapidly replaced, demonstrating regeneration after tubular epithelial injury [99].

1.4.1 Dedifferentiation and tubular epithelial regeneration

Bonventre [99] has shown that tubular regeneration occurs in principle after injury. Still, it remains controversial whether the source of replacement cells is from surviving terminally differentiated tubular epithelial cells or from a subpopulation of specialized progenitor/stem cells. There is recent evidence suggesting that the classical concept for tubular regeneration after injury is that pre-existing or surviving tubular epithelial cells dedifferentiate, proliferate, and replace lost neighbouring cells [100-103]. The contribution of surviving tubular epithelial cells to tubular regeneration was demonstrated by Kusaba et al. [104] using genetic cell lineage tracing techniques in mice. This experimental approach generated knock-in mouse constructs to track tubular epithelial cells after unilateral ischemia-

reperfusion injury (IRI) surgery. Using tamoxifen as a genetic tracer, the knock-in mouse carried a tamoxifen-inducible Cre recombinase (CreER^{t2}) under the control of the sodium-dependent inorganic phosphate transporter-1 (SLC34a1). This protein is not expressed in renal stem/progenitor cells but in the apical side of terminally differentiated epithelial cells. These SLC34a1 mice were crossed against mice carrying a construct of a Rosa26^{tomato} reporter line. They observed specific and efficient genetic labelling of the proximal tubule's different tubular epithelial cell segments. After the injury, the surviving epithelial cells restored the epithelium without diluting the labelling, suggesting that the regenerated epithelial cells were the product of the surviving terminally differentiated tubular cells [104].

In this model of proximal tubular regeneration, terminally differentiated proximal tubular epithelial cells rapidly enter the cell cycle upon injury to replace lost neighbouring tubular epithelial cells through proliferative self-duplication. Although the cellular and molecular mechanisms of tubular dedifferentiation are not fully understood, studies have reported the involvement of activation of transcription factors, including Transforming Growth Factor beta-1 (TGF- β 1), Inhibitor of differentiation-1 (Id1), and the helix-loop-helix transcription factor and the epithelial growth factor receptor signalling pathway [105, 106]. During this process, terminally differentiated cells undergo epigenetic reprogramming of their gene activity to achieve a less differentiated state that allows the cells to proliferate and redifferentiate into their parent cell type, specifically by losing their polarity and expression of genes associated with differentiation and undergo partial Epithelial-Mesenchymal transition (EMT, see 1.4.1.1), leading to the acquisition of a flattened morphology, increased proliferative capacity, and expression of some developmental and injury-related genes such as *PAX2*, *SOX9*, *NCAM-1* and *KIM-1* (**Fig. 5**) [99, 107].

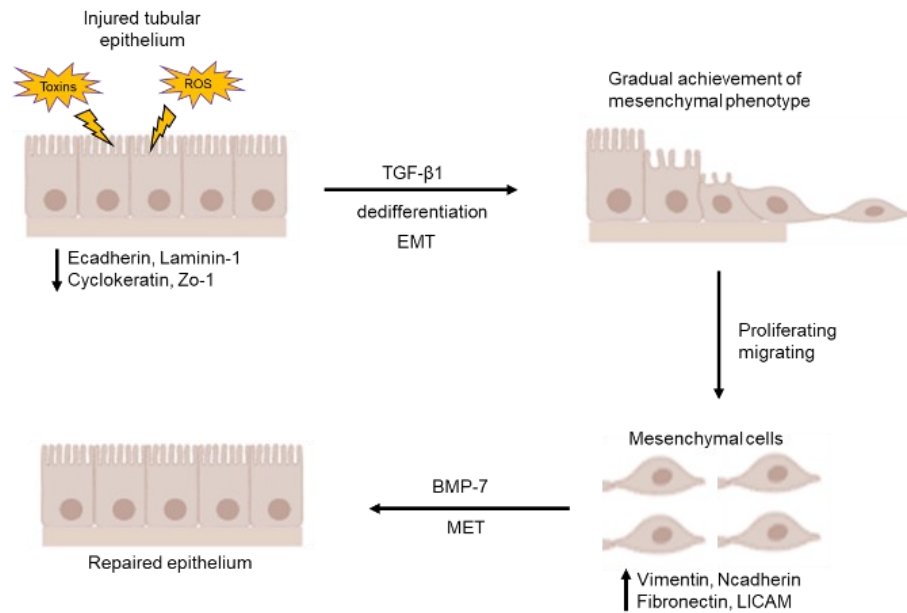


Figure 5: Dedifferentiation, a regenerative response to renal injury. In response to kidney injury, the tubular epithelial cells undergo a regenerative process called dedifferentiation. This process involves activating key transcription factors such as TGF-β1 and the Epithelial Growth Factor Receptor (EGFR) signaling pathway. As a result, the dedifferentiated epithelial cells lose their polarity and the expression of certain epithelial genes and undergo a partial epithelial-to-mesenchymal transition (EMT). These dedifferentiated cells acquire a flattened morphology, become migratory and proliferative, and re-express mesenchymal and developmental genes. This scheme was designed based on the research of Chang-Panesso and Humphreys [108] and Jiang *et al.* [109] and with the aid of Biorender.com. EMT = Epithelial-Mesenchymal Transition, MET = Mesenchymal-Epithelial Transition, TGF-b1 = Transforming Growth Factor beta-1, BMP-7 = Bone Morphogenetic Protein-7, ZO-1 = Zonula occludens-1, ROS = Reactive Oxygen Species.

1.4.1.1 Epithelial-Mesenchymal transition in tubular dedifferentiation

Epithelial-mesenchymal cell transition (EMT) and mesenchymal-epithelial cell transition (MET) are phenomena in which epithelial and mesenchymal cells can transform into each other under physiological and pathological conditions. They have been categorized into types I, II, and III [110, 111]. While type III EMT/MET has been reported in pathological processes such as solid tumour progression and metastasis [112-114], type I and II EMT/MET are central processes in embryogenesis, wound healing and tissue regeneration, respectively [115-117].

EMT is typified by the loss of apical-basal polarity, the breakdown of cell-cell contacts, and the reorganization of the cytoskeleton in epithelial cells (**Fig. 5**). Morphologically, this process is accompanied by the acquisition of an elongated, spindle-shaped structure and polarization from front to back [118, 119]. On a functional level, EMT enables the former epithelial cells to develop a motile phenotype, allowing them to leave their epithelial network without triggering anoikis, a programmed cell death in which epithelial cells invade the surrounding tissue by losing contact with the basement membrane [116]. At the molecular level,

EMT is associated with the downregulation of epithelial proteins such as E-cadherin, cytokeratin, and claudins and the upregulation of mesenchymal proteins such as vimentin, fibronectin, N-cadherin, and LICAM [117, 120]. Transcription factors of the ZEB (Zinc finger E-box binding homeobox), snail, micro RNAs (miRNA), and basic helix-loop-helix families most often mediate this frequently reversible switch in gene expression [120-123].

In proximal tubule regeneration, an EMT phenotype has been reported during the dedifferentiation of terminally differentiated tubular epithelial cells after AKI [108, 109, 124] (**Fig. 5**). In principle, after tubular injury, tubular epithelial cells undergo EMT and form proliferating mesenchymal cells expressing vimentin, smooth muscle actin, NCAM (neural cell adhesion molecule), matrix metalloproteinase 2 and 9 (MMP2 and 9), KIM1, and PAX2, a transcription factor critical for renal ontogenesis, and migrate into the empty areas of the basement membrane [99, 125-129]. This process has been reported to be tightly regulated by the transcription factor TGF- β 1 which interacts with proteins of the Smad family to form a complex with LEF1/TCF and Wnt-stabilized P-catenin in the nucleus to activate a gene program that converts the epithelial cells into mesenchymal cells [99, 115, 128, 130-132]. After the mesenchymal cells have restored the damaged areas of the basement membrane, they undergo MET to restore the epithelial properties of the cells. This conversion is regulated by Bone Morphogenetic Protein 7 (BMP7), which helps to reverse the TGF β 1-induced conversion of epithelial to mesenchymal cells by re-inducing the important epithelial cell adhesion molecule E-cadherin (**Fig. 5**) [131, 133]. Therefore, the correct balance between TGF β 1 and BMP7 signalling is essential for the physiological regeneration of the tubular epithelium. It has been previously reported that excess TGF β 1 leads to irreversible EMT, resulting in fibrosis of kidney tissue due to the accumulation of collagens [128, 129]. Whether EMT is followed by MET or fibrosis depends on the balance between these two opposing signals, as also shown by Zeisberg et al. [133], where pharmacologic doses of BMP7 reverse the fibrosis associated with EMT.

1.4.2 Renal stem/progenitor cells and tubular epithelial regeneration

Although there is evidence that dedifferentiation of surviving tubular epithelial cells seems to be the predominant mechanism of tubular epithelial regeneration, particularly following renal injury [102, 103], there is also evidence for the existence of a fixed stem/progenitor cell population in the adult human kidney [104, 134]. Bussolati et al. [135] provided the first evidence of a CD133⁺ progenitor cell

population in the adult human kidney. These cells were isolated from kidney tissue by magnetic cell sorting using the MACS system, were found to express PAX-2, an embryonic kidney marker, and were capable of expansion and self-renewal *in vitro* [135]. Interestingly, when these cells were implanted subcutaneously into immunocompromised mice, they formed tubules expressing renal epithelial markers [135]. After intravenous injection of CD133⁺ expressing cells into mice with acute tubular injury, they colonized the kidney and assimilated into the proximal and distal tubules [135]. This finding was also confirmed by an independent study conducted by Lindgren et al. [136] in 2011. This study also observed that progenitor cells isolated from adult kidney tissue by cell sorting due to their high ALDH enzyme activity were disseminated throughout the proximal and distal tubules and expressed CD133⁺CD24⁺CD106⁻ markers. They displayed stem cell attributes such as sphere formation and anchorage-independent growth [136]. When injected into SCID mice with acute kidney injury in a subsequent study by Angelotti et al. [137], they could engraft, form new tubule cells, and improve kidney function. These data, therefore, demonstrate that there is an adult stem cell population in the adult kidney that may be involved in tubule regeneration after injury (**Fig. 6**).

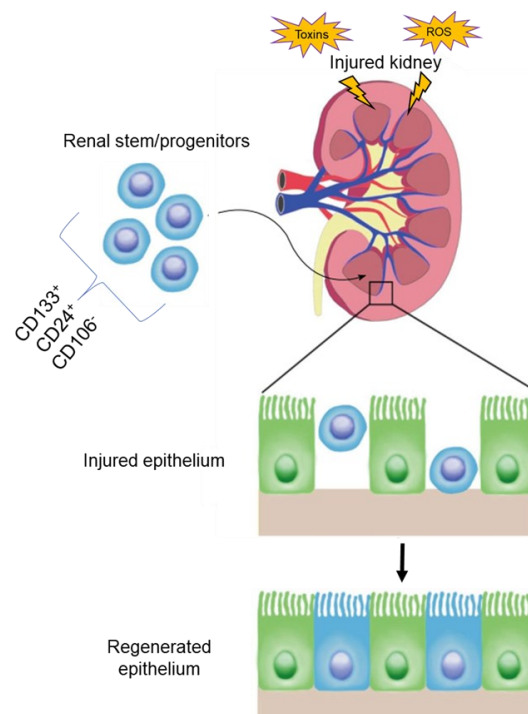


Figure 6: Regenerative capacity of adult renal stem/progenitor cells. Adult cells expressing the stem cell markers have been isolated and transplanted into immunocompromised mice with injured kidneys. These cells homed to the injury site and repopulated the renal tubular epithelium, thus supporting a model in which an adult stem cell population contributes to kidney regeneration and mild to moderate injury. This figure was modified/designed based on research by Chambers and Wingert [138], Bussolati et al. [135], and Angelotti et al. [137], and with the aid of Biorender.com.

Besides the kidney, adult stem/progenitor cells have also been isolated in many other tissues such as blood, intestine, skin, muscle, brain, and heart, which has contributed to a fundamental understanding of the regenerative potential of these tissues that is relevant to the field of developmental biology and regenerative medicine [139-141]. Adult stem cells (ASC), also referred to as somatic stem cells (SSC) or resident stem cells (RSC), are a rare population of multipotent undifferentiated cells that reside in a specialized structure called a micro niche within a differentiated organ. The niches maintain the local microenvironments that regulate stem cell growth and development. ASC can self-renew and differentiate into a limited number of mature cell types, maintaining tissue homeostasis [139, 142-144]. Usually, these cells are in a quiescent state in the tissue but can be activated upon injury to proliferate and differentiate into the desired cell type [145]. However, due to the difficulties associated with their accessibility, low quantity, limited differentiation potential, and complex and often unsuccessful *ex vivo* expansion, the utility of ASC *in vitro* as an essential source of tissue-specific stem cells for regenerative therapies is limited [139, 145, 146]. Alternatively, adult stem/progenitor cells can also be generated in the laboratory from human induced pluripotent stem cells (hiPSC) and differentiated directly into the various cell types or tissues of the body, thereby providing a platform to study cellular differentiation and the potential effects of toxins on this process. To this end, several protocols have been developed for the differentiation of iPSC into various cell types, including neurons, cardiomyocytes, hepatocytes, and kidney cells [147-150].

1.5 Induced pluripotent stem cells (iPSC)

Pluripotent stem cells are the cornerstone of regenerative medicine, as they can self-renew indefinitely and generate any cell type found in the three embryonic germ layers. This unique class of cells is epitomized by embryonic stem cells (ESC) and induced pluripotent stem cells (iPSCs) [151-153]. ESCs are naturally occurring stem cells that can be derived from the blastocyst (inner cell mass) and are a handy tool for the study of embryogenesis [154, 155]. However, their use in research has led to ethical and legal conflicts in many countries, including Germany, emphasizing the need for a reliable alternative model [156, 157]. Interestingly, the discovery of iPSCs circumvented these ethical concerns, and this discovery has wholly revolutionized the fields of stem cell biology and regenerative therapy, for which Sir John Gurdon and Shinya Yamanaka were given a Nobel Prize in Physiology and Medicine 2012. The foundation for this important discovery was first laid by Sir John Gurdon, who used the somatic cell nuclear transfer technique

(SCNT) in human oocytes to reprogram somatic cells into ESCs [158]. This approach was complemented by the group of Shinya Yamanaka, who used the four specific transcription factors OCT4 (Octamer-binding Transcription Factor 4), SOX2 (Sex determining region Y (SRY)-box 2), KIF4 (Krueppel-like factor 4), and c-Myc (transient transcription factor), which are expressed extensively in ESCs, to reprogram mouse fibroblasts into a pluripotent state [151]. These reprogrammed cells were termed iPSCs and have similar morphology, growth characteristics, and gene expression profiles to ESCs but without the ethical and legal issues associated with ESCs [22, 151]. However, since the c-Myc and KIF4 transcription factors used in identifying iPSCs are considered oncogenes, they are unsuitable for clinical applications. Based on this observation, further research by two independent groups, Takahashi et al. [159] and Yu et al. [160], have shown that the addition of LIN28 or NANOG (homeobox protein) instead of c-Myc and Klf4 with OCT4 and SOX2 can also induce the production of iPSCs from human somatic cells (**Fig. 7**) [159, 160]. Therefore, this discovery of a method to generate a pluripotent stem cell state in a human somatic cell *in vitro* has opened the possibility of studying regeneration or developmental processes in any cell type or tissue of the body *in vitro* and exploring the possible effects of xenobiotics on these processes [148, 151].

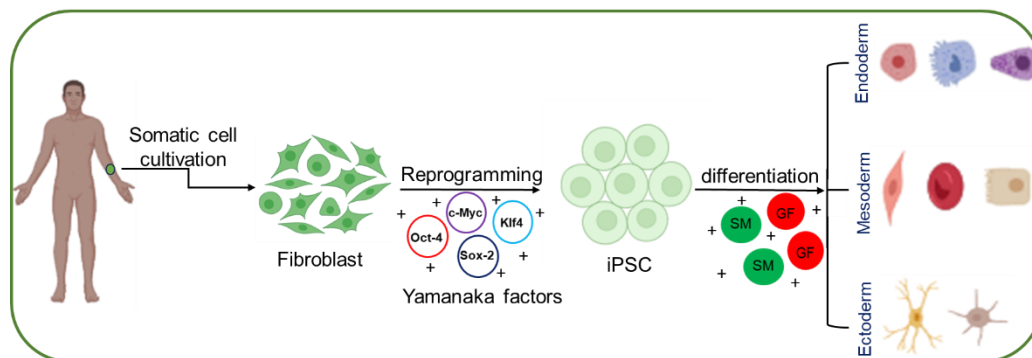


Figure 7: Schematic illustration of how human adult fibroblasts can be successfully reprogrammed to iPSC. The process involves culturing adult fibroblasts from human tissue and infecting them with lentiviruses containing the transcription factors OCT4, SOX2, KIF4 (LIN28), and c-Myc (NANOG) for reprogramming. By transducing the cells with these factors, they are expressed endogenously and induce a pluripotency state in the reprogramming fibroblast, thereby generating iPSCs. These iPSCs can then differentiate into cells of all three germ layers under controlled and appropriate culture conditions in the presence of small molecules and growth factors. The description is based on the research of Takahashi et al. [159] and Yu et al. [160], created with BioRender.com. iPSC: induced pluripotent stem cells, GF: growth factors, SM: signaling molecules. OCT4 = Octamer-binding Transcription Factor 4, SOX2 = Sex determining region Y (SRY)-box 2, KIF4 = Krueppel-like factor 4, c-Myc = transient transcription factor, and NANOG = Homeobox protein.

1.5.1 Somatic cell types and reprogramming methods used to generate iPSC

The first somatic cell type to be successfully reprogrammed into iPSCs by Takahashi and Yamanaka were skin fibroblasts from a skin biopsy [151]. Since then, research has shown that reprogramming fibroblasts can also be isolated from different tissues and organs of the body, including the heart, skin, lungs, or periodontal ligaments [161-164]. In addition to fibroblasts, iPSC induction can also be performed with other cell types. Umbilical cord blood CD34⁺ cells derived from cord blood at birth have been reported to be more efficient and faster to reprogram as they express many pluripotency markers, making them an excellent somatic cell type for cellular reprogramming. However, the availability and size of the donor pool for cord blood cell derivation are limited, paving the way for other blood cells, such as peripheral blood cells [165, 166]. Besides skin fibroblasts and blood cells, other accessible cell sources for reprogramming are exfoliated renal PTEC derived from urine and keratinocytes from plucked hair [167, 168]. Although it has been claimed that among the different cells used for reprogramming, renal tubular epithelial cells and keratinocytes stand out in terms of their accessibility, ease of isolation, less time required for reprogramming, and higher reprogramming efficiency, the somatic cell types currently used by therapeutic companies to generate iPSCs are fibroblasts and blood cells [168, 169].

Several methods exist for reprogramming different somatic cell types into a pluripotent state. These approaches can be subclassified into integrative and non-integrative transfer systems [170]. The integrative transfer system consists of viral vectors, which can be retroviruses or lentiviruses, and non-viral vectors, which are plasmids or transposons that perform the integration of the transcription factors into the host cell's genome. The non-integrative transfer system also consists of viral vectors such as adenovirus or Sendai virus and non-viral vectors such as episomal, protein, RNA, or microRNA vectors, which introduce the transgene into the host cells and enable the temporal, non-constitutive expression, and activation of the transgene in the host cell [171, 172]. The iPSCs used in this study were generated from foreskin fibroblasts by the Yu group [160]. They used the integrative transfer system with lentiviral vectors to integrate the OCT-3/4, SOX2, NANOG, and LIN28 transcription factors into human foreskin fibroblasts. Lentiviruses, mainly derived from the human immunodeficiency virus, were used for this reprogramming approach because they are well suited for gene delivery and can deliver their transgene to both proliferating and non-proliferating cells after infection, resulting in higher transduction efficiency [160].

1.6 *In vitro* differentiation of iPSC into proximal tubular epithelial-like Cells

As mentioned above, proximal tubular epithelial cells (PTEC) are one of the main targets for nephrotoxic substances in the renal nephron. They are, therefore, the focus of iPSC differentiation research as far as toxicological studies in the kidney are concerned. Many differentiation protocols have been described to differentiate iPSCs into PTEC-like cells, which follow different strategies. Several groups started by generating three-dimensional (3D) self-assembling structures from iPSCs, the so-called renal organoids, by recapitulating the multistep process of *in vivo* nephrogenesis [173-177]. These iPSC-derived 3D renal organoids contain nephron-like structures, including glomerular structures, proximal tubular cells, cells of the loop of Henle, distal tubular cells, and collecting duct structures, in a highly structured and organized manner, thereby recapitulating renal tissue *in vivo*. These iPSC-derived renal organoids, therefore, offer exciting possibilities in regenerative medicine and disease modelling and, to some extent, in the kidney's toxicity assessment. However, there are also some limitations associated with renal organoids, including toxicity testing in renal organoids. It is challenging because it is difficult to expose the cells exclusively from the apical or basolateral side and evaluate how much drug each cell type of the organoid is exposed to. It is also more challenging to analyse the specific effects on individual cell types in the organoid. In addition, kidney organoids are unsuitable for high-throughput applications due to the time and complexity of generation [178]. However, monocultures of a target cell type could overcome some of these shortcomings. Recently, several protocols have been developed to induce iPSCs directly into PTEC. Some of these differentiation protocols also follow the course of embryogenesis of the kidney to generate the PTEC-like cells in a stepwise manner, generating the various renal precursors. In 2014, Lam et al. [179] were able to differentiate cells expressing markers of the intermediate mesoderm *PAX2* and *LHX1* from human iPSCs by treating hiPSCs with glycogen synthase kinase 3 inhibitor (CHIR99021), fibroblast growth factor (FGF2) and retinoic acid. Withdrawal of FGF2 and retinoic acid after three days of incubation and without the addition of other factors after seven days produced PTEC-like cells. After implantation under the renal capsule of immunodeficient mice, these cells expressed renal PTEC markers such as Lotus tetragonolobus lectin, N-cadherin, and kidney-specific Cadherin-16 [179]. Chandrasekaran and colleagues also applied a multistep differentiation protocol involving a mixture of small molecules and growth factors on cell culture wells coated with Geltrex to transform hiPSCs into cells with a renal proximal tubular phenotype within 14 days. PTECs expressed

proximal tubular-specific genes and proteins, including megalin, paired box protein-2 (PAX-2), and parathyroid hormone-1 receptor (PTH-1R). They exhibited PTEC-like hormone responses, megalin-enhanced endocytosis, and P-glycoprotein efflux transport [23]. Another multistep protocol was presented by Ngo et al. [180] using a levitation-based approach that allows scalable cell culture to expand and differentiate hiPSCs into human PTEC cultured on Matrigel-coated alginate beads. With this protocol, kidney progenitors were generated 4 days after hiPSCs differentiation, and PTEC-like cells were generated after 8 days with an efficiency of 80 % and a 10-fold expansion in 24 days. PTEC-like cells on the beads also exhibited microvilli and distinct apicobasal localization of markers, and their functionality was demonstrated by the uptake of glucose, albumin, organic anions, and cations [180].

In addition to the multistep protocols, other protocols have been used to shorten the differentiation of PTEC from hiPSCs to a few days. In 2013, the research group of Zink [181] developed the first 1-step protocol for differentiating human ESCs into PTEC-like cells as a first step for application in *in vitro* toxicology assessment. In this protocol, incubation of human ESCs with renal epithelial growth medium (REGM) supplemented with bone morphogenetic protein 2 and 7 (BMP-2 and -7) resulted in the expression of aquaporin-1 (*AQP-1*), aminopeptidase (*CD-13*), γ -glutamyl transferase (*GGT*) and kidney-specific Cadherin (*CAD-16*) within 20 days. These ESC-derived PTEC-like cells showed similar morphology and function to PTEC *in vivo* and partially contributed to the formation of an epithelium after injection into mice [181]. Two years later, Kandasamy et al. [22] revised this protocol, allowing the differentiation of hiPSCs into PTEC-like cells in only 8 days. In this protocol, hiPSCs were also differentiated in REGM supplemented with BMP-2 and -7. This resulted in PTEC-like cells expressing PTEC markers such as *AQP-1*, *CD-13*, and *GGT*, while a reduction in stem cell markers *NANOG*, *OCT3/4*, and *SOX2* was observed. In addition, the PTEC-like cells showed morphological signs of tubulogenesis and formed domes. With this protocol, PTEC-like cells were generated with a purity of > 90 %, and screening of substances could also be performed directly after differentiation without the need to harvest or purify the cells [22].

2. Aim of the study

Nephrotoxic and ischemic damage to the kidney, especially to the proximal tubular epithelial cells (PTEC), leads to acute renal injury (AKI) and, in most cases, can lead to chronic kidney disease (CKD) or end-stage renal disease [20, 29-31]. However, the recovery of renal function after AKI depends on the regenerative potential of the kidney, which allows the replacement of damaged tubular epithelial cells with functional tubular epithelium either by stem cell differentiation or by restoring the proliferative properties of surviving PTEC through the acquisition of an EMT phenotype [94, 99] (**Fig. 8**). However, it is known that renal function declines, suggesting that the damaged cells are not replaced by fully functional cells. To better understand the possible causes of this loss of renal cell function, it would be beneficial to know the role of toxins during the tubular regeneration processes. Therefore, we investigated the response of human induced pluripotent stem cells (hiPSC) to known genotoxic and non-genotoxic nephrotoxins as well as to known oxidizing agents during their differentiation into proximal tubular epithelial-like cells (PTELCs), which in this context represents one of the two regeneration pathways in the kidney. For this reason, we aimed to establish a model of hiPSC differentiating into PTELCs. The progression from hiPSC to PTELCs will be monitored by analysing RNA and protein expression. Functional assays such as albumin transport, 6-carboxyfluorescein uptake and P-glycoprotein-mediated extrusion will also be used for functional characterisation. Using this model, the sensitivity of cells at the different stages of differentiation to selected known toxins such as cisplatin, cyclosporin A, hydrogen peroxide (H₂O₂), menadione and tert-butylhydroquinone (TBHQ) will be analysed using the Alamar Blue cell viability assay. In addition, the mode of action and underlying molecular mechanisms of these different toxins on cells at various stages of differentiation will be clarified by performing toxicity studies such as apoptosis, senescence, residual proliferation, and DNA damage foci analysis. Furthermore, to obtain a more holistic understanding of the role of toxins in the tubular regeneration process, in the second part of the project, we also aimed to investigate whether the differentiated PTELCs can regain their ability to proliferate after differentiation by mainly adopting an EMT phenotype, which is also an alternative regeneration pathway in the kidney. The influence of the various toxins on this EMT-driven dedifferentiation pathway of kidney regeneration will also be investigated in this project.

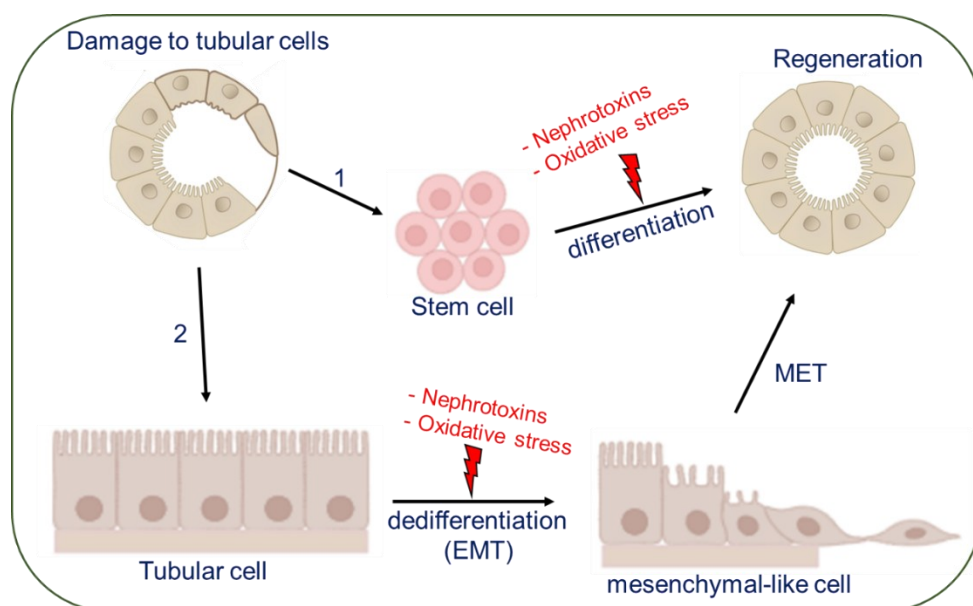


Figure 8: A schematic representation of the plan to study the effects of toxins on kidney regeneration processes. Two pathways are possible for the regeneration of damaged tubular epithelial cells in the kidney: by division and differentiation of (1) multipotent renal progenitor cells into functional tubular epithelial cells or by (2) dedifferentiation of fully differentiated tubular epithelial cells after acquisition of a mesenchymal-like phenotype and restoration of the epithelial phenotype. The influence of genotoxic and non-genotoxic nephrotoxins and oxidative stress on these cells of origin and their transformation processes will be investigated in this subproject. EMT = Epithelial-mesenchymal transition, MET = mesenchymal-epithelial transition.

2. Published data (international journal of molecular sciences, 25, 81, 2023)

2.1. Sensitivity of human induced pluripotent stem cells and thereof differentiated proximal tubular cells towards selected nephrotoxins

2.1.1. Introduction

The kidney is a detoxifying organ that filters and transports not only metabolic waste products from the body but also drugs and potentially toxic xenobiotics. More than 32 % of the 200 most important drugs are excreted via the kidney. The epithelial cells of the proximal tubular segment of the kidney are the major players in the reabsorption and secretion of chemical substances [5, 182]. This critical role makes proximal epithelial cells (PTEC) particularly vulnerable to damage caused by xenobiotics, which can lead to nephrotoxicity. In fact, an estimated 20 % of acute kidney injury (AKI) cases in hospitals are attributed to PTEC-mediated drug nephrotoxicity, making PTEC the most studied cell type in drug safety evaluations, regeneration therapies, and tissue modeling [20].

The tubular system has regeneration potential, which occurs even in the absence of specific insults to continuously replace aged cells to preserve the organ's structural and functional integrity. However, in the event of nephrotoxicity or other damage to the kidney, the basic cell turnover is significantly exceeded by the regeneration process to repair the damaged areas [92, 94]. This tubule cell regeneration occurs either by local stem cell proliferation or following epithelial–mesenchymal transition (EMT) of tubular epithelial cells near the injury site [94]. Ultimately, one or a combination of these pathways will restore organ structure and function. Despite the replacement of tubule epithelial cells in the kidney, there is unambiguous evidence that the kidney does not regain one hundred percent of its former function, especially in patients with post-AKI. These patients have an elevated risk of acquiring chronic kidney diseases (CKD), suggesting that the functioning of existing tubular cells may have been compromised or those cells replacing injured cells are not fully functional upon regeneration [183, 184]. Moreover, ageing, oxidative stress, and toxic agents can interfere with repairing damaged areas, possibly resulting in dysfunction and ultimately increasing the risk of renal failure [183].

Therefore, for meaningful risk assessments, it will be necessary to investigate the influence nephrotoxic substances have on renal regeneration. One promising avenue is the development of approaches based on human induced pluripotent

stem cell (hiPSC). These approaches could serve as a model for toxicity effects during regeneration, offering a new and exciting direction in this field [185]. hiPSCs are primarily derived from reprogrammed human somatic cells such as dermal fibroblasts. They have proven to be a robust and reproducible source of human cell types for regeneration and disease modelling, as hiPSCs are capable of extensive self-renewal and can differentiate into multiple somatic cell types within the three germ layers [159]. hiPSC allows studies without ethical concerns compared to animal and human embryonic stem cell (hESC) models [159]. In addition, their use is consistent with the 3Rs principles for next-generation toxicity assessment: replacement, reduction, and refinement of animal-based experiments with new methodological approaches [185, 186]. Interestingly, models using hiPSC have the potential to be more accurate in tailored toxicity assessment than traditional animal models, which have low predictive values and suffer from several limitations, including interspecies differences in transporter expression [187, 188]. They could also be more suitable than hESC-derived human proximal tubule-like cells, which have a low sensitivity [5, 22]. Moreover, using hiPSC would allow the generation of patient-specific immunocompatible tissues through personalized *in vitro* models [189].

Although various methods for direct differentiation of hESC and hiPSC into proximal tubular epithelial-like cells (PTELC) have been reported, the focus has mostly been on using these stem cell-derived renal cells to develop a suitable and reliable model for predicting nephrotoxicity [21-23, 180, 190]. Our study is the first to investigate the effects of distinct toxins on the differentiation process of hiPSC leading to tubular cells. Therefore, in this study, we adapted a previously published differentiation protocol [22] to generate PTELC and evaluated the progression of hiPSC to PTELC based on mRNA and protein expression. This differentiation protocol tested hiPSC, hiPSC differentiating into PTELC, and hiPSC differentiated into PTELCs for their sensitivity to selected nephrotoxins. This study not only confirms the potential of hiPSC to differentiate into PTELC but also provides hopeful insights into the effects of toxins on this differentiation process. In the future, after ensuring that PTELC are sufficiently similar to tubular cells *in vivo*, experiments with hiPSC differentiating into tubular cells may provide crucial information on the harmful effects of substances on the differentiation processes required for renal regeneration.

2.1.2. Materials and Methods

2.1.2.1. Materials

The text lists all chemical names and the companies from which they were purchased. The Appendix lists primers and antibodies used to detect the expression of various genes and proteins.

2.1.1.2. Methods

2.1.1.2.1. Cell culture of RPTEC and F4-hiPSC, and *in vitro* differentiation protocol

The human primary renal proximal tubular epithelial cell line (RPTEC-TERT1) was obtained from the American Type Culture Collection (ATCC, Manassas, VA, USA) and expanded as described by [191]. In brief, cells were grown into a 1:1 composition of DMEM with high glucose and Ham's F-12 nutrient mixture supplemented with 2 mM GlutaMAX (both from Thermo Fisher Scientific, Waltham, MA, USA), 100 U/mL Pen/strep, 5 µg/mL insulin, 5 µg/mL transferrin, 5 ng/mL sodium selenite, 10 ng/mL EGF, and 36 ng/mL hydrocortisone (all from Sigma-Aldrich, St. Louis, MO, USA). These cells were cultured and used until passage 10. The foreskin-4 (F4)-human induced pluripotent stem cell line (further referred to as hiPSC) was purchased from the WiCell Stem Cell Bank (Madison, WI, USA) at passage 29. These cells were generated from human foreskin fibroblasts through lentiviral transfection of Oct3/4, Sox2, Nanog, and Lin28 [48]. The hiPSC line was routinely cultured on six-well plates coated with human embryonic stem cell-qualified Matrigel for the F4 (Corning, New York, NY, USA) in mTeSR1 medium (StemCell Technologies, Vancouver, BC, Canada), supplemented with 10 mM Y27632 dihydrochloride (Sigma-Aldrich, St. Louis, MO, USA) to keep them in exponential growth, and passaged twice a week at a ratio of 1:6 when cultures reached a confluency of 70–90 %. For differentiation into renal proximal tubular epithelial-like cells (PTELC), a modified protocol, according to Kandasamy and colleagues [22], was used as illustrated (Figure 1A). Briefly, 3000 F4 cells/cm² were seeded into 12-well plates coated with growth factor-reduced Matrigel (Corning, NY, USA) in the renal epithelial growth medium (REGM) containing various growth factors and supplements (REGM BulletKit, Lonza, Basel, Switzerland) including 0.5 % fetal bovine serum and 10 mM Y-27632 dihydrochloride. After 24 h, the cells were switched to the REGM differentiation medium without Y-27632 dihydrochloride but supplemented with 10 ng/mL of bone morphogenetic protein (BMP) 2 (Sigma-Aldrich, St. Louis, MO, USA) and

2.5 ng/mL BMP7 (Thermo Fisher Scientific, Waltham, MA, USA) and cultured under these conditions for 9 days with a daily medium change to induce differentiation towards PTELC. On day 9, hiPSC-derived PTELCs were either directly treated with nephrotoxic substances or harvested for further experiments.

2.1.1.2.2. Analysis of cell viability

After 24 h treatment with vehicle controls (DMSO or basal medium) or with different concentrations of the model compounds cisplatin, a genotoxic nephrotoxin (Teva, Petach Tikva, Israel), and cyclosporin A, a non-genotoxic nephrotoxin (Enzo Life Sciences, Farmingdale, NY, USA), the cell viability of undifferentiated, differentiating, and differentiated cells was examined using the Alamar Blue Assay [192], which measures the reduction in the blue and non-fluorescent resazurin dye (Sigma, Steinheim, Germany) into pink and fluorescent resorufin by cell activity. Fluorescence intensity was measured in quadruplicates (excitation: 535 nm, emission: 590 nm on Tecan infinite 200, Tecan, Männedorf, Switzerland). Relative cell viability values were normalized to the respective vehicle controls and expressed as percentages.

2.1.1.2.3. Analysis of gene expression (RT-PCR)

Total RNA was separated and purified with the RNeasy Mini Kit (Qiagen, Venlo, The Netherlands) and RNase-free DNase Set (Qiagen, Venlo, The Netherlands), either manually or using the automated QIAcube (Qiagen, Venlo, The Netherlands). The RNA amount was quantified using the NanoVue Plus Spectrophotometer (GE Healthcare Life Sciences, Buckinghamshire, UK), stored at -80°C , or immediately used for cDNA synthesis. cDNA was synthesized from 2000 ng RNA using the High-Capacity RNA-to-cDNA Reverse Transcription Kit (Thermo Fisher Scientific, Waltham, CA, USA) in combination with the RiboLock Rnase Inhibitor (Thermo Fisher Scientific, Waltham, CA, USA). Quantitative real-time polymerase chain reaction (qRT-PCR) was performed using the SensiMix SYBR Hi-ROX (C) Kit (Bioline GmbH, Luckenwalde, Germany) on a CFX96 Touch Real-Time PCR Detection System (Bio-Rad Laboratories, Hercules, CA, USA), and the data were analysed using CFX Manager software (v3.1, Bio-Rad Laboratories, Hercules, CA, USA) according to the manufacturer's instructions. All samples were run with three technical replicates. The Cq values obtained for genes of interest were first normalized to the mean Cq values obtained for the

housekeeping genes *ACT-β* and *RPL-32* and then to the control samples and expressed as a fold of this mean value. Changes in ≤ 0.5 - and ≥ 2 -fold gene expression were considered biologically relevant. Gene-specific primer pairs used for amplification in this study (**Table 1**) were designed with NCBI (<https://www.ncbi.nlm.nih.gov/nucore/>). Using different cDNA concentrations, these primer sets were tested and validated for specificity in a qPCR.

2.1.1.2.4. Immunofluorescence analysis

To monitor the expression of prototypical proximal tubular-related proteins, cells were fixed with 4 % cold formaldehyde/PBS (Merck Millipore, Billerica, MA, USA) for 15 min, washed with PBS, and permeabilized twice with 0.1 % Triton X-100/PBS (Sigma-Aldrich, St. Louis, MO, USA) for 5 min at room temperature (RT). After blocking (5 % BSA/PBS, 1 h, RT), incubation with primary antibodies in the dilution indicated in Table S2 was performed at 4 °C overnight in a humid chamber. After washing with PBS, a fluorescence labelled secondary antibody (Alexa Fluor 488/550 goat polyclonal to mouse or rabbit, Abcam, Cambridge, UK) was added and incubated in the dark (1:1000; 2 h). Nuclear DNA was stained with Vectashield containing DAPI (4',6-diamidino-2-phenylindole, Vector Laboratories, Burlingame, CA, USA). Slides were sealed with nail polish and examined on a fluorescence microscope (BX43F Upright Microscope, Olympus, Shinjuku, Tokyo, Japan).

2.1.1.2.5. Westen blot analysis

Cell extracts were prepared through lysis of cells in Roti-Load buffer (Carl Roth GmbH, Karlsruhe, Germany) followed by heating (95 °C for 5 min). First, 25 µg of the isolated protein was separated by SDS-PAGE (10 to 12 %) and transferred to a nitrocellulose membrane. The membrane was blocked at RT for 1 h (5 % non-fat milk in TBS/0.1 % Tween 20) and incubated overnight at 4 °C with the primary antibodies in the dilution indicated in Table S2. After washing the membrane with TBS/0.1 % Tween 20, incubation with peroxidase-conjugated secondary antibodies (1:2000) was performed (2 h at RT on a shaker). Finally, the membrane was visualized using the ChemiDox™ Touch Imaging System (BioRad, Munich, Germany).

2.1.1.2.6. Flow cytometry-based quantitative detection of aquaporin-1

Flow cytometric analysis was performed for quantitative detection of the PTEC marker aquaporin 1. After trypsinization, at least 1×10^6 cells were pelleted by centrifugation (400 \times g, 4 min, 4 °C) and treated with 0.5 % Tween 20 in PBS (RT, 15 min). After centrifugation, cells were resuspended in 3 % BSA in PBS (RT; 15 min), followed by the addition of the primary antibody against aquaporin-1 (1:250). After washing twice with PBS, a fluorescently labelled secondary antibody (Alexa Fluor 488, goat, polyclonal to mouse, Abcam, Cambridge, UK) was added (1:1000; 30 min). The quantification of cells expressing aquaporin-1 was performed by flow cytometric analysis (Becton Dickinson, Accuri™ C6 plus, Heidelberg, Germany).

2.1.1.2.7. Albumin uptake assay

The ability of PTEC to reabsorb albumin as a surrogate marker of their functionality was assessed by adding fluorescence-labelled bovine serum albumin (BSA-FITC, 10 mg/mL) (Sigma Aldrich, St. Louis, MO, USA) to the culture medium. Following 2 h of incubation at 37 °C, uptake was stopped with ice-cold PBS. At this point, cells were either detached with trypsin, fixed with 0.5 % cold formaldehyde in PBS (15 min, RT), and analysed by flow cytometry (Becton Dickinson, Accuri™ C6 plus, Heidelberg, Germany) or fixed with 0.5 % cold formaldehyde in PBS (15 min, RT) followed by counterstaining of cell nuclei and visualization by fluorescence microscopy (BX43F Upright Microscope, Olympus, Shinjuku, Tokyo, Japan).

2.1.1.2.8. Statistical analysis

Statistical analyses were conducted on GraphPad Prism version 6 (GraphPad Software, San Diego, CA, USA). Data are shown in terms of mean and standard deviation of three independent experiments ($n = 3$). A comparison between the different sample groups was performed using Student's t-test (multiple-comparison test) or a one-way analysis of variance (ANOVA). Statistically significant differences between groups were assumed at a p -value ≤ 0.05 .

2.1.3. Results

2.1.3.1. Differentiation of hiPSC into proximal tubular epithelial-like cells

Dermal fibroblast-derived hiPSC Foreskin-4 (F4hiPSC) were differentiated into PTELC as described in the Material and Methods with the protocol shown in **Fig. 9A**. The F4hiPSC underwent morphological changes from the typical cobblestone-like appearance to larger spindle-like cells within nine days (**Fig. 9B**). They also formed domes and organized themselves in tubule-like patterns, features that were also observed in the human proximal tubular cell line RPTEC/TERT1 (**Fig. 9C**).

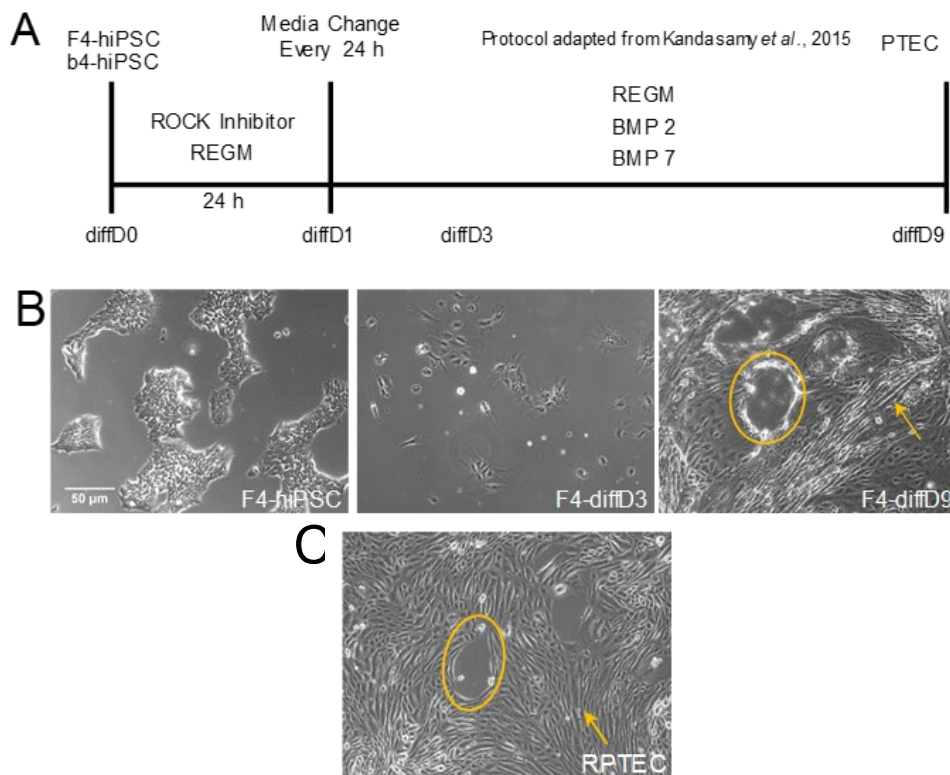


Figure 9. Differentiation protocol and physiological changes provoked by it. (A) Treatment scheme of hiPSC adapted from the protocol of Kandasamy et al. [13]. **(B)** Morphological appearance of the F4-hiPSC and cells on day 3 and day 9 of the differentiation process compared to a **(C)** commercially available kidney biopsy-derived proximal tubular cell line (RPTEC/TERT1). Yellow circles highlight domelike and yellow arrows show tubule-like patterns in the cell layers of the differentiated cells. BMP = bone morphogenetic protein, diffD = differentiation day, hiPSC = human induced pluripotent stem cells, PTELC = proximal tubular epithelial-like cells, REGM = renal epithelial cell growth medium, ROCK = rho-associated, coiled-coil-containing protein kinase.

Expression analysis revealed a significant downregulation of mRNA expression of stem cell marker genes *NANOG*, *OCT-3/4*, and *SOX-2* after nine days of differentiation in F4-hiPSC (**Fig. 10A**). The expression of markers of epithelial cells, especially *E-cadherin*, increased in the differentiated cells compared to the hiPSC strain. Out of four analysed markers of proximal tubular epithelial cells (PTEC), three of them, *AQP-1*, *CAD-16*, and the glucose transporter *GLUT-5*, were

significantly expressed. At the same time, *CD13* mRNA levels showed no difference after differentiation (**Fig. 10A**) in the hiPSC-derived cells. Basal expression and the expression change by differentiation of some markers were confirmed on the protein level, as seen in the immunocytochemical pictures in **Fig. 10C**. This method also detected a higher increase in protein levels where little or no increase in mRNA levels in the hiPSC-PTELC was measured, such as for *CD13* or *ZO-1*. FACS analysis revealed that at nine days post differentiation, almost all hiPSC-derived diffD9 cells expressed the PTEC marker AQP-1, more than three times as many cells as compared to undifferentiated hiPSC (**Fig. 10C**).

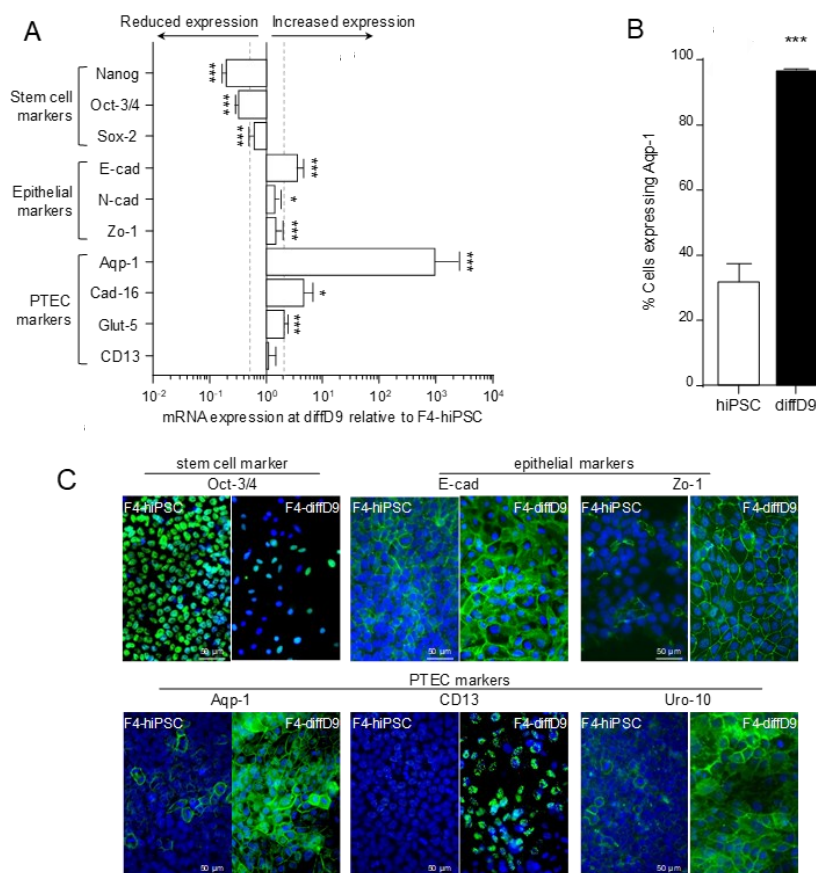


Figure 10. Changes in expression of differentiation markers in F4-hiPSC differentiated into proximal tubular epithelial cell-like cells (PTELC). (A) mRNA expression of stem cell, epithelial cell, and PTEC markers in differentiated F4-hiPSC relative to expression in undifferentiated F4-hiPSC analysed by quantitative RT-PCR. (C) Visualization of selected proteins by immunocytochemical staining on F4-hiPSC and F4 on differentiation day 9. Antibodies against the different markers are visualized with FITC-coupled secondary antibodies, and nuclei are stained with DAPI. (B) Flow cytometry analysis of the PTEC typical protein aquaporin-1 in F4-hiPSC and F4 on differentiation day 9. Data from at least 3 independent experiments (qPCR also included 3 technical replicates) are shown as mean + SD. * $p \leq 0.05$, ** $p < 0.01$ and *** $p < 0.001$ vs. hiPSC (Student's t-test). Aqp-1 = aquaporin1, Cad-16 = cadherin 16, CD13 = alanyl aminopeptidase, DAPI = 4',6-diamidino-2-phenylindole, diffD = differentiation day, E-cad = E-cadherin, FITC = fluorescein isothiocyanate, Gapdh = glyceraldehyde 3-phosphate dehydrogenase, Glut-5 = fructose transporter 5, hiPSC = human induced pluripotent cells, Nanog = homeobox protein, N-cad = N-cadherin, Oct-3/4 = octamer-binding transcription factor 3/4, PTEC = proximal tubular epithelial cells, Sox-2 = sex determining region Y-box 2, Uro-10 = urothelial glycoprotein, Zo-1 = zonula occludens-1.

2.1.3.2. Transporter expression and transport capacity of hiPSC-derived PTELCs

As a pre-requisite for the cells to respond to toxic substances, they must have suitable transporters to import them. **Fig. 11A** shows that after nine days of differentiation, many of the transporters studied in hiPSC-diffD9 were significantly more expressed than in the hiPSC, and these include transporters for cisplatin and albumin. Other transporters, such as organic cation transporter 2 (*OCT-2*) and multidrug resistance protein 1 (*MDR-1*), were significantly downregulated in hiPSC-diffD9. But Western blot and immunocytochemical staining confirmed the expression of the *OCT-2*, the two copper transporters *CTR-1* and *-2*, which are crucial for the uptake of cisplatin into cells, and megalin, which is important for the transport of albumin, also on protein level in hiPSC-diffD9 (**Fig. 11B, C**). Additionally, the Western blot showed that the amount of *OCT-2* was not reduced in the hiPSC-diffD9 compared to the undifferentiated hiPSC, as quantified by PCR.

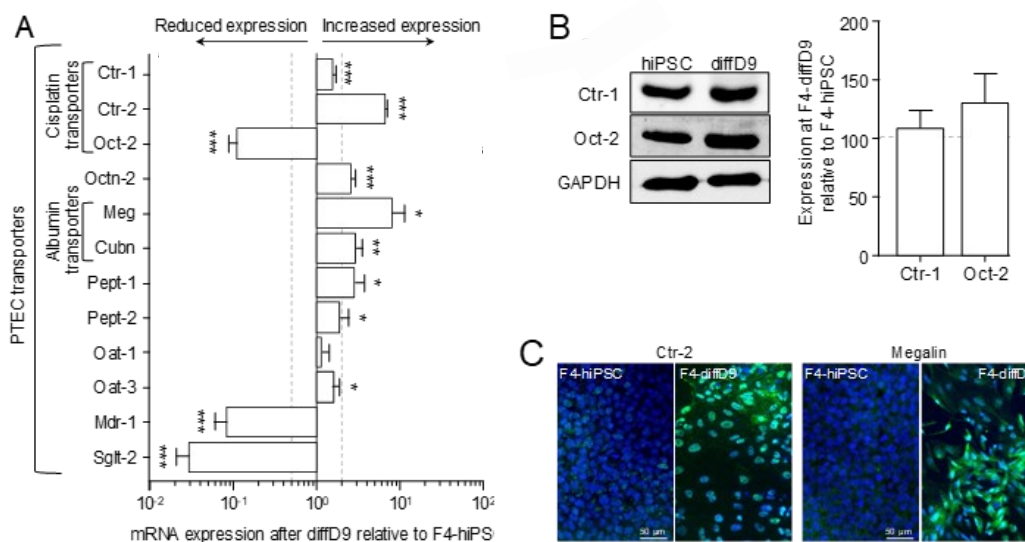


Figure 11. Expression changes in functional proteins in hiPSC differentiated into PTELCs. (A) mRNA expression of PTEC transporters and transporters of cisplatin relative to expression in F4hiPSC analysed by quantitative RT-PCR. (B) Expression of selected transporter proteins in F4hiPSC and F4hiPSC on differentiation day 9 analysed by Western blotting. Shown are representative blots as well as their quantification. (C) Visualization of selected proteins by immunocytochemical staining on F4-hiPSC and F4 on differentiation day 9. Antibodies against the different markers are visualized with FITC-coupled secondary antibodies, and nuclei are stained with DAPI. Data from at least 3 independent experiments (qPCR also included 3 technical replicates) are shown as mean ± SD. * p ≤ 0.05, ** p < 0.01, *** p < 0.001 vs. hiPSC (Student's t-test). Ctr-1/copper transporter 1/2, Cubn = cubilin, DAPI = 4',6-diamidino-2-phenylindole, diffD9 = differentiation day 9, FITC = fluorescein isothiocyanate, hiPSC = human induced pluripotent cells, Mdr-1 = multidrug resistance protein 1, Meg = megalin, Oat-1/3 = organic anion transporter 1, Oct-2 = organic cation transporter 2, Octn-2 = organic cation/carnitine transporter 2, Pept-1/2 = peptide transporter 1/2, Sglt-2 = sodium/glucose cotransporter 2.

F4-hiPSC differentiated for 9 days (diffD9) into PTELCs were analysed for their ability to take up albumin as an indication of their functionality in comparison to the LLC-PK1 (porcine proximal tubular cell line, positive control) and to the RPTEC cell line (negative control). Differentiated PTELCs showed a clear uptake of labelled albumin, as depicted in **Fig. 12A**, proving the functionality of the transporters for albumin. LLC-PK1 cells, on the other hand, also showed an increase in the uptake of albumin (**Fig. 12C**), whereas RPTEC cells did not show any significant uptake of albumin (**Fig. 12B**).

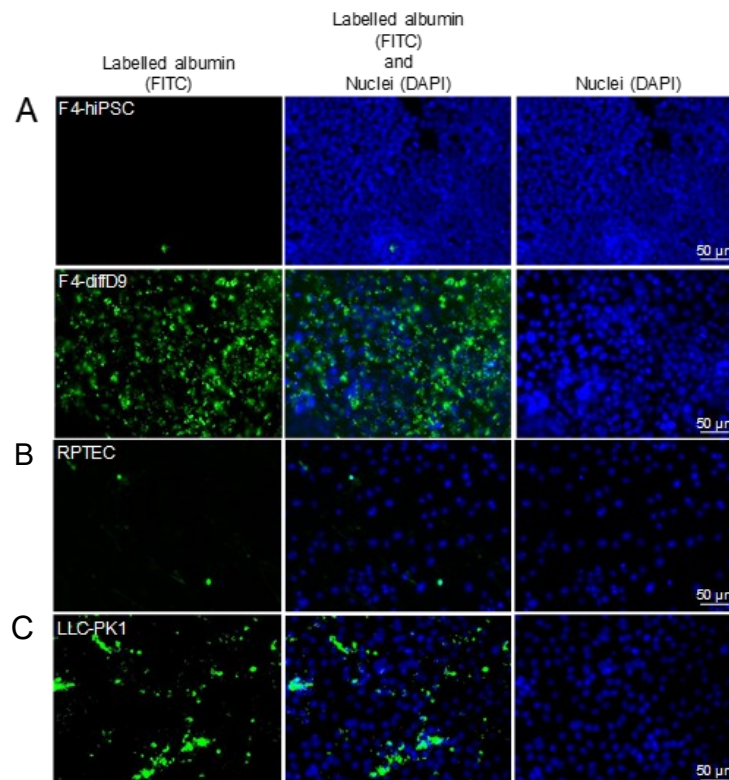


Figure 12. Gain of functional albumin transport in hiPSC differentiated into PTELCs. Analysis of albumin uptake into the undifferentiated and differentiated F4 cells (A), as well as in RPTEC- (B) and LLC-PK1 (C) cells with the help of FITC-labelled BSA. Shown are representative pictures. BSA = bovine serum albumin, DAPI = 4',6-dimidino-2-phenylindole, diffD9 = differentiation day 9, FITC = fluorescein isothiocyanate, hiPSC = human induced pluripotent cells, RPTEC = renal proximal tubular epithelial cells.

2.1.3.3. Comparison of marker and transporter expression as well as transport capacity of PTELC with the human renal proximal tubular epithelial cell line RPTEC/TERT1

Gene expression analysis of selected genes in PTELC differentiated from F4-hiPSC showed up-, down-, and unregulated expression of genes in the differentiated cells (**Fig. 13**). Expressed at the same level as in RPTEC/TERT1 were the transporter *OCT-2*, *E-cadherin*, and *OAT-1* in PTELC originating from F4-hiPSC. The pluripotent stem cell marker *OCT-3/4*, one marker of the proximal

tubules, *AQP-1*, and a subunit of the albumin transporter, *megalyn* were highly increased compared with expression in RPTEC/TERT1. The expression of all other genes examined was downregulated compared with the expression in RPTEC/TERT1.

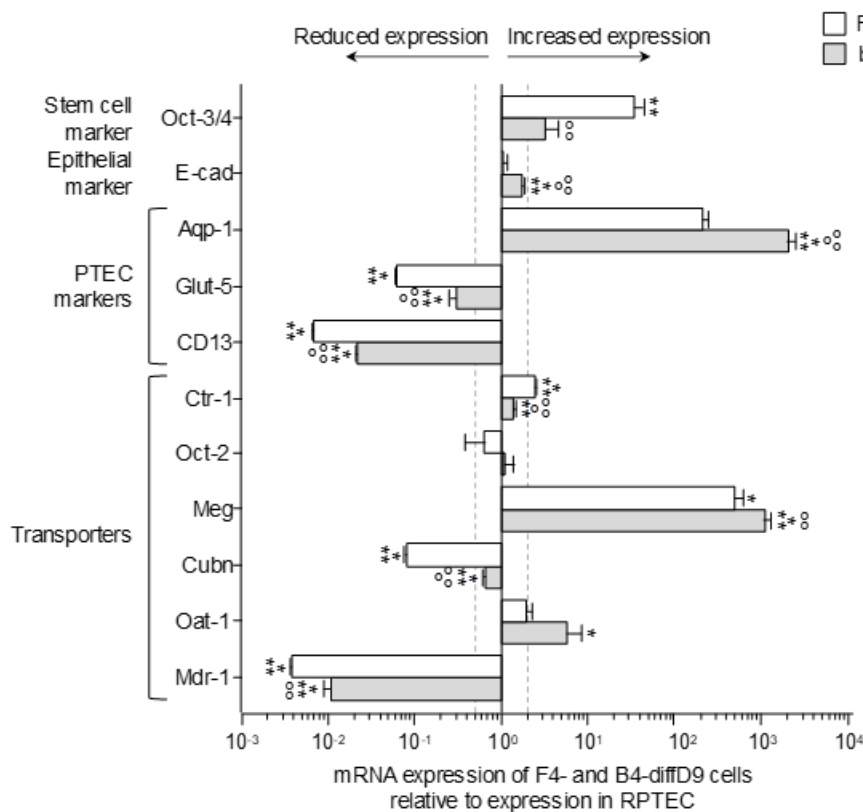


Figure 13: Expression changes of selected genes in F4-hiPSC differentiated into proximal tubular epithelial cell (PTEC)-like cells compared to the expression in a commercial renal proximal tubule epithelial kidney cell line (RPTEC/TERT1). mRNA expression of a stem cell marker, an epithelial marker, several PTEC markers, and transporters relative to expression in RPTEC/TERT1 were analyzed by quantitative RT-PCR. Data from at least 3 independent experiments (qPCR also included 3 technical replicates) are shown as mean \pm SD. * $p < 0.05$, ** $p < 0.01$ and *** $p < 0.001$ vs. RPTEC/TERT1 (ANOVA). BSA = bovine serum albumin, DAPI = 4',6-diamidino-2-phenylindole, diffD9 = differentiation day 9, FITC = fluorescein isothiocyanate, hiPSC = human induced pluripotent cell. Aqp-1 = aquaporin-1, CD13 = alanyl aminopeptidase, Ctr-1 = copper transporter 1, Cubn = cubilin, diffD9 = differentiation day 9, E-cad = E-cadherin, Glut-5 = fructose transporter 5, hiPSC = human induced pluripotent cell, Meg = megalin, Oct-3/4 = octamer-binding transcription factor 3/4, P-gp = P-glycoprotein, RPTEC = renal proximal tubule epithelial cells.

2.1.3.4. Sensitivity of hiPSC, hiPSC differentiating into PTELC, and hiPSC differentiated into PTELC towards a genotoxic nephrotoxin and a non-genotoxic nephrotoxin

F4-hiPSC, F4-hiPSC in the process of differentiating into PTELC on differentiation day three, and F4-hiPSC after nine days of differentiation were treated with two different nephrotoxins. **Fig. 14A** shows the response of the cells to the genotoxic

nephrotoxin cisplatin. The highly proliferating F4-hiPSC and differentiating F4-hiPSC showed the same sensitivity towards cisplatin, with an IC_{50} of around 1 μ M. F4-diffD9 cells were not as sensitive, with an almost twenty times higher IC_{50} of 18 μ M. Regarding the non-genotoxic CsA, cells of all three differentiation states showed the same sensitivity with IC_{50} values around 10 μ M (**Fig. 14B**).

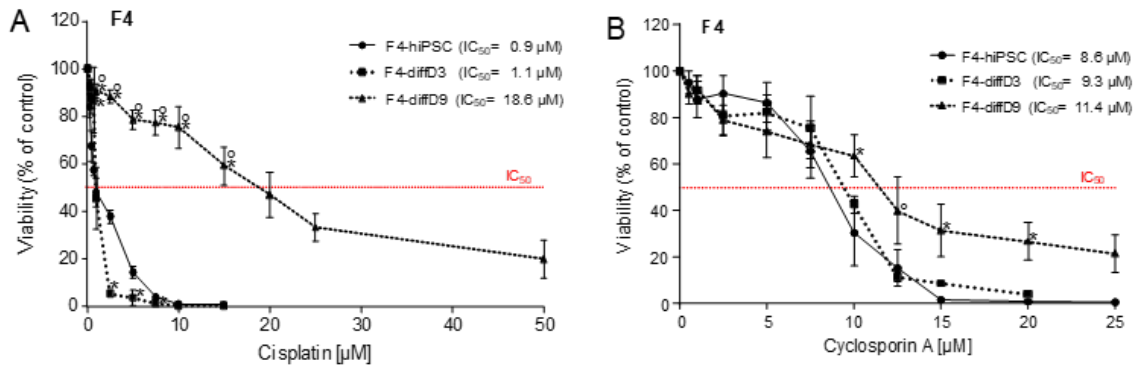


Figure 14: Sensitivities of hiPSCs and cells on differentiation days 3 and 9 to selected nephrotoxins. Cell viability was measured with the Alamar Blue assay on cells of differentiation days 0 (F4-hiPSC), 3 (diffD3) and, 9 (diffD9) after 24 h treatment with (A) cisplatin, (B) CsA, in the indicated concentrations. The concentrations at which 50 % of the cells were dead are given as IC_{50} values in the graphs. Data from at least 3 independent experiments are shown as mean \pm SD. * $p \leq 0.05$ vs. F4-hiPSC, $^{\circ}p \leq 0.05$ vs. diffD3 (One-way ANOVA). CsA = cyclosporin A.

2.1.3.4. Impact of toxin treatment on marker expression and transporter function

For further studies on the influence of toxins on the function of differentiated cells, we focused on F4 cells. Treatment of the diffD9 cells with the IC_{20} and IC_{50} of cisplatin resulted in a significant decrease in the expression of almost all tested genes except *CTR-2*, as well as *megalyn* and *GLUT-5* at IC_{20} (**Fig. 15A**). *CAD-16* was the only gene to show a significant increase after treatment with the IC_{50} . A dose-dependent response was also observed for almost all genes. The reduced expression of the PTEC marker AQP-1 could also be observed at the protein level, but no dose dependency was found here. IC_{20} lowered AQP-1 expression by 50 %, just like IC_{50} (**Fig. 15B**). Furthermore, a significant dose-dependent decrease in albumin transport was detected, possibly caused by a reduction in the expression of the responsible transporter components, megalin and cubilin (**Fig. 15C**). The IC_{20} and IC_{50} of CsA did not have as pronounced an effect on the expression of the selected genes as cisplatin did. Although the expression of some genes was significantly decreased or increased, only *ZO-1*, *CD13*, *CTR-1*, and *cubilin* approached or exceeded the 0.5- or 2-fold change in mRNA levels set as biologically relevant (**Fig. 15D**). IC_{50} caused higher changes in expression than

IC₂₀. Identical to cisplatin, a dose-independent reduction in the protein expression of the specific marker of proximal tubular cells, AQP-1, was observed after CsA treatment (Fig. 15E). This was reduced to 50 % by cisplatin, although mRNA levels had decreased less. Even more pronounced than after cisplatin treatment, albumin transport was decreased by CsA (Fig. 15F). The only slightly reduced expression of *megalyn* and *cubilin* after CsA treatment may not have been the only relevant factor for this effect.

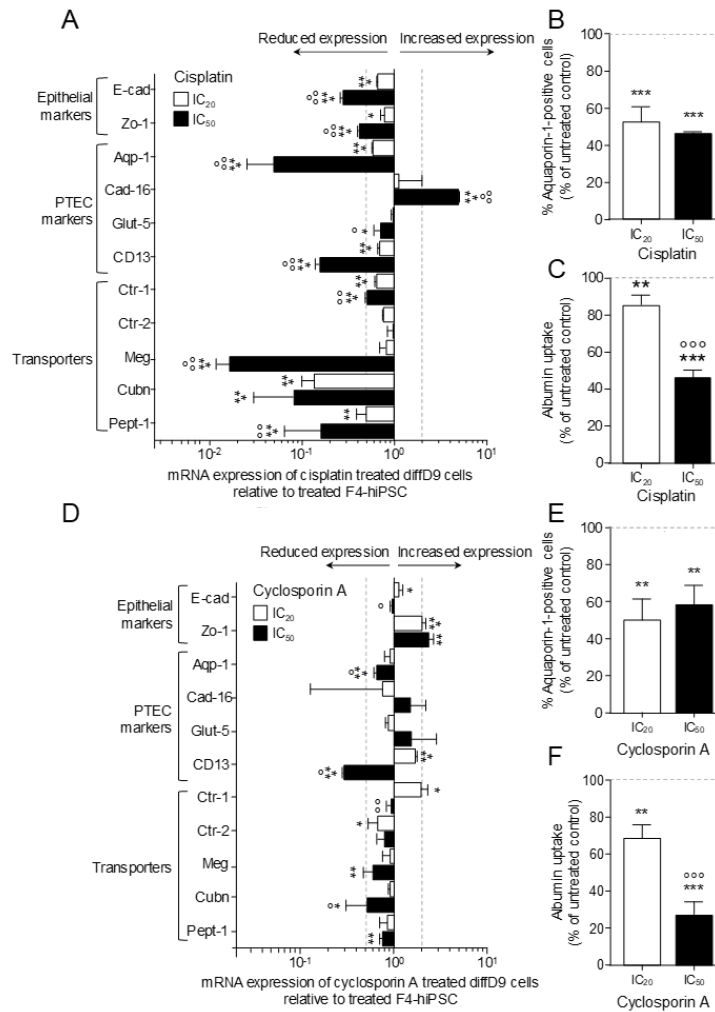


Figure 15: Effects of cisplatin and cyclosporin A on marker gene expression and transport function in F4-hiPSC differentiated into PTELCs. mRNA expression of marker genes in diffD9 F4 cells after 24 h treatment with the IC₂₀ and IC₅₀ concentrations of cisplatin (A) and cyclosporin A (D) relative to their expression in F4-hiPSC analyzed by quantitative RT-PCR. Flow cytometry analysis of the PTEC typical protein aquaporin-1 in diffD9 F4 cells treated 24 h with the IC₂₀ and IC₅₀ concentrations of cisplatin (B) and cyclosporin A (E). Flow cytometric analysis of albumin uptake into diffD9 F4 cells after 24 h treatment with the IC₂₀ and IC₅₀ concentrations of cisplatin (C) and cyclosporin A (F) with the help of FITC-labelled albumin. Data from at least 3 independent experiments (qPCR included 3 technical replicates) are shown as mean + SD. *p≤0.05, **p<0.01 and ***p<0.001 vs. treated F4-hiPSCs, °°°p<0.001 vs. diffD9 cells treated with IC₂₀ (ANOVA). Aqp-1 = aquaporin-1, Cad-16 = cadherin 16, CD13 = alanyl aminopeptidase, Ctr-1/2 = copper transporter 1/2, Cubn = cubilin, diffD9 = differentiation day 9, E-cad = E-cadherin, Glut-5 = fructose transporter 5, hiPSC = human induced pluripotent cell, Meg = megalin, Pept-1 = peptide transporter 1, Zo-1 = zonula occludens 1.

2.1.4. Discussion

For the first time, hiPSC, hiPSC differentiating into PTELCs, and hiPSC differentiated into PTELCs were studied for their sensitivity to selected nephrotoxins. These included the genotoxic nephrotoxin cisplatin and the non-genotoxic nephrotoxin cyclosporin A. The cells at different stages of differentiation showed different sensitivity to the nephrotoxic agents tested, which may be explained in part by the nature of the agents. The differentiation of the F4-hiPSC using the protocol published by Kandasamy et al. [22] changed the morphology of the cells to a renal cell-like morphology, which allowed conclusions about the functional competence of the cells, as they formed tubular-like structures and domes. Dome or hemicyst formation occurs by polarized epithelial cells under culture conditions performing trans-epithelial fluid transport [193]. In agreement with Kandasamy et al. [22], most of the markers analysed in F4hiPSC, such as the pluripotent markers *OCT3/4*, *NANOG*, and *SOX2*, the epithelial markers *E-cadherin* and *ZO-1*, the PTEC markers *CAD-16* and *AQP-1*, and five out of nine transporters, showed a comparable change in the levels of mRNA expression. The post-differentiation expression levels are also consistent with the data of overlapping markers of PTELCs differentiated from hiPSC by another research group using an utterly different differentiation protocol [23]. Consistent with the mRNA data, OCT-3/4 levels were also reduced at the protein level after differentiation, as demonstrated by immunocytochemistry, as also shown by Chandrasekaran et al. [23]. At the same time, the expression of epithelial and PTEC markers increased with the correct cellular localization, except CD-13, which is consistent with the corresponding markers studied by the other two groups [22, 23]. Moreover, more than 95 % of F4hiPSC-derived cells were positive for the PTEC marker, aquaporin-1, after differentiation, as determined by flow cytometry, suggesting that the differentiation process was quite efficient, which was also observed by Kandasamy et al. [22]. However, an important aspect that must be considered when differentiating cells from hiPSC and analysing expression differences is that RT-qPCR cannot determine an absolute number of genes but only a relative number. This means that the expression of the differentiated cells is related to the expression of the undifferentiated hiPSC. Nevertheless, it is not known how much of the examined mRNA the hiPSC has already expressed under basal conditions. To reach the pluripotent state during hiPSC reprogramming, fibroblasts undergo a mesenchymal-to-epithelial transition, losing mesenchymal markers and gaining epithelial ones [194]. They also form adherens junctions, tight junctions, and polarity [195, 196]. This could explain the minor changes in epithelial

markers observed in the gene expression analyses, which were inconsistent with the corresponding protein expression analyses. In addition to gene and protein expression patterns similar to those of PTEC, PTELCs also expressed essential tubular transporters such as megalin and cubilin, which are responsible for the uptake of albumin, an important function of the proximal tubule and were more highly expressed after differentiation than in undifferentiated hiPSC. The incorporation of albumin further demonstrates the functionality of our differentiated PTELCs, similar to that of LLC-PK1, which served as a positive control. RPTEC/TERT1, on the other hand, had reduced albumin uptake activity. The lack of functional albumin uptake in RPTEC/TERT1 cells has already been reported [23, 194]. Some of the other studied transporters, such as *OCT-2*, *MDR-1*, and *SGLT-2*, decreased their mRNA expression levels compared to the hiPSC. For *OCT-2*, one of the transporters responsible for cisplatin uptake [197, 198], we could show no significant difference at the protein level in F4-hiPSC, in contrast to the result of reduced mRNA expression. As cell epithelialization seems crucial to gain pluripotent characteristics [195], it can be expected that further genes characteristic for epithelial cells besides the common epithelial markers currently tested are already basally expressed by the hiPSC, for example, transporters. Reports indicate that pluripotent stem cells already express, e.g., the glucose transporter *SGLT-2* [199, 200], which appears strongly downregulated in our differentiated cells compared to the hiPSC. When investigating the sensitivity of cells at different stages of differentiation to cisplatin, it was found that the defence system of the cells against cisplatin must have changed considerably with the differentiation process, as the undifferentiated hiPSC were the most sensitive, followed by the differentiating cells, while the fully differentiated cells were the least sensitive. This was expected because, as a DNA-damaging agent, cisplatin interferes with cell division, and the proliferation rate of the differentiated cells was much lower than that of the not-yet-differentiated cells. Surprisingly, the differentiating cells were as sensitive as the F4-hiPSC, even though the former already exhibited greatly reduced proliferation. Future experiments are needed to reveal whether this comparable sensitivity in the presence of reduced proliferation may be due to the differentiating cells being more vulnerable to the cytotoxic effects of cisplatin. These include mitochondrial damage, direct activation of apoptosis via the TNF family, and triggering of stress at the endoplasmic reticulum (as summarized by [195]). A few studies have examined the dose response to cisplatin in stem cells and differentiated cells. The IC_{50} values of our F4-hiPSC were in the range of other stem cells, and hiPSC and hESC were equally sensitive [196, 197].

A two- to three-fold increase in sensitivity, as we saw with the F4-hiPSC, has already been observed by others [196]. Stem cells derived from amniotic fluid alone were less sensitive [198]. Cells differentiated from stem cells lose viability only at 10- to 100-fold higher cisplatin concentrations [199, 200], as did ours. Even far less sensitive to cisplatin are renal organoids generated from stem cells or differentiated PTELC growing on beads [180, 201]. We are aware of only one study that determined the sensitivity of the differentiated cells as well as the sensitivity of the original hiPSC cells, as we did. Here, the IC₅₀ of the hiPSC was in the same range as in our hiPSC, whereas the neurons differentiated from them were so resistant that no IC₅₀ could be determined [196]. To date, no study has measured the sensitivities of cells in the process of differentiation. With respect to CsA, the cellular defence system against this substance did not appear to have changed significantly with differentiation, as the cells showed concordant sensitivities, suggesting a more general cytotoxic mechanism of CsA. Effects of CsA have not been studied in detail in stem cells. Therefore, IC₅₀ values for CsA from stem cells or differentiating cells are not available in the literature so far. Most evidence of CsA in association with stem cells is related to the improved survival of transplanted hiPSC-derived neural precursor cells due to administered CsA (i.e., reviewed by Antonios et al. [202]). Only hiPSC differentiated into brain-like endothelial cells were investigated regarding their sensitivity to CsA and showed an IC₅₀ value of more than 15 µM after 7-day incubation [203], which is not comparable to the value of our differentiated cells, which already exhibit a lower IC₅₀ after 24 h. In monocytes, on the other hand, an IC₅₀ value was determined at approximately 5 µM after 72 h [204]. In relation to non-stem cells, the literature on CsA contains very contradictory information. On the one hand, CsA induces apoptosis, leading to mitochondrial damage and EMT at concentrations between 1 and 5 µM [204-206]. On the other hand, it protects against apoptosis and EMT induced by other substances at similar concentrations [207, 208]. Future studies will reveal which of the acute effects is causing the observed cytotoxicity in our model. Cisplatin and CsA treatments not only reduced the viability of the cells tested here but also impaired the function of the fully differentiated cells and the expression of markers linked with differentiation. Thus, cisplatin, in particular, induced decreased mRNA expression of a number of transport proteins and reduced albumin uptake. It is known that cisplatin binds to megalin, preventing it from absorbing its ligands, which include albumin [209]. This could explain the reduced albumin uptake we saw after cisplatin treatment. Other nephrotoxins, such as aristolochic acid, are also known to reduce the expression of megalin [210]. To

our knowledge, this has not yet been reported for cisplatin. However, the mechanism exerted by these toxins seems to be via the upregulation of TNF α [210], which is also increased by cisplatin [211]. On the other hand, aquaporins have been documented to be reduced in expression by cisplatin exposure, which we also observed, but the mechanism is not yet known for aquaporin-1 [212, 213]. CsA is also known to inhibit various transporters, including Mdr-1, peptide transporter-1 (Pept-1), organic anion transporters, and sodium transporters [214-216]. However, no change in the expression of these transporter molecules could be detected [216, 217]. Other transporters, such as sodium transporters, are downregulated by CsA treatment *in vivo*, but this is most likely related to a change in blood pressure [218]. Regarding the impact of CsA on the gene expression of other transporters, only indirect hints could be found; for example, in rats with kidney transplants, the expression of several transporters (among them, glucose transporter 3, sodium-dependent phosphate cotransporter and nucleoside transporter 2) was lower in the animals receiving CsA compared to the non-treated animals [219]. No evidence of CsA reducing the expression of megalin could be found. Because the reduction in mRNA of *megalyn* and *cubulin* was higher in cisplatin-treated cells than in CsA-treated cells, but albumin uptake was more impaired in the latter, the loss of expression cannot be the only cause of reduced albumin uptake.

Overall, the differentiation protocol adapted from Kandasamy et al. [22] resulted in cells that resemble proximal tubule cells not only morphologically but also in their mRNA and protein expression pattern. Of course, only part of the transcriptome was verified, but important PTEC markers could be found in the differentiated cells. Functional albumin transport was also detected. The sensitivity of the cells to cisplatin changed dramatically during differentiation, which was only partly due to the decrease in proliferation rate. In contrast, all cell stages were equally sensitive to CsA. In addition, treatment with the two toxins had an adverse effect on differentiation marker expression. Surprisingly, the expression levels of the quantified transporter genes were clearly reduced by the toxins, which severely impaired the functional albumin uptake of the differentiated cells. On the other hand, it can also be assumed that the transport capacity of the kidney will be affected by the substances *in vivo*. An effect of CsA on the expression of various ion channels was recently demonstrated in rats and kidney transplant patients [220]. Our results lay the foundation for investigating changes in transport function in newly formed cells after regeneration.

The data shown here constitute the first step towards a model that might be useful in the future to investigate the influence of toxins on regeneration processes in the kidney. Cells in the differentiation process are at least as sensitive, if not more sensitive, to the known nephrotoxins used here as model substances than the finally differentiated cells. This suggests a possible vulnerability of the newly forming cells in injured tubules, which may play a role in the observed loss of kidney function after AKI. This vulnerability has yet to be confirmed *in vivo*, as well as for other substances that may be present in the kidney during AKI.

3. Unpublished data

3.1. Increased DNA damage response and decreased expression of genes associated with the maintenance of genome integrity during differentiation

Our first published results showed that differentiating hiPSC were as sensitive to the genotoxic nephrotoxin cisplatin as undifferentiated hiPSC, although the former already exhibited significantly reduced proliferation [221]. Therefore, we hypothesised that this comparable sensitivity with reduced proliferation could be due to differentiating cells being more sensitive to the cytotoxic effects of cisplatin, such as DNA damage and activation of apoptosis [34, 47]. Therefore, to investigate this experimentally, we analysed the ability of cisplatin to induce DNA damage in cells at different stages of differentiation by examining the formation of DNA damage foci with phosphorylated histone H2AX (γ -H2AX), a known robust and sensitive biomarker for DNA damage quantification [222, 223]. Interestingly, we observed that although cisplatin and ionising radiation (as a positive control) also induced DNA damage in hiPSCs and differentiated PTELCs, as indicated by the high frequency of nuclei with foci, the frequency of γ -H2AX-positive cells increased significantly in the differentiating cells (**Fig. 16A**), suggesting that differentiating cells were more susceptible to the DNA-damaging effect of cisplatin. Therefore, this finding prompted us to analyse the ability of cells to repair DNA at the different stages of differentiation. In this study, however, we did not measure DNA repair per se. Instead, we first analysed the basal mRNA expression levels of a subset of genes linked with different DNA repair pathways, which gives an indication of deficient repair. We found that mRNA levels of most genes representing the different repair pathways were downregulated in differentiating cells compared to hiPSCs and differentiated PTELCs (**Fig. 16B**). More specifically, we observed that most of the repair genes involved in cisplatin-induced DNA damage repair, including the formation of DNA-cisplatin mono adducts (base excision repair), DNA-cisplatin intrastrand adducts (nucleotide excision repair), and DNA-cisplatin interstrand adducts (homologous recombination repair) [224-226] were downregulated in differentiating cells compared to hiPSCs and differentiated PTELCs (**Fig. 16B**), indirectly indicating a general decrease in DNA repair capacity during differentiation.

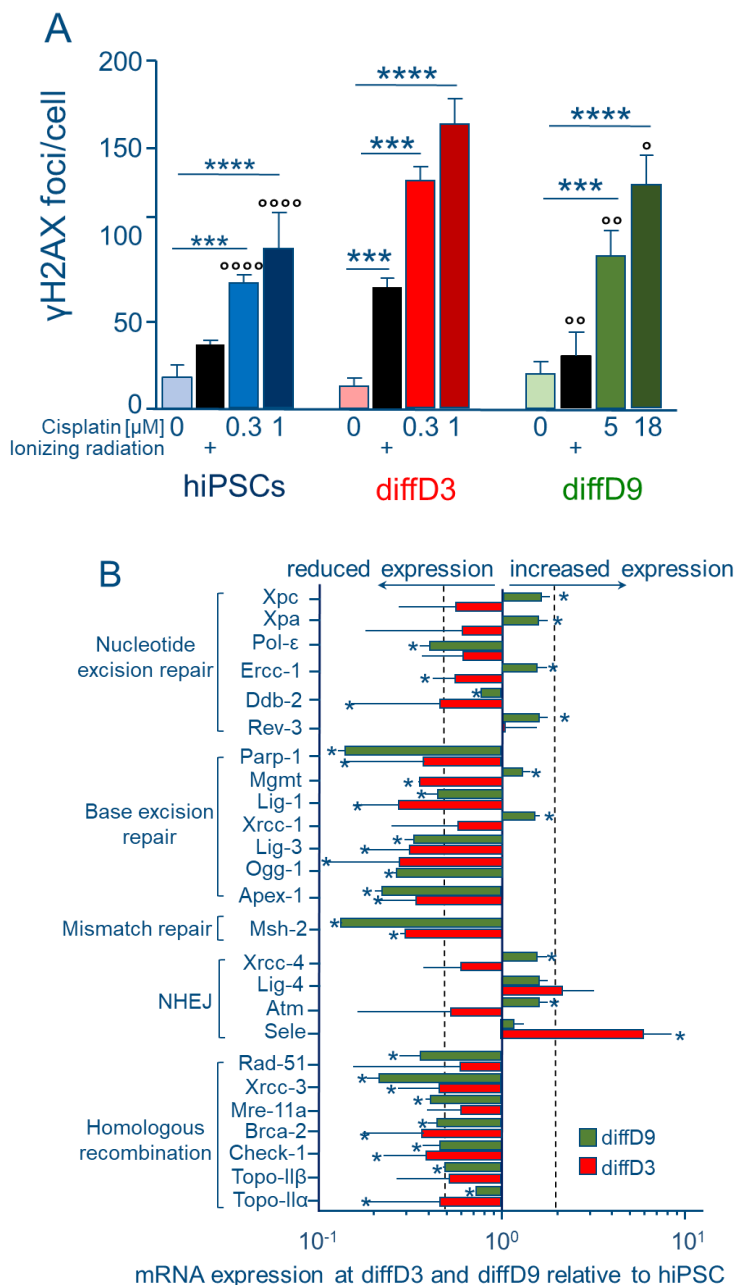


Figure 16: Changes in expression of genes of DNA repair proteins and DNA damage in PTELC differentiated from F4-hiPSC. (A) Antibody detection of DNA double-strand breaks (via the surrogate marker γ H2AX) in hiPSC, differentiating and differentiated PTELC after treatment with cisplatin and ionizing radiation. (B) mRNA expression in differentiating (diffD3) and differentiated (diffD9) F4-hiPSC relative to expression in undifferentiated hiPSC analyzed by quantitative RT-PCR. Data from at least 3 independent experiments (qPCR also included 3 technical replicates) are shown as mean \pm SD. One-way ANOVA (A) and Student's t-test (B): * $p \leq 0.05$, ** $p < 0.01$ and *** $p < 0.001$ vs. respective controls, and $^{\circ}p \leq 0.05$, $^{\circ\circ}p < 0.01$ and $^{\circ\circ\circ}p \leq 0.0001$ compared to diffD3 treated cells (One-way ANOVA). Apex = Apurinic/aprimidinic endonuclease 1, Atm = Ataxia telangiectasia mutated homolog, Brca 2 = Breast cancer 2, Check 1 = checkpoint kinase 1, Ddb 2 = Damage specific DNA binding protein 2, Ercc 1 = Excision repair cross-complementing rodent repair deficiency, Lig 1,3,4 = Ligase I, III, IV, Mgmt = O-6-methylguanine-DNA methyltransferase, Mre 11a = Meiotic recombination 11 homolog A, Msh 2 = MutS homolog 2, Ogg 1 = 8-oxoguanine DNA-glycosylase 1, Parp 1 = Poly (ADP-ribose) polymerase 1, Rad51 = RAD51 homolog, Rev 3 = REV3-like, catalytic subunit of DNA polymerase zeta RAD54 like, Sele = Selectin, Topo II α Topoisomerase II alpha, beta, Xpa = Xeroderma pigmentosum, complementation group A, Xpc = Xeroderma pigmentosum, complementation group C, Xrcc 1, 3, 4 = X-ray repair complementing defective repair in Chinese hamster 1, 3, 4, Pol ϵ = Polymerase epsilon.

3.2. Impact of nephrotoxins and oxidants on survival and function of renal proximal tubular epithelial cells differentiated out of hiPSC

3.2.1. Introduction

As the primary route for the excretion of drugs and other chemicals from the body, the kidneys play an integral role in preserving homeostasis. This crucial function, however, also makes renal cells highly susceptible to damage triggered by xenobiotics and their toxic metabolites [3, 5]. In particular, the epithelial cells lining the proximal convoluted tubule are most affected by these toxic urinary substances due to their role in glomerular filtrate concentration and transport and metabolism of these toxic compounds that can lead to acute kidney injury (AKI). Therefore, proximal tubular epithelial cells (PTEC) have become the focus of extensive research in renal toxicity assessment and regenerative medicine [20, 227].

To ensure the organ's functionality, cells must be replaced constantly, even without a specific injury, due to ageing cells. These regenerative properties reach an even higher level in the presence of nephrotoxicity or damage to the kidney compared to essential cell turnover [93, 228]. Tubular regeneration is done either by a local stem cell population or by the dedifferentiation of surviving PTEC after acquiring an epithelial-mesenchymal phenotype. Either one or an interplay of both regenerative pathways maintains the organ's functionality and structure [94, 99]. However, while remarkable, the regenerative capacity of PTEC in the kidney is often fraught with challenges. The processes are often inefficient, impaired and dysregulated, resulting in some replaced cells not regaining full functionality after injury [127, 229, 230]. In addition, 50 % to 70 % of AKI patients have impaired kidney function even after recovery, increasing their chances of developing chronic kidney disease (CKD) and end-stage renal disease (ESRD). This suggests that the damaged cells are not replaced by fully functional cells or that their functionality may have been compromised during the regeneration process [30, 31, 183, 184, 230].

Since ineffective regeneration is linked to the progression of AKI to CKD and ESRD, it is essential to understand the causes of this reduced functionality of tubular epithelial cells after regeneration. One common cause of impaired renal function observed in clinical practice is drug-induced nephrotoxicity. Drugs in clinical use often trigger off-target effects on PTEC, which have been implicated in 19-25 % of AKI in critically ill patients [231]. In addition to the non-target effects of drugs on PTEC, oxidative stress (OS) has also been shown to be a common and significant pathobiological factor in PTEC injury [72]. OS refers to an increase in

intracellular reactive oxygen species (ROS) levels emanating from an imbalance between the cellular generation of ROS and the ability of cells to scavenge them [232]. While ROS play an integral role in intracellular signalling and cell homeostasis, excessive ROS causes OS. It has been documented to drive mitochondrial dysfunction characterized by mitochondrial swelling and loss of mitochondrial membrane potential, ultimately leading to cell death [73]. PTECs are a significant source of ROS in the kidney due to the high mitochondrial density, which is needed for their enormous energy requirements to maintain secretory and reabsorptive functions [72]. Consequently, PTECs are highly vulnerable to ROS-induced damage leading to AKI [233]. Given the role of nephrotoxic drugs and OS in PTEC injury, it is reasonable to expect these stressors to compromise the integrity and functionality of newly replaced PTECs during regeneration, leading to maladaptive repair. Therefore, conducting meaningful risk assessments that explore the impact of nephrotoxins and OS on renal regeneration is necessary beyond merely predicting the nephrotoxicity of matured PTEC.

A promising and exciting strategy to investigate the role of drugs and OS in renal regeneration is the use of human induced pluripotent stem cell (hiPSC)-based models [185]. hiPSCs, primarily derived from reprogrammed human somatic cells such as skin fibroblasts, represent an increasingly viable alternative to animal models. They have been shown to be an ethically safe, powerful and reproducible source of various human tissues for disease modelling and regeneration [159]. Their ability to extensively self-renew and differentiate into different cell lineages characterises them and opens up the possibility of studying the mechanisms of regeneration and how toxic substances can affect the regenerative processes in the body [234].

As proof of principle for the use of hiPSCs to model renal regeneration, using a protocol previously reported by Kandasamy et al. [22], we recently showed a hiPSC-based *in vitro* model that allows toxicity assessment during PTEC generation from hiPSCs [221]. The results showed that hiPSC differentiation resulted in cells that resembled PTECs not only morphologically but also in their mRNA and protein expression patterns and functionality. When treating the cells in the different differentiation stages with known nephrotoxins, we also observed that the cells in the differentiation process reacted more sensitively to the toxins than the fully differentiated cells. This increased sensitivity could have an unfavourable effect on the regeneration processes [221]. Here, we not only characterised the different molecular mechanisms that contribute to the sensitivity of preferentially

differentiating cells to nephrotoxins but also investigated the effects of other stressors, such as OS-inducing substances which may be present in the kidney during AKI. These stressors could affect the susceptibility of cells at different stages of differentiation, as OS is also a recognised trigger for PTEC damage [232].

3.2.2. Materials and Methods

3.2.2.1. Materials

The human induced pluripotent stem cell line Foreskin-4 (F4 WB66699) (from now on referred to as hiPSCs) was purchased from WiCell Stem Cell Bank (Madison, USA) at passage 27 and used until passage 47. Human embryonic stem cell qualified Matrigel and Reduced Growth Factor Basement Membrane Matrix were from Corning (New York, USA). mTeSR1 medium was from StemCell Technologies (Vancouver, Canada), while renal epithelial growth medium (REGM) containing various growth factors and supplements (REGM BulletKit) was from Lonza (Basel, Switzerland). Y-27632 dihydrochloride and BMP-2 were from Sigma-Aldrich (St. Louis, USA), and BMP-7 was supplied by Thermo Fisher Scientific (Waltham, USA). All chemicals were purchased from Sigma-Aldrich (St. Louis, USA), Enzo Life Sciences (Farmingdale, NY, USA), and Teva (Petach Tikva, Israel). The primers were purchased from Eurofins Genomics (Val Fleuri, Luxembourg), while antibodies were purchased from Abcam (Cambridge, UK) and BD Bioscience (Heidelberg, Germany), and the fluorophore-conjugated secondary antibody Alexa Fluor 488 was purchased from Life Technologies (Carlsbad, California, USA). The primers and antibodies used to detect the expression of various genes and proteins are listed in Tables 1 and 2 in the Appendix.

3.2.2.2. Methods

3.2.2.2.1. Cultivation of F4-hiPSC and formation of proximal tubular epithelial cells

The hiPSC line F4-hiPSC, derived from human foreskin fibroblasts by lentiviral transfection of OCT3/4, SOX2, NANOG, and LIN28 [235], was cultured on 6-well plates plated with human embryonic stem cell-qualified Matrigel in serum-free, defined mTeSR1 medium supplemented with 10 mM Y-27632 dihydrochloride. The authentication was done before purchasing and after the completion of experimentations. In addition to this, the cells were regularly checked for Mycoplasma, Bacterial, and Fungi. Cells were maintained following the recommendations from WiCell, which include but not limited to thawing one vial into three wells of a six-well plate and culturing in a humidified 5 % CO₂ atmosphere at 37 °C and passaged twice weekly at a 1:6 ratio when cultures reached 70-90 % confluence to maintain them in exponential growth. A modified protocol, according to Kandasamy and colleagues [22], was used for differentiation into renal proximal

tubular epithelial-like cells (PTELCs), as previously reported by Mboni-Johnston et al. [221] (**Fig.17A**). In brief, 3000 hiPSC/cm² were seeded in renal epithelial growth medium (REGM) supplemented with Y-27632 dihydrochloride and specific growth factors (BMPs 2/7) were added from day 2 onwards and cultured under these conditions for 9 days, changing the medium daily to induce differentiation to PTELC. hiPSC-derived PTELCs were treated directly with toxins or harvested on day 9 for further analysis.

3.2.2.2.2. Cytotoxicity assay

Undifferentiated hiPSCs, hiPSCs differentiating into PTELCs, and hiPSCs differentiated into PTELCs were treated with different concentrations of the genotoxic nephrotoxin cisplatin and the non-genotoxic nephrotoxin cyclosporin A as well as the oxidizing agents hydrogen peroxide (H₂O₂), menadione, and tert-butylhydroquinone (TBHQ). Following 24 h of exposure, the viability of the undifferentiated, differentiating, and differentiated cells was examined using the Alamar Blue Assay [192], which measures the reduction of blue and non-fluorescent resazurin dye (Sigma, Steinheim, Germany) into pink and fluorescent resorufin by cell activity. Fluorescence intensity was measured in quadruplicate (excitation: 535 nm, emission: 590 nm (Tecan infinite 200, Tecan, Männedorf, Switzerland)). The relative viability of the cells in the corresponding untreated controls was set to 100 %.

3.2.2.2.3. RT-qPCR

RNA was isolated from hiPSCs, hiPSCs differentiating into PTELCs, and hiPSCs differentiated into PTELCs treated with and without the different toxins using the RNeasy Mini Kit and RNase-free DNase Set (Qiagen, Venlo, The Netherlands) according to the manufacturer's protocol. In brief, cells were lysed in 350 µl of RLT buffer. The supernatant was first mixed with an equal volume of 70 % ethanol and centrifuged through a gDNA eliminator column. After several washing steps, the RNA was eluted in 25 µl RNase-free water. After quantification with the NanoVue Plus spectrophotometer (GE Healthcare Life Sciences, Buckinghamshire, UK), a total of 500-2000 ng of RNA was used as input for cDNA synthesis using the High-Capacity RNA-to-cDNA Reverse Transcription Kit in combination with the RiboLock Rnase Inhibitor (Thermo Fisher Scientific, Waltham, CA, USA), and qRT-PCR based on the SensiMix SYBR Hi-ROX (C) kit (Bioline GmbH, Luckenwalde, Germany) was performed using a CFX96 Touch Real-Time PCR Detection System (Bio-Rad Laboratories, Hercules, CA, USA).

3.2.2.2.4. Analysis of gene expression data

The primer sequences used for the mRNA expression analyses were designed with the help of NCBI and tested and validated for specificity in a qPCR with different cDNA concentrations. At the end of the run, data were analyzed using CFX Manager software (Bio-Rad Laboratories, Hercules, CA, USA) according to the manufacturer's instructions. All samples were run with three technical replicates. The Cq values obtained for the genes of interest were first normalized to the mean Cq values obtained for the housekeeping genes *ACT-β* and *RPL-32* and then for the control samples and expressed as a fold of this mean value. Changes in ≤ 0.5 - and ≥ 2 -fold gene expression were considered biologically relevant.

3.2.2.2.5. Immunofluorescence analysis

To analyze the expression of markers of epithelial-mesenchymal transition (EMT) and the induction of 4-hydroxynonenal, a lipid peroxidation marker, cells coated on coverslips were fixed with 4 % cold formaldehyde (15 min, RT) and incubated in 0.5 % Triton/PBS to permeabilize the cells. After blocking non-specific binding sites with 5 % BSA/PBS for 1 h at RT, incubation with primary antibodies in the dilution indicated in Table S2 was performed at 4 °C overnight in a humid chamber. After thoroughly washing the primary antibodies, a 2-hour incubation with secondary antibodies was performed. Cell nuclei were stained with Vectashield containing DAPI (4',6-diamidino-2-phenylindole, Vector Laboratories, Burlingame, CA, USA). Cells were analyzed with a fluorescence microscope (BX43F Upright Microscope, Olympus, Shinjuku, Tokyo, Japan).

3.2.2.2.6. TUNEL assay

To verify whether the nephrotoxins cisplatin and cyclosporin A and the oxidants menadione and TBHQ induced apoptosis in the cells at different stages of differentiation, the TUNEL assay was performed using the In Situ Cell Death Detection Assay Kit (Roche, GmbH, Germany). The TUNEL (terminal deoxynucleotidyl transferase-mediated dUTP-fluorescein nick-end labeling) assay can detect cells undergoing apoptosis. In principle, the cell's DNA is fragmented during apoptosis, resulting in free hydroxyl groups within the DNA strand breaks. These free hydroxyl groups can be visualized by labeling with modified nucleotides through an enzymatic reaction [236]. Therefore, this assay kit contains the enzyme

TdT, which catalyzes the modified nucleotide fluorescein deoxyuridine triphosphate (dUTP) polymerization to the free hydroxyl groups. The modified nucleotide can be visualized under the microscope. For this purpose, coverslip-coated cells at different stages of differentiation with or without drug exposure were washed with PBS and fixed with 3.7 % PFA for 15 min at RT. Following three washes with PBS, cells were incubated with 0.5 % Triton-X/PBS for 10 min at RT and then blocked with 3 % BSA/PBS for 1 h at RT. After washing with PBS, one coverslip of- each cell type was incubated with 150 U/ml DNase for 10 min at RT as a positive control. Subsequently, all coverslips were treated with labelling solution (5 µl enzyme solution + 45 µl labelling solution per coverslip) for one hour in the dark at 37 °C, and apoptotic cells were labelled with TdT and fluorescein-dUTP. After another washing step, coverslips were mounted with VECTASHIELD® Antifade Mounting Medium containing DAPI and sealed with nail polish. Fluorescence images were acquired using an Olympus BX43 fluorescence microscope at 200X magnification and analyzed using ImageJ 1.51j8 (<https://imagej.nih.gov/ij/>). TUNEL-positive cells were referenced to the total number of cells and normalized to the untreated control.

3.2.2.2.7. Analysis of cell proliferation

To investigate the effect of toxins on the proliferation rate during the differentiation of hiPSCs into PTECs, the incorporation of EdU into S-phase cells was determined using the EdU-Click 488 assay according to the manufacturer's protocol (Baseclick GmbH, Tutzing, Germany). In brief, cells coated on coverslips were labelled with fluorescent 5-ethynyl-2'-deoxyuridine (EdU) for 2 h at 37 °C. Cells were then fixed with 4 % cold formaldehyde (15 min, RT) and permeabilized with 0.5 % Triton/PBS. After adding Alexa Fluor 488-conjugated dye-reaction cocktail (30 min, RT in the dark) and washing with PBS, the nuclei were counterstained with DAPI. At least 7 to 10 different pictures containing cells were captured with a fluorescence microscope (Olympus BX43) in dual-channel images (DAPI and FITC), and proliferating and non-proliferating cells were assessed with ImageJ 1.51j8 (<https://imagej.nih.gov/ij/>).

3.2.2.2.8. Albumin uptake assay

The effect of toxins on the functionality of hiPSC-derived PTELC was examined by adding fluorescently labelled bovine serum albumin (FITC-BSA) (Sigma Aldrich, 10 mg/ml) to the culture medium. Cells were incubated with serum-free medium with/without 100 µg/ml FITC-albumin for 2 h at 37 °C, and uptake was stopped with ice-cold PBS. Cells were then harvested from Matrigel-coated wells with trypsin/EDTA, and albumin uptake was analyzed by flow cytometry (Becton Dickinson, Accuri™ C6 plus (Heidelberg, Germany)) as previously reported by Mboni-Johnston et al. [221].

3.2.2.2.9. Statistical analysis

Statistical analysis was conducted using GraphPad Prism version 6 (GraphPad Software, San Diego, CA). Data are presented as the mean with a standard deviation of three independent experiments (n = 3). The normal distribution was checked using Kolmogorov-Smirnov tests with Dallal-Wilkinson-Lilie for p-values. The multiple comparisons two-tailed unpaired Student's t-test was performed to compare two-sample groups comprising parametric distributed datasets. For non-normally distributed values, the Mann-Whitney U-test was used. Parametric data, including multiple groups, were tested by one-way analysis of variance (one-way ANOVA) for statistical significance with Tukey's and Dunnett's post hoc test. Non-parametrical datasets of multiple groups were analyzed with Kruskal-Wallis one-way ANOVA on ranks test. Statistically significant differences between the groups were assumed at a p-value <0.05.

3.2.3. Results

An *in vitro* model based on induced pluripotent stem cells (iPSC) was used to investigate the influence of the genotoxic nephrotoxin cisplatin and the non-genotoxic nephrotoxin cyclosporin A as well as the oxidizing agents hydrogen peroxide (H_2O_2), menadione, and TBHQ on the renal tubular differentiation processes. Treatment with the respective compounds was performed on differentiation day 0 (undifferentiated hiPSC), three days after the start of the differentiation process (diffD3) and after the ninth day of differentiation (diffD9). Analyses were performed after 24 h of exposure, as indicated in **Fig. 17A**. In previous work, the sensitivity of the cells at different stages of differentiation to the genotoxic nephrotoxin cisplatin and the non-genotoxic nephrotoxin cyclosporin A has already been investigated and published [221]. Therefore, the respective IC_{20} and IC_{50} values determined in this former study were used in this study to characterize the cellular mechanisms that contribute to the cell's sensitivity to these agents.

3.2.3.1. hiPSC-derived tubular progenitors are particularly sensitive to oxidative stress induced by known oxidizing agents

The *in vitro* differentiation of hiPSCs into PTELCs was performed according to the differentiation protocol shown in **Fig. 17A**, previously published by Mboni-Johnston et al. [221]. This differentiation protocol was used to analyze the sensitivity of undifferentiated hiPSCs, hiPSCs differentiating into PTELCs (diffD3), and fully differentiated PTELCs to different oxidants. For this purpose, the cells were treated with three different oxidants, H_2O_2 , menadione, and TBHQ, for 24 h, and their sensitivity to the respective substances was analyzed using the Alamar Blue assay. **Fig. 17B** shows the response of the cells at different stages of differentiation to the oxidizing agent H_2O_2 . The highest H_2O_2 sensitivity was observed in diffD3 cells ($IC_{50} = 15 \mu M$). Meanwhile, undifferentiated hiPSCs ($IC_{50} = 158 \mu M$) and differentiated PTELCs ($IC_{50} = 594 \mu M$) showed approximately 10- and 40-fold lower sensitivity, respectively, compared to diffD3 cells (**Fig. 17B**), with differentiated PTELCs being the most resistant. Similar to the results obtained with H_2O_2 , hiPSCs differentiating into PTELCs (diffD3) also showed the highest sensitivity to another oxidizing agent, menadione, with an IC_{50} of about $4.1 \mu M$, which is four times lower than that of hiPSCs and terminally differentiated PTELCs (**Fig. 17C**). The sensitivity of hiPSC to menadione ($IC_{50} = 16.2 \mu M$) was like that of

terminally differentiated PTELCs ($IC_{50} = 17.6 \mu\text{M}$). The cells were also exposed to a third oxidizing agent, TBHQ, to further confirm these findings. Interestingly, as shown in **Fig. 17D**, hiPSC differentiating into PTELCs (diffD3) also showed the highest sensitivity to TBHQ with an IC_{50} of approximately $2.8 \mu\text{M}$, which is 7- and 12-fold lower than hiPSC and hiPSC-derived diffD9 cells, respectively. Although hiPSCs were not as sensitive to TBHQ compared to diffD3 cells, they were 2-fold more sensitive ($IC_{50} = 18.5 \mu\text{M}$) to TBHQ in comparison to hiPSC-derived PTELC, which showed the highest resistance to TBHQ ($IC_{50} = 34.5 \mu\text{M}$). Overall, the data suggests that cells at different stages of differentiation with the same genetic background displayed differential sensitivity to known oxidants, with the hiPSC differentiating into PTELC precursors being the most sensitive.

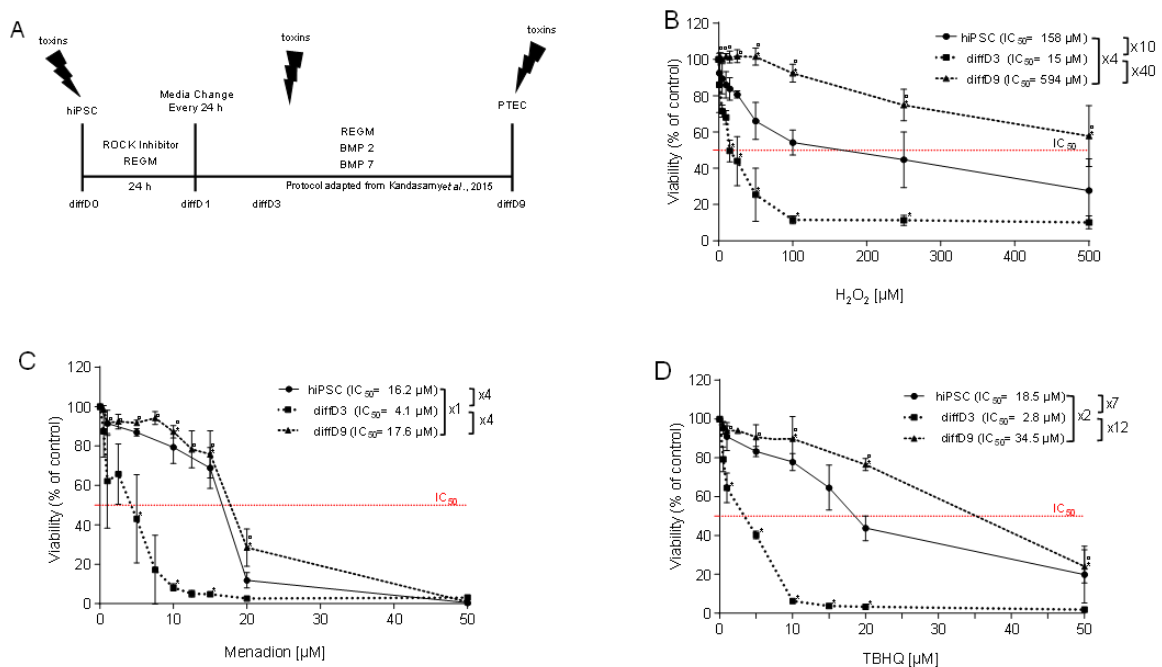


Figure 17: Influence of selected oxidizing agents on the viability of hiPSC and cells at differentiation days 3 and 9. **A:** Schematic representation of the protocol for differentiating hiPSCs into PTELC and for the treatment time points during differentiation. Cell viability was measured on cells at differentiation days 0 (hiPSC), 3 (diffD3), and 9 (diffD9) following 24 hours of treatment with the indicated concentrations of **(B)** hydrogen peroxide, **(D)** tert-butylhydroquinone and **(C)** menadione using the Alamar Blue assay. The concentrations at which 50 % of the cells died are indicated in the diagrams as IC_{50} values. Data from at least 3 independent experiments are given as mean \pm SD. * $p \leq 0.05$ vs. hiPSC, $^{\circ}p \leq 0.05$ vs. diffD3 (one-way ANOVA).

3.2.3.2. Influence of oxidizing agents on gene expression and transport in proximal tubular epithelial-like cells

Our previous study analysed and reported the impact of the nephrotoxins cisplatin and CsA on the gene expression and function of terminally differentiated PTELCs. Treatment with both toxins had a negative effect on the expression of differentiation markers and strongly impaired the functionality of differentiated PTELCs [221]. Therefore, in this current study, we have delved further and analysed the effect of oxidants, starting with menadione and TBHQ, on the function of differentiated PTELCs. Our analysis showed that treatment of PTELCs with menadione selectively affected the mRNA expression of individual PTEC markers and transporters. Notably, treatment with IC_{20} and IC_{50} of menadione resulted in a significant and dose-dependent decrease in the mRNA expression of *AQP-1* and *megalin* (**Fig. 18A**). Significantly reduced expression of *PEPT-2* was also observed after treatment with IC_{50} , but not in a dose-dependent manner. *CD13* and *PEPT-1* were the only genes that increased significantly after treatment with IC_{50} of menadione. In contrast, all other genes (among them *CAD-16*, *cubilin*, *GLUT-5*, *OAT-3*, and *N-CAD*) showed either a decrease or an increase in expression or both, but their mRNA expression levels did not exceed the 0.5- or 2-fold change classified as biologically relevant. Meanwhile, menadione treatment also altered the differentiation-induced decrease in mRNA expression of the pluripotency markers *OCT-3/4* and *NANOG*, but not significantly. Furthermore, since we have previously observed an effect of the nephrotoxins cisplatin and CsA on the albumin uptake capacity of PTELCs [221], we checked the effects of known oxidising agents on the albumin transport capacity of PTELCs. Interestingly, a significant decrease in albumin transport was observed only after treatment with IC_{50} of menadione (**Fig. 18C**). Similarly, treatment with the IC_{20} and IC_{50} of TBHQ also altered the differentiation-related decrease in the mRNA expression of the pluripotency markers *OCT-3/4* and *NANOG*, but not significantly (**Fig. 18B**). Of the PTEC-specific genes analysed, *AQP-1* was the only gene that showed a significant dose-dependent decrease after treatment with IC_{20} and IC_{50} of TBHQ. Interestingly, the mRNA expression levels of genes such as *CAD-16*, *megalin*, and *PEPT-1* increased at least above the 2-fold biologically relevant levels after treatment with the IC_{50} of TBHQ, although only the expression level of *CAD-16* was statistically significant. Surprisingly, in contrast to the menadione treatment, the albumin transport capacity of differentiated PTELCs significantly increased dose-dependently after treatment with TBHQ (**Fig. 18D**), which was unexpected. However, this increase was accompanied by a slight increase in megalin

expression, at least at the IC₅₀. Overall, our data provide valuable insights into the impact of oxidants on PTELCs and highlight the selective effects of different oxidants on gene expression and function.

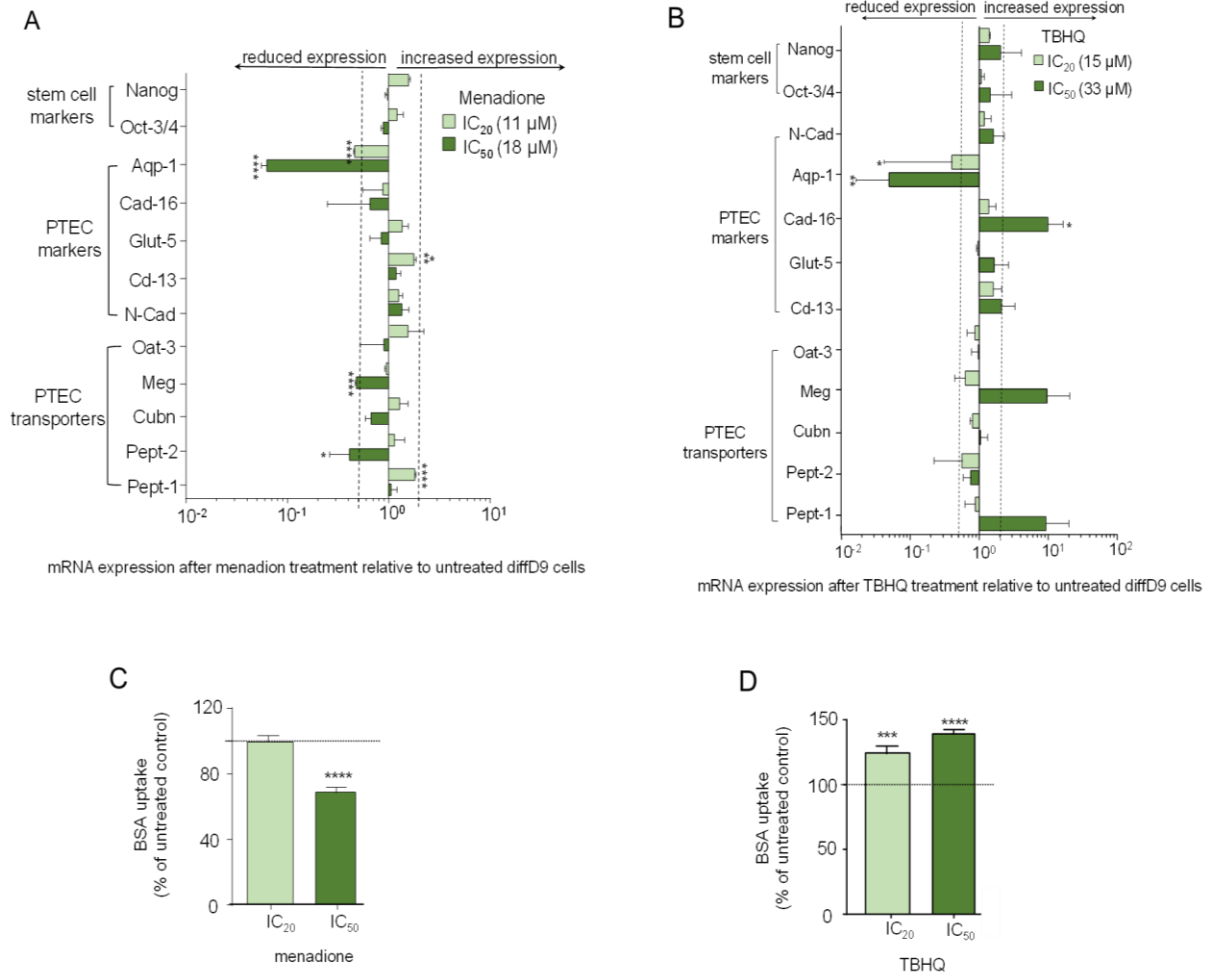


Figure 18: Influence of oxidizing agents on marker gene expression and transport function in hiPSC differentiated into proximal tubular epithelial cells (PTEC). mRNA expression of marker genes in diffD9 cells after 24-hour treatment with the IC₂₀ and IC₅₀ concentrations of menadione (**A**) and TBHQ (**B**) compared to their expression in untreated diffD9 cells, analysed by quantitative RT-PCR. Flow cytometric analysis of albumin uptake in diffD9 cells after 24 hours of treatment with the IC₂₀ and IC₅₀ levels of menadione (**C**) and TBHQ (**D**) using FITC-labelled albumin. Data from at least 3 independent experiments (RT-qPCR also included 3 technical replicates) are expressed as mean + SD. *p<0.05, **p<0.01, ***p<0.001 and ****p<0.0001 compared to untreated diffD9 cells (Student's t-test). Aqp-1 = aquaporin-1, Cad-16 = cadherin 16, CD13 = alanyl aminopeptidase, Oat-3 = organic anion transporter 1, Oct-3/4 = octamer-binding transcription factor 3/4 and Nanog = homeobox gene, Cubn = cubilin, diffD9 = differentiation day 9, Glut-5 = fructose transporter 5, hiPSC = human induced pluripotent cell, Meg = megalin, Pept-1/2 = peptide transporter 1.

3.2.3.3. Mode of toxicity contributing to the cell's sensitivity at the different stages of differentiation towards nephrotoxins and oxidative stress

To investigate the underlying cellular mechanisms contributing to the sensitivity of cells to nephrotoxins and oxidative stress, first the manner of cell death induced by the different toxins was studied. Apoptosis induction was analyzed by the TUNEL assay, which measures nuclear fragmentation, one of the hallmarks of apoptotic cell death. For this purpose, cells at the three differentiation stages were treated with the respective equitoxic concentrations of the genotoxic nephrotoxin cisplatin and the non-genotoxic nephrotoxin CsA, as well as with the oxidizing agents menadione and TBHQ, as determined by dose-response analysis. As shown in **Fig. 19A**, the frequency of TUNEL-positive fragmented nuclei increased with cisplatin concentration in undifferentiated hiPSCs, differentiating hiPSCs, and fully differentiated PTELCs, indicating that cisplatin treatment resulted in the induction of apoptosis in the cells (**Fig. 19A and B**). In agreement with these data, cell viability data showed significant restoration of cell viability in all stages of differentiation when the cells at the different stages of differentiation were co-treated with cisplatin and the pan-caspase inhibitor QVD compared to their cisplatin mono-treatment counterpart (**Fig. 19C**). Interestingly, the percentage of cell viability rescued by QVD was also very similar in undifferentiated hiPSCs, differentiating hiPSCs, and hiPSC-derived PTELCs and the respective untreated control. (**Fig. 19E**). Overall, our data suggest that the sensitivity of undifferentiated hiPSCs, differentiating hiPSCs and hiPSC-derived PTELCs to cisplatin may be entirely due to preferential activation of apoptotic cell death mechanisms.

For the non-genotoxic nephrotoxin CsA, the frequency of TUNEL-positive cell nuclei also increased with rising concentrations in hiPSCs, differentiating hiPSCs (diffD3) and differentiated PTELCs (diffD9), indicating the presence of apoptosis (**Fig. 19C**). Consistent with this observation, the percentage of viable cells at the different stages of differentiation was significantly higher when cells were treated with CsA and QVD together than when treated with CsA alone (**Fig. 19F**). However, in contrast to cisplatin, the viability of the cells could not be rescued entirely by simultaneous treatment by this co-treatment compared to the untreated control. Therefore, this result indicates that the sensitivity of cells to CsA at all stages of differentiation is not exclusively dependent on the activation of apoptotic cell death signaling.

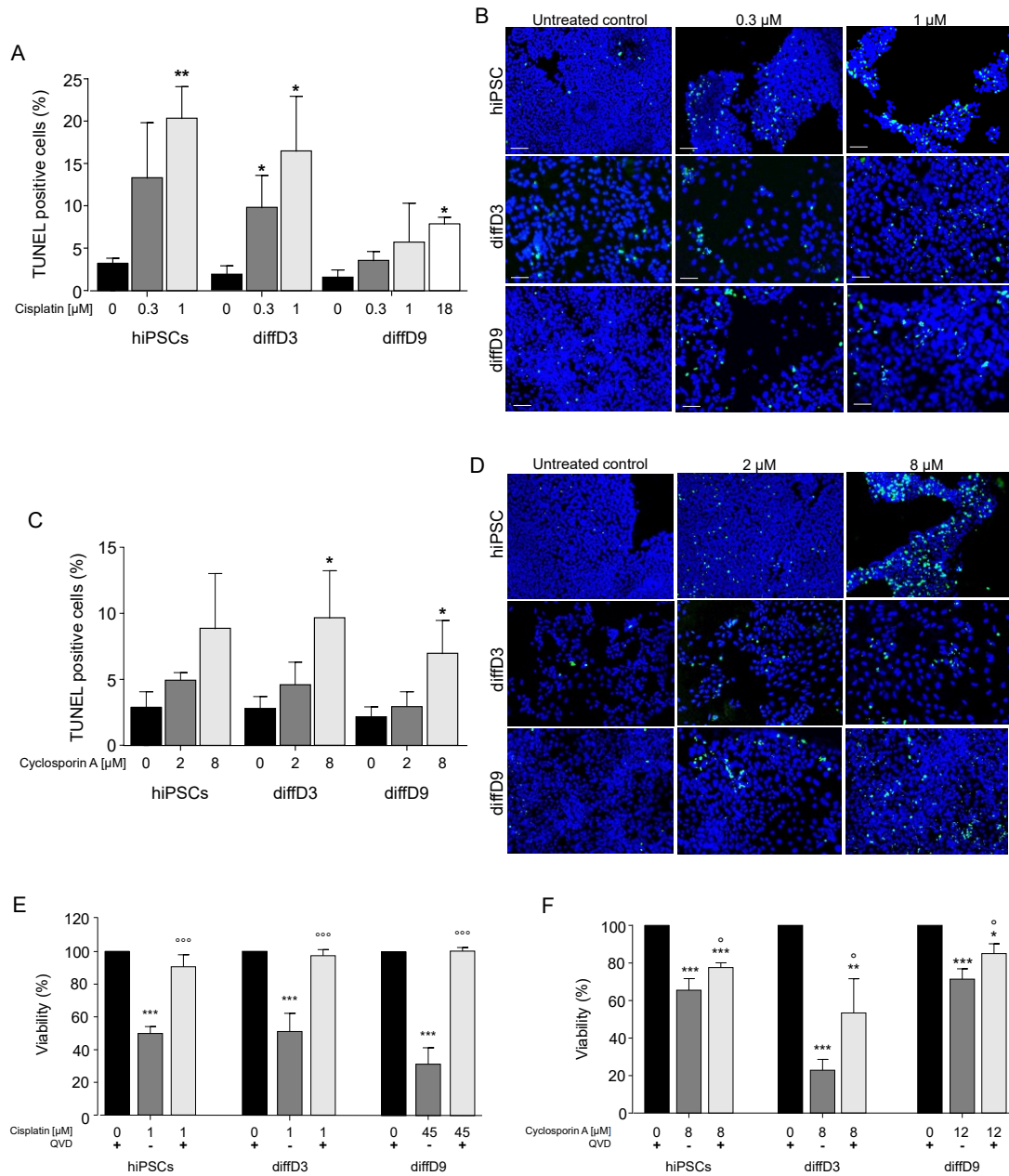


Figure 19: Stimulation of cell death mechanisms in hiPSC, diffD3, and diffD9 by cisplatin and CsA. hiPSC, diffD3, and diffD9 cells were treated with the indicated equitoxic doses of cisplatin and cyclosporin A for 24 hours. After treatment, apoptosis was measured with the TUNEL assay (A, B, C, D). A, C: Apoptosis was quantified by counting the number of TUNEL-positive cells. B, D: Representative overlay images of TUNEL-positive cells and cell nuclei from treated and untreated hiPSC, diffD3, and diffD9 cells from three independent experiments are shown. The cell nuclei were counterstained with DAPI (blue colour). FITC (green colour) indicates the incorporation of dUTP. Scale bar: 50 μm. The pan-caspase inhibitor (10 μM) QVD was used to verify apoptosis (E, F). Cell viability was measured in cisplatin (E) and cyclosporin A (F) treated cells of all stages with or without the addition of 10 μM QVD. All the data are presented as mean + SD of three independent experiments. One-way ANOVA, * $p \leq 0.05$, ** $p < 0.01$, *** $p < 0.001$ vs. control, and ° $p \leq 0.05$ and °°° $p \leq 0.001$ vs. QVD treated cells. TUNEL = terminal deoxynucleotidyl transferase-mediated dUTP-fluorescein nick-end labelling, dUTP = deoxyuridine triphosphate, SC = solvent control, QVD = pan-caspase inhibitor.

When treated with oxidizing agents, the frequency of TUNEL-positive fragmented cell nuclei was significantly higher in both menadione- (Fig. 20A and B) and TBHQ- (Fig. 20C and D) treated differentiating cells than in undifferentiated

hiPSCs and differentiated PTELCs. Thus, treatment with both oxidizing agents preferentially induced apoptosis signaling only in differentiating hiPSCs.

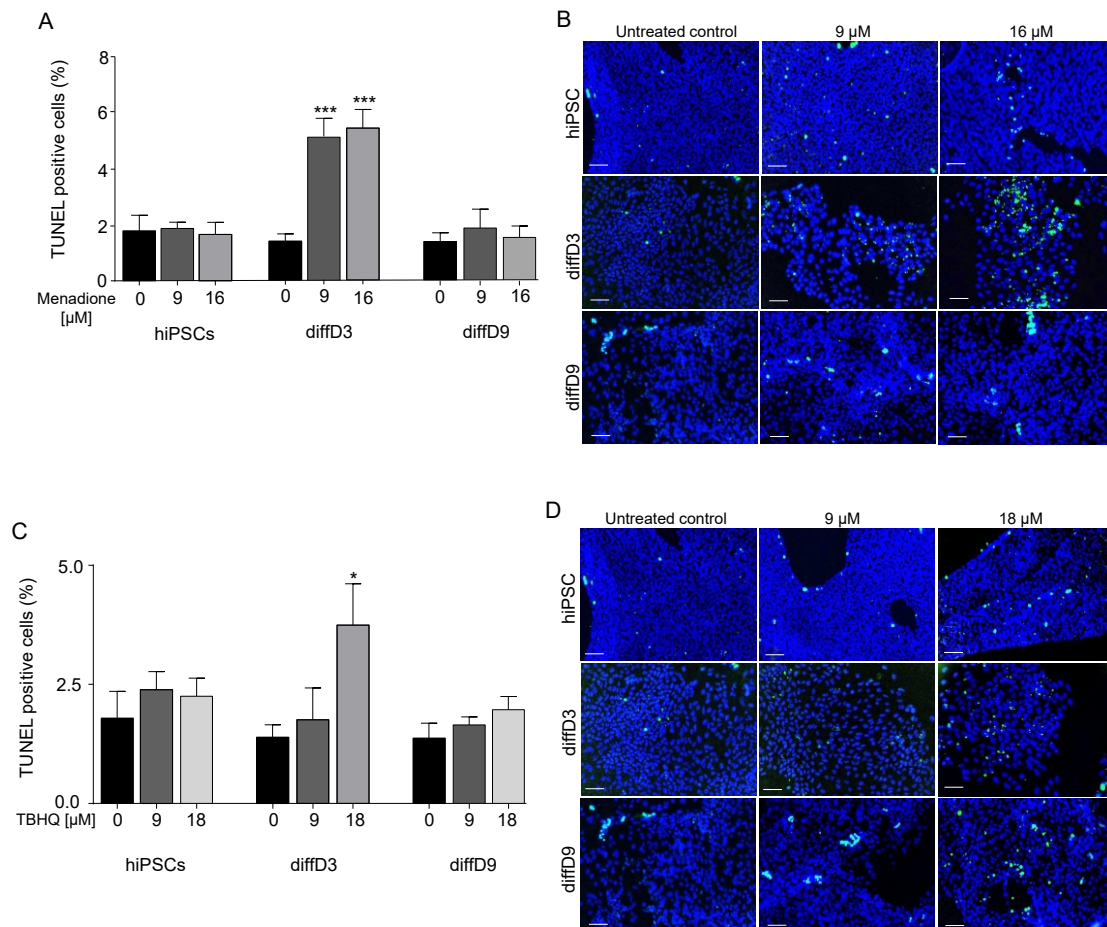
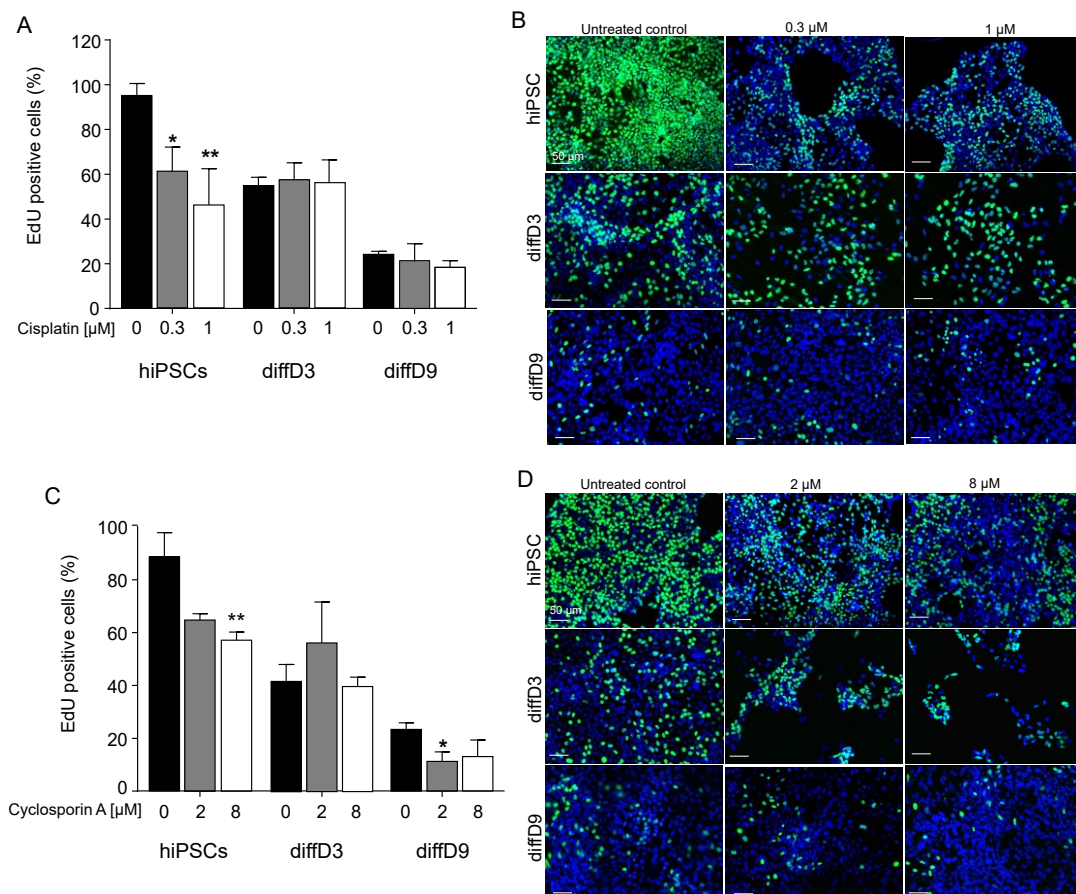


Figure 20: Stimulation of cell death mechanisms by oxidants in hiPSC, diffD3, and diffD9. hiPSC, diffD3, and diffD9 cells were treated with the indicated concentrations of the oxidants menadione (A, B) and TBHQ (C, D) for 24 hours, and apoptosis was analysed using the TUNEL assay. (A, C) Apoptosis was quantified by determining the number of TUNEL-positive cells. Data are expressed as mean + SD of three independent experiments. One-way ANOVA, *p<0.05, ***p<0.001 compared to the corresponding untreated controls. (B, D): Representative overlay images of TUNEL-positive nuclei from treated and untreated hiPSC, diffD3, and diffD9 cells from three independent experiments are shown. The cell nuclei were counterstained with DAPI (blue colour). FITC (green colour) indicates the incorporation of dUTP. Scale bar: 50 μm.

In order to investigate the mode of toxicity of the various active substances further, cell proliferation was analyzed by measuring EdU incorporation. For this purpose, cells at different differentiation stages were treated with equitoxic doses of the nephrotoxins cisplatin, CsA, and the oxidizing agents menadione and TBHQ. As shown in **Fig. 21A**, treatment with the genotoxic nephrotoxin cisplatin inhibited EdU incorporation in undifferentiated hiPSCs in a dose-dependent manner. However, this was not the case in differentiating hiPSCs (diffD3) and hiPSC-derived PTELCs, in which EdU incorporation was relatively similar (**Fig. 21A**). This result suggests that cisplatin treatment explicitly reduces the proliferation of undifferentiated hiPSCs from approximately 90 % to 40 % at the time of exposure. Regarding the non-genotoxic

nephrotoxin CsA, EdU incorporation in undifferentiated hiPSCs treated with CsA was decreased from approximately 90 % to 50 % compared to the untreated control, but only significantly at the higher concentration. EdU incorporation was also decreased from approximately 30 % to 10 % in hiPSC-derived PTELCs after treatment with CsA compared to the untreated control, although this was only significant at the lower concentration. However, no significant difference in EdU incorporation was observed in CsA-treated differentiating hiPSCs at all concentrations tested compared to the untreated controls (**Fig. 21C**).

Surprisingly, in the case of oxidative stress-inducing agents, EdU incorporation was significantly reduced from approximately 70 % to 30 % only in differentiating hiPSCs treated with menadione and TBHQ compared to the untreated control. In contrast, no significant differences in EdU incorporation were observed when undifferentiated hiPSCs and differentiated PTELCs were treated with both menadione and TBHQ compared with the untreated control (**Fig. 21E and F**). Taken together, our data suggest that nephrotoxic treatment preferentially affects the proliferation rate of undifferentiated hiPSCs. In contrast, oxidant exposure preferentially affects the proliferation of hiPSCs undergoing differentiation at the time of exposure.



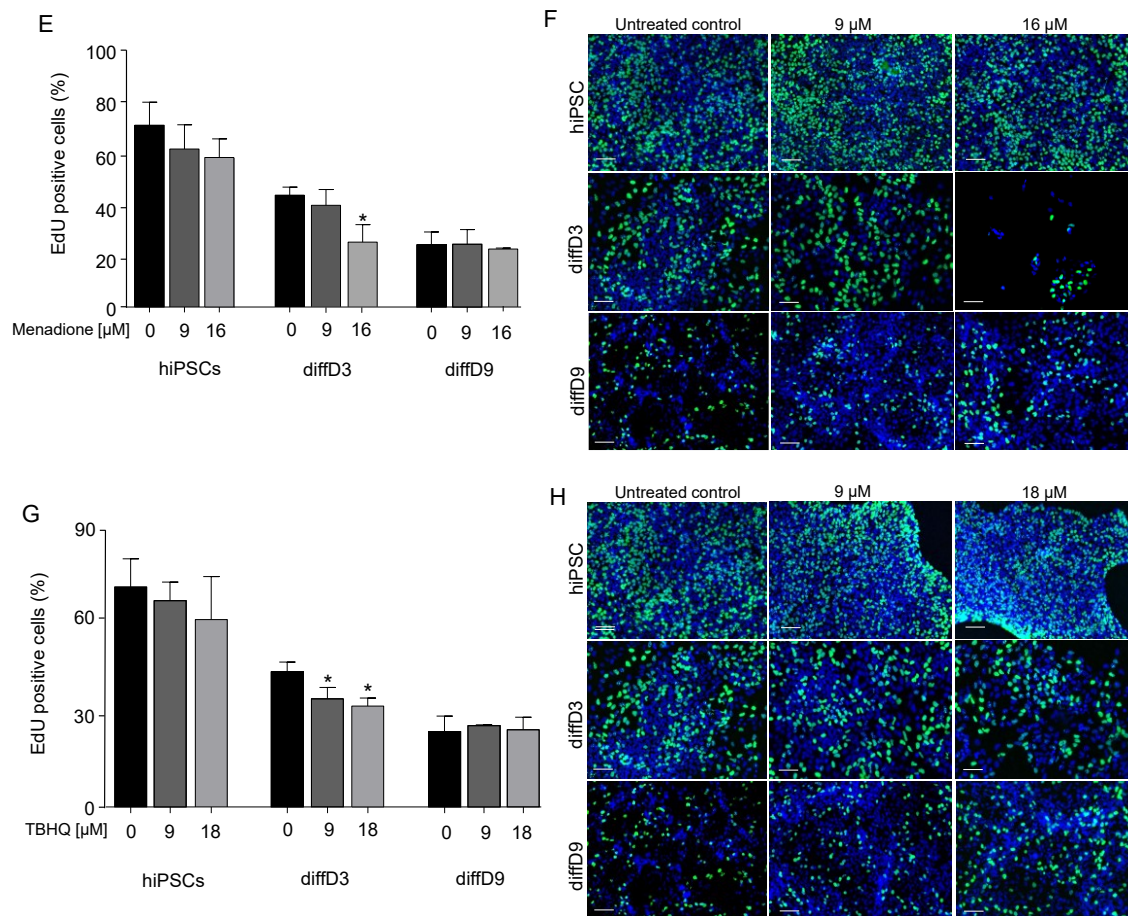


Figure 21: Influence of genotoxins and oxidizing agents on proliferation. Undifferentiated hiPSC, hiPSC differentiating into PTELC (diffD3), and terminally differentiated PTELC (diffD9) were treated for 24 h with the indicated concentrations of cisplatin (A, B), cyclosporin A (C, D), menadione (E, F) and TBHQ (G, H). After treatment, cell proliferation was determined by measuring the incorporation of EdU. (A, C, E, F): Proliferation was quantified by counting the number of EdU-positive cells. Data from at least three independent experiments are expressed as mean + SD. One-way ANOVA, * $p < 0.05$ and ** $p < 0.01$ compared to untreated control. (B, D, F, H): Representative overlay images of EdU-positive cells and cell nuclei from treated and untreated hiPSC, diffD3, and diffD9 cells from three independent experiments are shown. The cell nuclei were counterstained with DAPI (blue colour). FITC (green colour) indicates the incorporation of EdU. Scale bar: 50 μm. EdU = 5-ethynyl-2'-deoxyuridine, PTELC = Proximal tubular epithelial-like cells, DAPI = 4',6-diamidino-2-phenylindole, FITC = fluorescein isothiocyanate.

Investigating the molecular mechanisms involved, no apparent senescence-associated secretory phenotype was observed at the different stages of differentiation after treatment with the genotoxic nephrotoxin cisplatin, as only significant expression of *p21* mRNA levels was observed in the differentiating hiPSCs and hiPSC-derived PTELCs after 72 h of analysis (Fig. 22A). However, the non-genotoxic nephrotoxin CsA preferentially stimulated genes involved in senescence in undifferentiated hiPSCs, as indicated by the significant mRNA expression of the senescence-associated β -galactosidase, senescence-associated secretory cytokine *IL-8* and the cyclin-dependent kinase inhibitor *p21*, only *IL-8* mRNA expression increased in a dose-dependent manner in differentiating cells.

In contrast, both *IL-8* and *p21* were increased in differentiated PTELCs by the higher concentration (Fig. 22B). As for oxidative stress-inducing agents, no clear senescence-associated secretory phenotype was observed when the cells were treated with both TBHQ and menadione at different developmental stages, as shown in Fig. 22C and D, where only *IL-8* levels were tendentially increased after TBHQ treatment in differentiating hiPSCs and menadione treatment in differentiated PTELCs after 72 h of analysis.

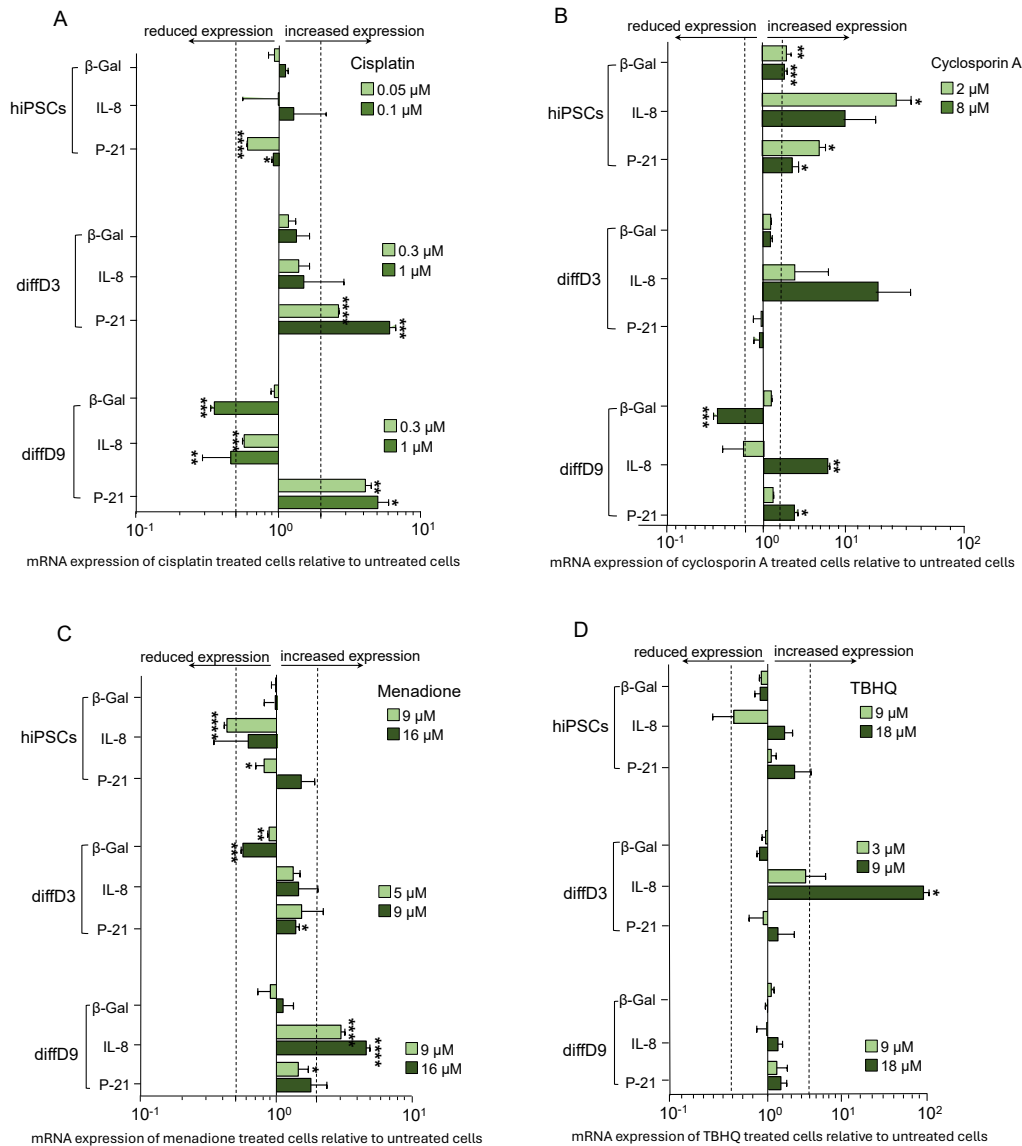


Figure 22: Influence of nephrotoxins and oxidants on the activation of senescence mechanisms. Undifferentiated hiPSC, hiPSC differentiating into PTELC (diffD3), and terminally differentiated PTELC (diffD9) were treated for 24 h with the indicated concentrations of cisplatin (A), cyclosporin A (B), menadione (C) and TBHQ (D). After treatment, quantitative RT-PCR analysis of the mRNA expression of senescence-associated markers (β -Gal, IL-8, P-21) was performed 48 h after 24 h of treatment. The relative mRNA expression of untreated cells was set to 1. Data from two independent experiments (qPCR also included three technical replicates) are expressed as mean + SD. Student's t-test, * $p \leq 0.05$, ** $p < 0.01$, *** $p < 0.001$, and **** $p < 0.0001$ compared to vs. respective untreated control. β -Gal = β -Galactosidase, IL-8 = Interleukin 8, P-21 = Protein 21, PTELC = Proximal tubular epithelial cell-like cell.

3.2.3.4. Influence of nephrotoxins and oxidants on the induction of EMT phenotype in proximal tubular epithelial-like cells

To investigate whether treatment of differentiated PTELC with subtoxic doses of the various toxins also triggers activation of an EMT phenotype, we analyzed the PTELC expression profile for genes and proteins belonging to the epithelial (E-cadherin and Collagen IV) and mesenchymal (Licam, Cadherin 11, Fibronectin, and N-cadherin) genetic programs. As shown in **Figs 23A and B**, both cisplatin and CsA, after 24 h of exposure at the indicated concentration, increased all tested mesenchymal markers and decreased the epithelial markers with the exception of *E-cadherin*, which was rather slightly increased after CsA treatment. Consistent with this data, when staining for the protein expression of the mesenchymal and epithelial markers, we also observed a decreased protein expression of Fibronectin and an increased expression of E-cadherin after treatment with cisplatin and CsA compared to the untreated control (**Fig. 23C**). However, treatment of PTELCs with the oxidants menadione and TBHQ did not have as pronounced an effect on the expression of selected mesenchymal and epithelial marker genes as cisplatin and CsA did, as none of the individual EMT genes analyzed in this study exceeded the 0.5- or 2-fold threshold expression levels set as biologically relevant (**Fig. 23D and E**). The expression patterns of the mesenchymal marker Fibronectin and the epithelial marker E-cadherin observed at the protein level via immunocytochemical analyses (**Fig. 23C**) also confirmed the qPCR-based results, indicating the absence of an EMT induction after oxidants exposure. Our findings suggest that the nephrotoxins cisplatin and CsA induced the EMT phenotype in the hiPSC-derived PTELC. However, a possible EMT phenotype was not observed after treatment of PTELC with both oxidizing agents.

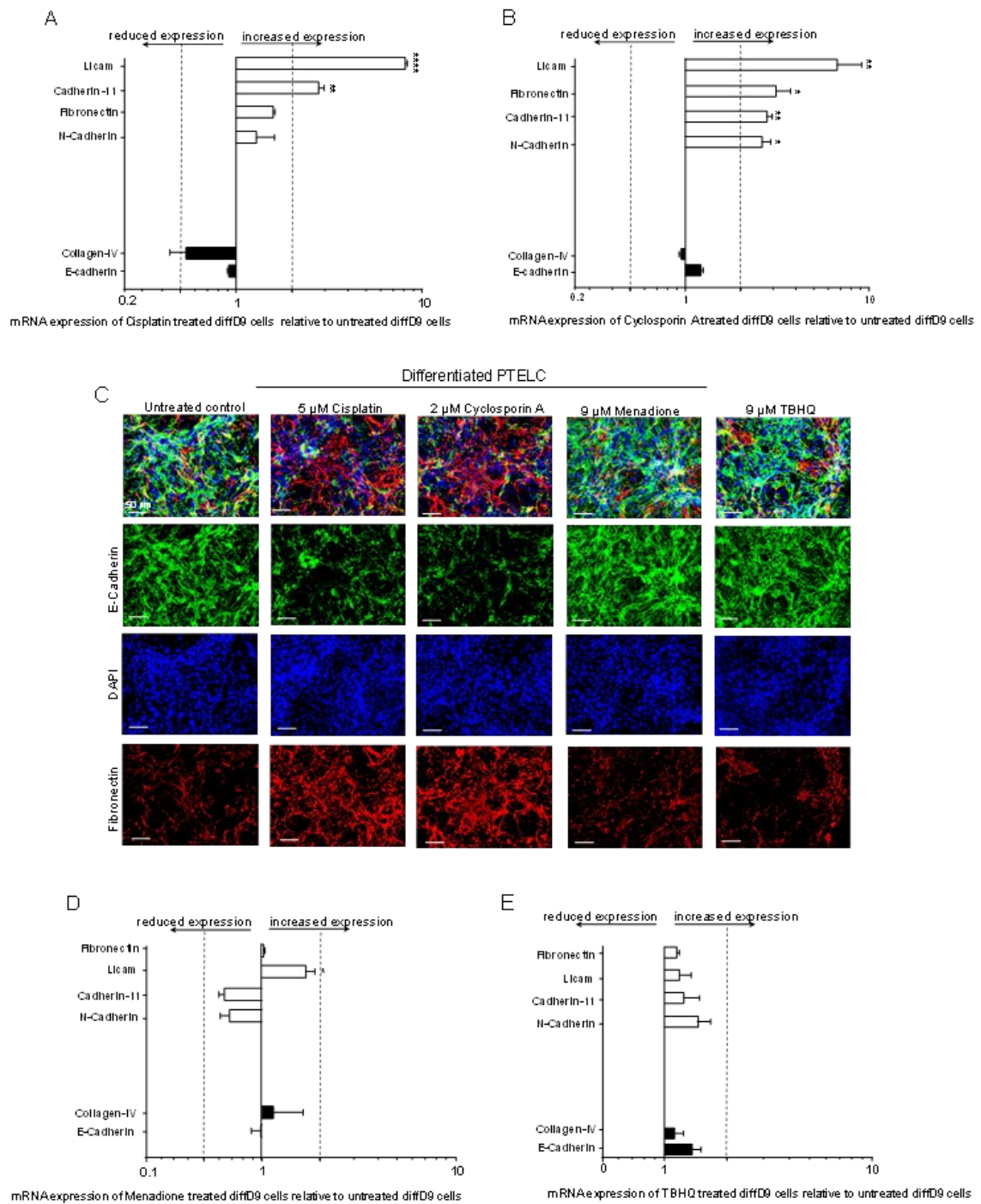


Figure 23: Induction of the EMT phenotype by nephrotoxins and oxidants in hiPSC-derived PTELCs. Quantitative RT-PCR analysis of mRNA expression of EMT-associated markers (E-cadherin, Collagen-IV, N-cadherin, Cadherin-11, Licam, Fibronectin) after 24 h exposure of hiPSC-derived PTELCs to **(A)** 5 μ M cisplatin, **(B)** 2 μ M cyclosporin A, **(C)** 9 μ M menadione and **(D)** 9 μ M TBHQ. Relative mRNA expression of untreated cells was set to 1.0. Data from at least three independent experiments (qPCR also included three technical replicates) are expressed as mean + SD. One-way ANOVA, * p < 0.05, ** p < 0.01 and **** p < 0.0001 vs. untreated control. **E:** Immunocytochemical analyses of the protein expression of EMT markers E-cadherin and Fibronectin of PTELC analyzed after 24 h after treatment with the respective toxins. Nuclei were counterstained with DAPI (blue) and EMT markers are colored green (Ecadherin) and Red (Fibronectin). EMT = Epithelial-to-Mesenchymal Transition, TBHQ = Tert-Butylhydroquinone, PTELCs = Proximal tubular epithelial cell-like cells.

3.2.4. Discussion

In this study, we tested the response of human induced pluripotent stem cells (hiPSC) to known nephrotoxins and oxidants exposure during their differentiation into proximal tubular epithelial-like cells (PTELCs). We focused on the genotoxic nephrotoxin cisplatin, the non-genotoxic nephrotoxin CsA, and the oxidizing agents H₂O₂, menadione and TBHQ. The results we obtained unequivocally demonstrate the high sensitivity of the differentiating cells to these known nephrotoxic and oxidizing agents. Depending on the agent, this sensitivity leads to apoptosis, early signs of cellular senescence, and EMT, which can have an unfavourable effect on the tubular regeneration processes.

In our previous study, we successfully established a PTELCs differentiation model from hiPSC using a protocol published by Kandasamy and colleagues in 2015 [22]. By triggering proximal tubular epithelial cell (PTEC) differentiation with the proteins BMP 2 and 7, we were able to produce hiPSC-derived PTELCs with similar morphology to PTECs, which expressed prototypical PTEC markers and were able to undergo albumin endocytosis [221]. Additionally, when we treated the cells at the different stages of PTELC differentiation with the known nephrotoxin cisplatin, hiPSC and differentiating hiPSC were more sensitive to cisplatin than differentiated PTELCs [221]. To uncover the molecular mechanisms underlying the hypersensitivity of hiPSC and differentiating hiPSC to cisplatin, our present study reveals that the differing cisplatin sensitivity of hiPSC and differentiating hiPSC compared to differentiated PTELCs may stem from variations in proliferation rates as indicated by the results obtained from the EdU incorporation measurements. This was expected because cisplatin is a DNA-damaging agent that has been previously reported to interfere with DNA synthesis and replication in rapidly proliferating cells, such as stem cells [35]. Interestingly, cisplatin treatment did not significantly affect the proliferation rate of differentiating hiPSC compared to hiPSC despite their similar sensitivity to cisplatin. This suggests that the differentiating cell's sensitivity to cisplatin may be linked to other cytotoxic effects of the drug. Indeed, all stages of differentiation, including hiPSC and differentiated PTELCs, exhibited susceptibility to cisplatin-induced cell death rather than senescence. Importantly, co-treatment with cisplatin and the pan-caspase inhibitor QVD, a broad-spectrum caspase inhibitor that prevents apoptosis, effectively restored cell viability. This observation suggests that the cell death induced by cisplatin is predominantly apoptotic. This result is somewhat unexpected as, in addition to apoptosis, cisplatin is also recognised to induce other forms of cell death in cisplatin-treated cells, such as ferroptosis and necrosis [237-239]. Forthcoming

experiments would be needed for further clarification. While only a few studies examined the mode of toxicity of cisplatin in stem cells [196, 197] and fully differentiated PTEC [21, 22], to the best of our knowledge, none has investigated the mode of toxicity of cisplatin during the tubular differentiation process. While Lawrence et al. [21] only specifically reported oxidative stress induced by cisplatin and other nephrotoxins in hiPSC-derived renal organoids containing PTEC, Kandasamy and colleagues also observed oxidative stress associated with DNA double-strand breaks and the induction of inflammatory response after cisplatin treatment in hiPSC-derived PTEC, but the mechanism of apoptotic cell death was not analyzed in either study [21, 22]. Nevertheless, the results obtained in the present study with cisplatin-treated differentiated PTELCs are consistent with clinical data and the results of animal studies, in which it has already been well-documented that cisplatin exhibits dose-limiting nephrotoxicity and is apoptotic to renal proximal tubular epithelial cells of humans and experimental animals [43, 240].

Furthermore, tubular epithelial injury resulting from xenobiotic-induced nephrotoxicity can lead to epithelial-to-mesenchymal transition (EMT) in tubular epithelial cells. EMT in tubular epithelial cells is a well-established mechanism in tubular repair and the development of tubulointerstitial fibrosis [94, 241]. It is characterized by the loss of apical-basal polarity, breakdown of cell-cell contacts and reorganization of the cytoskeleton in epithelial cells. At the molecular level, EMT is associated with the downregulation/loss of epithelial proteins, e.g. E-cadherin, claudins and cytokeratins, and the upregulation/increase of mesenchymal proteins, e.g. vimentin, LICAM, N-cadherin and fibronectin [117, 242]. In agreement with this concept, it has been previously reported that cisplatin-induced proximal renal tubular apoptosis preceded by the induction of an EMT phenotype involving actin cytoskeletal reorganization, associated with disruption of cell-matrix and cell-cell adhesion [243]. Consistent with this observation, we found a reduced epithelial marker expression and increased mesenchymal markers expression at both the RNA and protein levels, indicating a phenotypic switch characteristic of EMT induction in our differentiated PTELCs after cisplatin-mediated injury.

Concerning the non-genotoxic nephrotoxin CsA, we have also shown previously that, unlike cisplatin, all differentiation stages were equally sensitive to CsA with IC₅₀ values around 10 μ M [221]. Although all stages of differentiation showed similar sensitivity to CsA, we equally had a look at the mode of toxicity of CsA at

the different stages of differentiation. We found that the proliferation rate of undifferentiated hiPSC and differentiated PTELCs were particularly susceptible to CsA treatment. While the effect of CsA has not been studied in detail in stem cells, however, the impact of CsA on the proliferation rate of renal cell types appears to be consistent, as a reduction in the proliferative capacity of cultured tubular epithelial cells (52 % with 4.2 μ M CsA), mesangial cells (50 % with 1 μ g/ml CsA) and endothelial cells was also observed in previous studies [244-246]. To investigate whether this observed decrease in proliferation is related to the activation of possible senescence mechanisms, we observed that CsA preferentially stimulated early signs of premature senescence mechanism in undifferentiated hiPSC but not in differentiated PTELCs, which contrasts with previous studies by Jennings and colleagues showing that CsA stimulates cellular senescence in human renal tubular epithelial cells [247]. However, since we only analysed the mRNA expression of selected senescence-associated marker genes, further experiments are required for clarification, such as staining for senescence-associated β -galactosidase, determination of telomere length, and cell cycle analysis. Nonetheless, the lack of evidence of early signs of premature senescence in differentiating hiPSC and differentiated cells may suggest that their sensitivity to CsA was not dependent on senescence activation. Indeed, we have shown that differentiating hiPSC and differentiated PTELC, but also undifferentiated hiPSC, were particularly susceptible to CsA-induced cell death, and we were able to verify this observation with our cytotoxicity data that this cell death mechanism is apoptotic-related. Consistent with this finding, CsA was previously shown to induce an apoptotic cell death mechanism in a renal proximal tubular cell line [244, 248]. Additionally, like cisplatin, we discovered that CsA-induced nephrotoxicity also stimulated the EMT phenotype in PTELCs. This observation led us to speculate that EMT could serve as either an initial response to repair CsA-induced damage in PTELCs or a precondition for renal fibrosis and apoptosis of damaged PTELCs. Corroborating our findings, McMorro and colleagues [249] demonstrated that CsA directly induced EMT in renal tubule epithelial cells. Their study also alluded to the significance of CsA-induced EMT as a critical event in the development of interstitial fibrosis, a frequent complication associated with long-term CsA treatment.

In addition to assessing the effects of nephrotoxins on the tubular differentiation process [221], we also explored the impact of the oxidative stress triggers H₂O₂, menadione, and TBHQ on cells at various stages of tubular differentiation. Our findings revealed for the first time that differentiating hiPSC were more susceptible

to these oxidants than undifferentiated hiPSC and fully differentiated PTELCs. This observation is toxicologically relevant as it suggests that the stem cells differentiating into PTELCs are particularly vulnerable to oxidative stress induced by oxidizing agents. Consistent with this observation, our gene expression analysis revealed a decline in antioxidant defences as cells differentiated, with essential antioxidant genes showing downregulation in differentiating cells compared to differentiated cells (**see SFig. 3**). This decrease in antioxidant defences could explain why differentiating cells are more susceptible to oxidative stress. Our findings are in line with previous studies demonstrating that antioxidant defence decreases with differentiation [250]. The increased expression of redox genes in the differentiated PTELCs compared to differentiating cells may have contributed to increased antioxidant defence against oxidative stress induced by our test agents, thereby explaining their increased resistance. Based on the low expression of redox genes in differentiating cells, we speculated that stem cells differentiating into PTELCs most likely have significantly reduced redox properties on the third day of differentiation. As a result, their antioxidant defences would be weakened, and the oxidative stress induced by the oxidants would increasingly exceed the buffering capacity of the cell, resulting in a considerable reduction in viability.

The sensitivity of oxidizing agents to human stem cells and thereof differentiated counterparts has not been extensively researched, resulting in a lack of readily available IC₅₀ values in the literature. While H₂O₂ has been shown to play a role in the proliferation, survival, and differentiation of neural stem cells into sessile CNS cells [251], only rat bone marrow-derived multipotent adult progenitor cells have been examined for their sensitivity to H₂O₂, with an IC₅₀ value of over 25 µM after 48 h of incubation [252]. However, this value cannot be directly compared to the IC₅₀ value of our undifferentiated hiPSC, which showed an IC₅₀ value of 158 µM after just 30 min of incubation, as different H₂O₂ incubation times were used in both studies. Regarding non-stem cells, while there are no available studies on the effects of oxidants on differentiated PTELCs, previous research on human kidney epithelial cell lines has reported IC₅₀ values ranging from 200 to 800 µM after 24 h of incubation with H₂O₂ [242, 253], which although similar to the range observed in our differentiated cells, cannot be directly compared due to different exposure times that the substance was allowed to act on the cells. Regarding TBHQ sensitivity, our differentiated cells demonstrated a significant reduction in cell viability with an IC₅₀ of 35 µM, while endothelial cells from Karimi et al. [254] and mammary epithelial cells from Jin et al. [255] showed IC₅₀ values of 60 µM and 50 µM, respectively. These findings imply that different cell types have varying

sensitivity to TBHQ. In contrast, the human Hep G2 cell line exhibited cytotoxicity to menadione with an IC₅₀ value of approximately 18-19 µM after 18 h of incubation [256], which is very similar to the IC₅₀ value of 17 µM observed in our differentiated cells, albeit with a slightly longer incubation time (24 h).

For further studies on the molecular mechanisms contributing to the preferential hypersensitivity of differentiating cells to oxidizing agents, we focused on the oxidants menadione and TBHQ because they were more stable in the cells and, therefore, easily handled compared to H₂O₂. Moreover, all three agents showed similar effects on the viability of our cells at the different stages of differentiation. Interestingly, we found that menadione and TBHQ inhibited proliferation and induced apoptosis in differentiating cells. In contrast with this finding, Xiao and colleagues investigated the effect of H₂O₂-induced oxidative stress on bone marrow stem cells (MAPCs), their endothelial differentiation, and underlying mechanisms *in vitro* [252]. Instead, they observe a significant inhibition of proliferation and a dose-dependent induction of apoptosis in the undifferentiated MAPCs [252]. However, the effect of H₂O₂ on MAPCs differentiating into endothelial cells and on MAPC-derived endothelial cells was not analysed in this study. Furthermore, H₂O₂-mediated oxidative stress has previously been shown to induce EMT in the rat PTEC line (NRK-52E) [257, 258]. Nevertheless, we could not identify the phenotypic switch characteristic of EMT induction in our differentiated PTELCs after menadione- and TBHQ-mediated injury. On the other hand, a similar finding was reported by Khan et al., who also failed to observe EMT induction in a human PTEC model with H₂O₂-mediated injury [253].

In addition to the effects of menadione and TBHQ treatment on cell viability at different stages of tubular differentiation, further analysis revealed that these oxidizing agents also selectively impaired the functionality of fully differentiated PTELCs, and the expression of individual marker genes associated with tubular differentiation. However, while menadione exposure significantly decreased mRNA expression of the PTEC transporter megalin, which could be an explanation for the loss of ability to take up albumin, TBHQ, on the other hand, increased megalin expression, leading to a corresponding increase in albumin uptake in differentiated PTELCs. Although these two oxidants appear to have opposite effects on megalin expression in our study, Kurosaki et al. showed that H₂O₂-induced oxidative stress also increased megalin expression in the HK-2 cell line [259]. Megalin is an important endocytic receptor that is highly expressed in PTEC in the kidney and is involved in the uptake of proteins, including albumin and certain

drugs that are filtered in the glomeruli via the megalin/cubilin endocytosis system [260]. Although other toxic substances with oxidative stress-inducing properties, such as cisplatin, are known to bind to megalin and prevent its interaction with its ligand, which includes albumin, to our knowledge, this has not yet been reported for menadione or TBHQ. Additional studies are required to elucidate how these oxidative stress-inducing agents affect megalin expression in PTEC. In addition to megalin, we found that both compounds significantly reduced the PTEC marker aquaporin 1 in the differentiated PTELCs. However, there was no evidence found in the literature that these oxidizing agents reduce the expression of aquaporin 1. However, Liu et al.[261] showed that mitochondrial oxidative stress induced by the use of manganese (III) tetrakis (4-benzoic acid) porphyrin chloride (MnTBAP) in obstructive kidney disease also led to downregulation of aquaporins, including aquaporin 1 [261].

In conclusion, this study provides the first comprehensive characterisation and mechanistic understanding of the effect of the nephrotoxins cisplatin and cyclosporin A, as well as the oxidising agents H₂O₂, menadione, and TBHQ, on hiPSC during their differentiation into PTELCs. The small selection of compounds analysed in this study underscores the diverse response of cells at different stages of differentiation to substances with varying mechanisms of action. While it is apparent that the DNA-damaging compound cisplatin had its most significant effect on rapidly growing proliferating cells, the deleterious effect of oxidants on differentiating cells was unexpected, although oxidant-induced oxidative stress is already a recognised trigger for PTEC injury, which can lead to maladaptive repair and the occurrence of AKI [232, 253]. Consequently, these observations lend support to our hypothesis that nephrotoxins and oxidative stress may impede tubular epithelial regeneration.

3.3. Influence of nephrotoxins on the efficacy of hiPSC differentiation into proximal tubular epithelial-like cells

3.3.1. Introduction

The persistence of acute kidney injury (AKI) as an independent predictor of in-hospital mortality remains a concern for healthcare professionals despite advances in medical care [31, 262]. AKI often results in chronic kidney disease (CKD), with survivors having an approximately 9-fold, 3-fold and 2-fold incidence of progression to CKD, end-stage renal disease and mortality compared to patients without AKI [29, 30]. Unfortunately, there are no definitive therapies to prevent or treat established AKI, emphasizing the need for urgent and comprehensive research to understand the pathophysiology of this disease.

Death of proximal tubular epithelial cells (PTEC) is the most common cause of AKI and often occurs due to ischemic, nephrotoxic, septic or obstructive insults, as they play an essential role in glomerular filtrate accumulation and the transport and metabolism of organic compounds, making PTEC the most frequently studied cell type in the kidney in the context of *in vitro* drug safety evaluation [3, 20, 263, 264]. However, the regenerative capacity of PTEC, which occurs either via differentiation of local renal stem cells or through restoration of the proliferative properties of PTEC near the site of injury through epithelial-mesenchymal transition (EMT), can lead to restoration of epithelial morphology and renal function after AKI [94, 99]. Nonetheless, renal function is often reduced, suggesting that damaged cells are not replaced by fully functional cells [183, 184, 229].

Despite this observation, research to date has mainly focused on the development of *in vitro* assays to predict PTEC toxicity to various toxins using PTEC lines and induced pluripotent stem cell (iPSC)-derived proximal tubular epithelial cells (PTELCs). While this approach is a commendable initiative, we propose a more holistic and comprehensive approach, namely the development of an iPSC-based approach that could serve as a model for the prediction of PTEC toxicity and investigate how toxic agents affect the PTEC regeneration process. In this study, we therefore aimed to investigate for the first time the effects of known nephrotoxins on the differentiation efficiency and function of iPSCs differentiating into PTELCs, which in this context represent one of the tubular regeneration pathways, by using a modified one-step differentiation protocol according to Kandasamy et al. [22], previously published by Mboni-Johnston et al. [221].

3.3.2. Materials and Methods

3.3.2.1. Materials

All materials used in this study, such as cell lines, media, growth factors, small signalling molecules, antibodies, kits, primers, chemicals, and reagents, were purchased from the respective companies previously listed in Mboni-Johnston *et al.* [221]. The primers and antibodies used to detect the expression of various genes and proteins are listed in Tables 1 and 2 in the Appendix.

3.3.2.2. Methods

In this study, an *in vitro* model based on human-induced pluripotent stem cells (hiPSC) was used to investigate the influence of the genotoxic nephrotoxin cisplatin and the non-genotoxic nephrotoxin CsA on renal tubular differentiation processes. For this purpose, a modified protocol, according to Kandasamy and colleagues [22], was used for the differentiation of hiPSC into renal proximal tubular epithelial-like cells (PTELCs), as previously reported by Mboni-Johnston *et al.* [221] and as illustrated in **Fig. 24A**. In brief, 3000 hiPSC/cm² were seeded in renal epithelial growth medium (REGM) supplemented with Y-27632 dihydrochloride, and the growth factors BMP2/7 were added from the second day and cultured under these conditions for 9 days, changing the medium daily to induce tubular epithelial differentiation. During the differentiation of hiPSCs into PTELCs, PTELCs precursors (diffD3) were directly treated with IC₂₀ and IC₅₀ of cisplatin and CsA for 24 h. After subsequent daily media changes, cells were harvested at diffD9 and qPCR analysis, immunocytochemistry, and functional albumin assays were performed, as previously reported by Mboni-Johnston *et al.* [221], to investigate the effects of these toxins on the tubular differentiation process. Data were expressed as mean + standard deviation of three independent experiments, and statistical analysis was performed using GraphPad Prism version 6 (GraphPad Software, San Diego, CA). Comparison between sample groups was performed using Student's t-test (multiple-comparison test), and a p-value ≤ 0.05 was considered statistically significant.

3.3.3. Results

Using an adapted *in vitro* model by Kandasamy et al. [22] based on human induced pluripotent stem cells (hiPSC), which was previously published by Mboni-Johnston *et al.* [221], the influence of the genotoxic nephrotoxin cisplatin and the non-genotoxic nephrotoxin CsA on the tubular differentiation processes of the kidney was investigated. The treatment with the respective substances was performed three days after the differentiation process had been initiated (diffD3), and the marker genes associated with tubular differentiation and albumin uptake activity were analysed on the ninth day of differentiation (diffD9), as shown in **Fig. 24A**.

3.3.3.1. Impact of nephrotoxins treatment on the expression of marker genes associated with renal tubular epithelial differentiation

To investigate whether treatment of differentiating hiPSCs with cisplatin and CsA influences the subsequent differentiation process of the surviving PTELCs progenitor cell fraction into terminally differentiated PTELCs, mRNA and protein expression of tubule epithelial marker genes and proteins associated with renal tubular differentiation was analyzed in the differentiated PTELCs after treatment of PTELCs progenitor cells (diffD3) for 24 h with IC₂₀ and IC₅₀ of cisplatin and CsA. As shown in **Fig. 24B**, cisplatin significantly impacted the differentiation-induced decrease in mRNA expression of the pluripotency markers *NANOG* and *OCT3/4*. In addition, treatment of diffD3 cells with IC₂₀ and IC₅₀ of cisplatin resulted in a significant reduction in mRNA expression of almost all tested tubular epithelial marker genes in the terminally differentiated PTELCs, except for *PEPT-1*, *GLUT-5* and *CAD-16* genes. However, of those three, only *CAD-16* was significant at IC₅₀. Reduced expression of the PTEC marker *AQP-1* was also observed at the protein level in differentiated PTELCs after treatment at diffD3 with cisplatin compared to the untreated control (**Fig. 24C**).

In contrast to cisplatin, the IC₂₀ and IC₅₀ doses of CsA had no significant effect on the differentiation-related decrease in mRNA expression of the pluripotency markers *Nanog* and *OCT3/4*. CsA also did not have as pronounced an impact on the expression of the selected tubule epithelial genes as cisplatin. Except the expression of the gene *AQP-1*, which decreased significantly, the mRNA expression of *GLUT-5*, *megalyn*, *cubilin*, *PEPT-1* and *OAT-1* either decreased or increased at IC₂₀ and IC₅₀, but their mRNA expression did not reach or exceed the 0.5- or 2-fold change in mRNA levels that is considered biologically relevant (**Fig.**

24D). As with cisplatin, decreased protein expression of the specific marker for PTEC, *AQP-1*, was also observed in differentiated PTELCs after treatment with IC₅₀ of CsA at diffD3 in comparison to the untreated control (**Fig. 24C**).

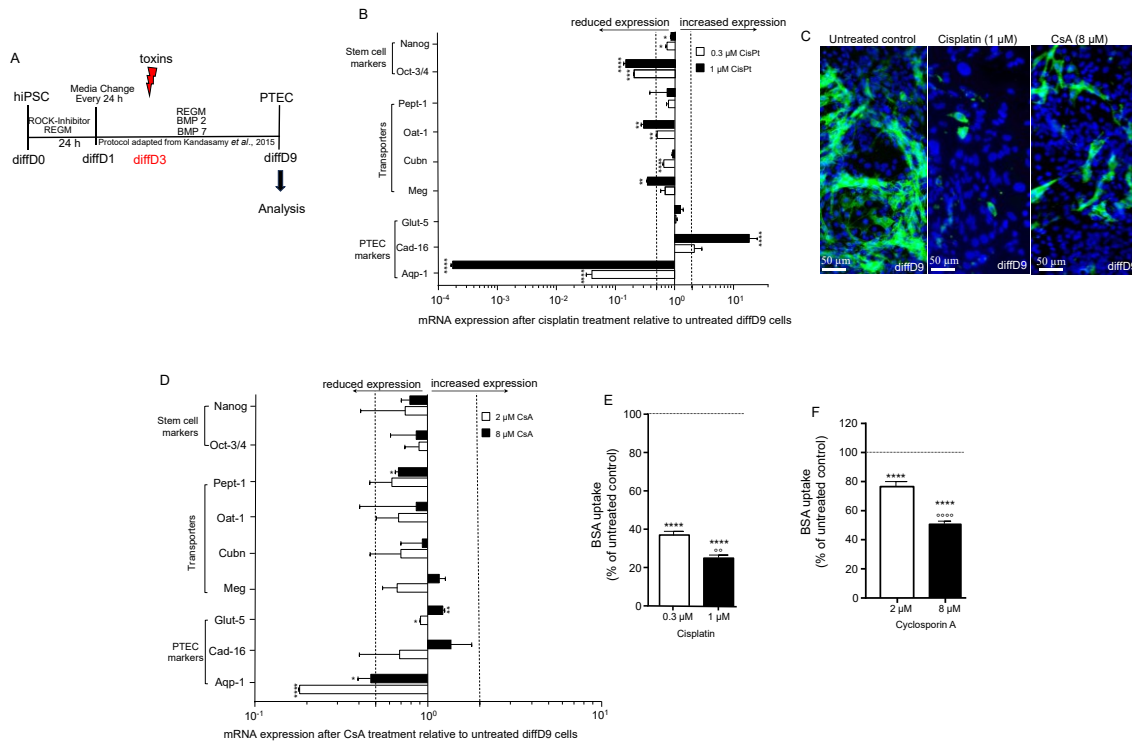


Figure 24: Effect of cisplatin and cyclosporin A on marker gene expression and transport function during the differentiation of hiPSC into proximal tubular epithelial cell-like cells (PTELCs). PTELCs treated with the indicated concentrations of cisplatin and cyclosporin A on day 3 of the differentiation process (diffD3), were analyzed on day 9 of differentiation (diffD9) and compared with untreated diffD9 cells. Quantitative RT-PCR analysis of mRNA expression of hiPSC-derived PTELCs after 24 h of treatment with 2 different concentrations of cisplatin (**B**) and cyclosporin A (**D**) at diffD3 and later analyzed on diffD9 for the mRNA expression of prototypic stem cell markers (Nanog, Oct-3/4) and PTEC markers/transporters (Aqp-1, Cad-16, Glut-5, Meg, Cubn, Pept-1, Oat-1) compared to their expression in untreated diffD9, which was set to 1. (**C**) Antibody detection of Aqp-1 on diffD 9 after treatment with toxins at diffD3. Images were captured with a fluorescence microscope and the scale bar represents 50 μm. Flow cytometric analysis of albumin uptake in diffD9 cells after 24 h of treatment with the indicated concentrations of cisplatin (**E**) and cyclosporin A (**F**) on diffD3 compared to untreated diffD9 cells using FITC-labeled albumin. Data from at least 3 independent experiments (qPCR also included 3 technical replicates) are expressed as mean + SD. *p≤0.05, **p<0.01, ***p<0.001 and ****p<0.0001 compared to untreated diffD9 (Student's t-test), °p≤0.01 and °°°p≤0.0001 vs. diffD3 (one-way ANOVA). Aqp-1 = aquaporin-1, Cad-16 = cadherin 16, Cubn = cubulin, Glut-5 = fructose transporter 5, hiPSC = human induced pluripotent cell, Meg = megalin, Pept-1 = peptide transporter 1, Oat-1 = organic anion transporter 1, Oct-3/4 = octamer-binding transcription factor 3/4, Nanog = homeobox protein, CisPt = cisplatin, and CsA = cyclosporin A.

3.3.3.2. Impact of nephrotoxins exposure on the functionality of differentiated proximal tubular epithelial-like cells

The selective uptake of albumin from the glomerular filtrate is an essential function of mature PTEC. This receptor-mediated albumin endocytosis in PTEC is carried out by megalin and cubilin, which are abundantly expressed in PTEC. To investigate whether treatment of PTELCs progenitor cells with cisplatin and CsA affects the subsequent functionality of the surviving progenitor cell fraction into terminally differentiated PTELCs, the albumin uptake capacity of differentiated PTELCs was analyzed by incubating terminally differentiated PTELCs with 100 µg/ml FITC-albumin for 2 h. Interestingly, a significant dose-dependent decrease in albumin transport was observed in differentiated PTELCs after treatment with IC_{20} and IC_{50} of cisplatin at diffD3 compared to the untreated control, possibly due to a reduction in the expression of the responsible transporter components *megalyn* and *cubilin* (**Fig. 24C**). Although not to the same extent as with cisplatin, treatment of diffD3 with IC_{20} and IC_{50} of CsA also resulted in a significant dose-dependent decrease in albumin uptake capacity of terminally differentiated PTELCs compared to the untreated control. Considering that albumin uptake is a critical function of PTECs, the data provide evidence that exposure of differentiating PTELC precursors to nephrotoxins impairs the functionality of surviving terminally differentiated PTELCs.

3.3.4. Discussion

The role of toxic substances in the renal tubular epithelial regeneration process remains a subject of limited understanding, although previous studies have shown that renal tubular epithelial function tends to decline after regeneration [94, 183]. Therefore, in this study, we rigorously attempted to investigate the influence of known nephrotoxins on the tubular epithelial differentiation process. Specifically, we used our modified one-step protocol [221] to generate proximal tubule-like cells (PTELCs) from human induced pluripotent stem cells (hiPSCs), which represent one of the regeneration pathways of the renal tubular epithelium. We then subjected PTELC-associated progenitor cells to IC₂₀ and IC₅₀ of the two known nephrotoxins cisplatin and CsA, derived from an earlier study, during their differentiation into PTELCs, and examined the effects of these toxins on the efficiency of their differentiation into functional PTELCs.

Our findings showed that cisplatin treatment of PTELCs precursors impaired the functionality of differentiated progeny and the expression of individual markers associated with differentiation. In particular, the down-regulation of the pluripotent markers *NANOG* and *OCT3/4* in differentiated progeny suggests that cisplatin treatment of the precursors of PTELCs does not prevent differentiation towards their differentiated progeny. However, the significant reduction in mRNA and protein expression of the key PTECs marker *AQP-1* indicated that cisplatin prevented the surviving population of PTELCs progenitor cells from differentiating efficiently into terminally differentiated PTELCs. To our knowledge, no study has reported the effect of cisplatin on *AQP-1* expression in the context of the tubular epithelial differentiation process. However, it has been documented that the expression of *AQP-1* and other members of the aquaporin family is reduced by cisplatin [212, 213], which we also observed in this study.

In addition to *AQP-1*, we observed that cisplatin treatment of PTELCs progenitor cells led to reduced mRNA expression of several PTEC-related transporters, including the albumin transporters *megalin* and *cubilin*, in terminally differentiated PTELCs. This is consistent with our finding that cisplatin treatment significantly reduced albumin uptake capacity in the differentiated progeny, suggesting reduced cell functionality after differentiation. This is in line with previous studies showing that cisplatin binds to megalin and prevents it from absorbing its ligands, including albumin [209]. This could explain the reduced albumin uptake we observed after cisplatin treatment.

Furthermore, we observed that CsA, a different nephrotoxin with a different mode of action, has a similar effect on PTELC progenitors as cisplatin. CsA treatment of PTELCs progenitors also did not prevent differentiation, as reflected by the downregulation of the pluripotent markers *NANOG* and *OCT3/4* in the differentiated progeny. However, their differentiation to matured PTELCs was impaired by CsA treatment, as evidenced by reduced expression of the major PTEC marker *AQP-1* at both the RNA and protein levels and by reduced mRNA expression of a number of transport proteins and by reduced albumin uptake function of terminally differentiated PTELCs. Although the effect of CsA on the expression of PTEC markers associated with tubular regeneration has not been reported, CsA is also known to inhibit various PTEC-related transporters, including peptide transporter-1 (PEPT-1), organic anion transporter, MDR-1, sodium transporter, glucose transporter 3, and sodium-dependent phosphate cotransporter [214-216, 219].

In conclusion, the results of our study are of great importance as they provide new information on the effects of nephrotoxins on the differentiation process of PTEC. These initial results suggest a potential vulnerability of the renal tubular epithelial regeneration process to nephrotoxic noxae, a finding that could potentially explain the observed loss of renal epithelial function after regeneration from AKI. This study highlights the urgent need for further studies, both *in vivo* and of other substances that may be present in the kidney during AKI, to provide a comprehensive view of their role in renal regeneration.

3.4. Influence of nephrotoxins on the dedifferentiation process of hiPSC-derived proximal tubular epithelial cells

3.4.1. Introduction

Acute kidney injury (AKI) is a clinically prevalent condition defined as a rapid decline in renal function recognised by a decreased glomerular filtration rate reflected by an increase in creatinine or blood urea nitrogen [265]. The leading cause of AKI is acute tubular necrosis resulting from nephrotoxic and oxidative injury [30, 71]. Proximal tubular epithelial cells (PTECs) are the central segment of injury in AKI as these cells rely on aerobic respiration due to their fluid and electrolyte reabsorption functions and are therefore uniquely very susceptible to ischemic and nephrotoxic injury [3, 20, 263, 264]. However, the recovery of renal cell function after AKI depends on the regenerative potential of the kidney, which allows the replacement of damaged tubular PTECs with functional tubular epithelium either by stem cell differentiation or by dedifferentiation of surviving PTEC after the acquisition of a mesenchymal-like phenotype and restoration of the epithelial phenotype [94, 99]. Nonetheless, it is known that renal function declines, suggesting that the damaged cells are not replaced by fully functional cells [183, 184]. Given the link between nephrotoxic-induced tubular damage, maladaptive repair, and the onset of AKI, understanding the role of toxins in renal tubular epithelial regeneration processes would help us better understand the possible causes of this loss of renal epithelial cell function associated with AKI. One possible avenue could be the development of human induced pluripotent stem cell (hiPSC)-based approaches that could serve as a platform for toxicity assessment during regeneration [185]. As a proof of principle, our recent study investigating known nephrotoxins on the differentiation efficiency and function of hiPSC differentiating into proximal tubular epithelial-like cells (PTELC) has shown promising results [221]. It shows that the known nephrotoxins cisplatin and cyclosporin A impair the tubular regeneration process by selectively altering the expression of marker genes associated with tubular epithelial differentiation and the functionality of the surviving differentiated PTELCs. This observation, therefore, raises the question of whether a similar situation could be observed in the above-mentioned second renal tubular epithelial regeneration pathway starting from surviving PTECs. To clarify this, we investigated in this current study whether the terminally differentiated PTELC can regain their ability to proliferate, which is a prerequisite for EMT-based tubular epithelial dedifferentiation, and what effects toxic substances have on this process.

3.4.2. Materials and Methods

3.4.2.1. Materials

All the material resources used in this study, such as cell lines, media, growth factors, small signalling molecules, antibodies, kits, primers, chemicals, and reagents, were purchased from the respective companies previously listed in Mboni-Johnston et al., [221]. The primers and antibodies used to detect the expression of various genes and proteins are listed in Tables 1 and 2 in the Appendix.

3.4.2.2. Methods

In this current project, an *in vitro* model based on human induced pluripotent stem cells (hiPSC) was used to investigate the influence of the genotoxic nephrotoxin cisplatin and the non-genotoxic nephrotoxin cyclosporin A (CsA) on renal tubular dedifferentiation processes. To this end, a modified protocol according to Kandasamy and colleagues [22] was used for differentiation into renal proximal tubular epithelial-like cells (PTELCs), as previously reported by Mboni-Johnston et al. [221] (**Fig. 25A**). In brief, 3000 hiPSC/cm² were seeded in renal epithelial growth medium (REGM) supplemented with Y-27632 dihydrochloride and the growth factors BMP 2/7 were added from day 2 and cultured under these conditions for 9 days, with the medium changed daily to induce differentiation into PTELCs. After differentiation, hiPSC-derived PTELCs were either directly treated with toxic doses of cisplatin for 24 h to induce tubular injury with subsequent daily medium change for 6 days or passaged once to allow the cells to dedifferentiate. During the dedifferentiation process, the dedifferentiating PTELCs (day 3) were directly treated with IC₂₀ and IC₅₀ of cisplatin and CsA generated with differentiated PTELCs from an earlier study for 24 h. After subsequent daily medium changes without BMP 2/7, the cells were harvested on day 7, and qPCR analysis, proliferation analysis, and immunocytochemistry were then performed as previously reported by Mboni-Johnston et al. [221] to investigate the effects of these toxins on the tubular dedifferentiation process. The data were expressed as mean and standard deviation of three independent experiments, and statistical analysis was performed using GraphPad Prism version 6 (GraphPad Software, San Diego, CA). Comparison between sample groups was performed using Student's t-test, and a p-value ≤ 0.05 was considered statistically significant.

3.4.3. Results

3.4.3.1. Differentiated hiPSC-derived PTELCs regain proliferation ability by undergoing EMT after passaging

An essential feature of proximal tubular dedifferentiation is the ability of proximal tubular epithelial cells (PTEC) to increase their proliferative capacity after injury, which is necessary for tubular epithelial regeneration [266]. In line with this concept, we wanted to address whether our differentiated PTELCs can also regain their capacity to proliferate after differentiation. To this end, PTELCs were generated from hiPSCs according to the differentiation protocol shown in **Fig. 25A** and two approaches were employed. In the first approach (**Fig. 25A₁**), PTELCs were passaged after differentiation and at 3 days post-passage, cell proliferation was analyzed by measuring EdU incorporation. As shown in **Fig. 25B**, EdU incorporation was significantly higher in passaged cells than in non-passaged PTELCs, indicating that PTELCs regained their ability to proliferate again after differentiation. Consistent with this observation, the morphology of the cells also changed from the characteristic cuboidal or cobblestone-shaped cells to elongated and spindle-shaped cells with anterior-to-posterior polarity, i.e. to a fibroblast-like morphology, within 7 days of cultivation (**Fig. 25C**). In addition, FITC-phalloidin staining of actin cytoskeletal organization showed a non-epithelial distribution, and tight-junction protein ZO-1 was expressed in the nuclei instead of its usual membrane location in passaged cells compared to unpassaged PTELCs (**Fig. 25C**).

To verify whether this increase in proliferation and change in morphology of passaged PTELCs was associated with the acquisition of an EMT phenotype, we characterized the mRNA and protein expression profiles for genes and proteins belonging to the epithelial (E-cadherin, Collagen IV, and ZO-1) and mesenchymal (Licam, Cadherin 11, Fibronectin, N-cadherin, Matrix metalloproteinase-2) genetic program in passaged and non-passaged PTELCs. As shown in **Fig. 25D**, after seven days of culture, all tested mesenchymal markers were up-regulated, whereas epithelial markers were down-regulated in passaged cells compared to non-passaged PTELCs (**Fig. 25D**). Consistent with these data, when staining for protein expression of the mesenchymal N-cadherin marker and epithelial E-cadherin marker, we also observed an increase in N-cadherin protein expression and a decrease in E-cadherin expression at seven days after passaging compared with non-passaged PTELCs, suggesting that PTELCs undergo EMT to start proliferating again (**Fig. 25E**).

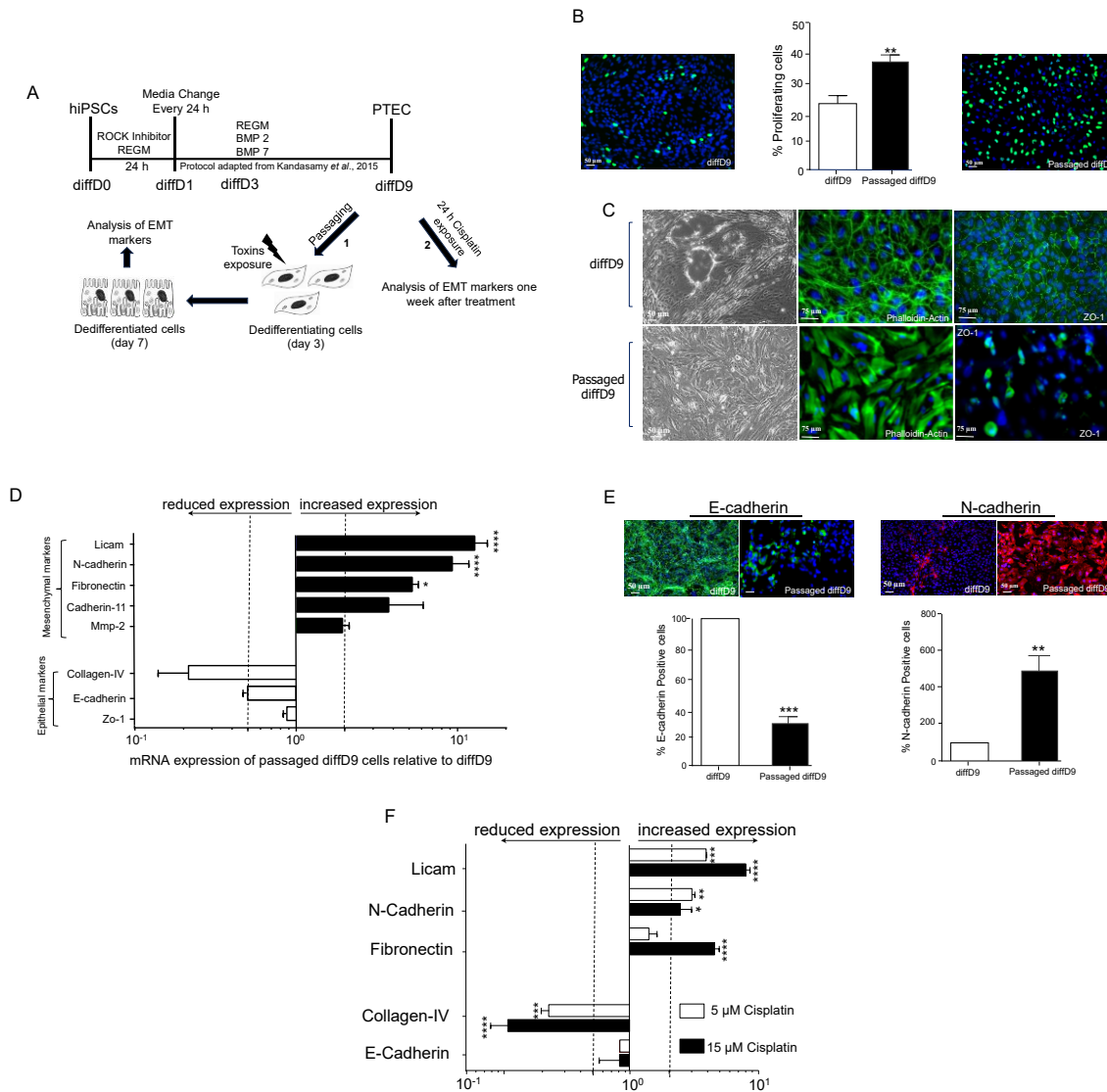


Figure 25: PTELCs regain their Proliferation capacity by undergoing EMT. (A) PTELCs were differentiated from hiPSCs according to the modified protocol of Kandasamy and colleagues. Differentiated PTELCs were either passaged and treated with cisplatin for 24 hours on day 3 (1) or directly treated with cisplatin for 24 hours (2) and analyzed after 7 days with daily medium changes. (B) The proliferation rate before and after the passage of diffD9 cells was quantified by the incorporation of fluorescent 5-ethynyl-2'-deoxyuridine (EdU) into the S-phase cells. The mean percentage of proliferating cells from 3 independent experiments and representative images are shown. (C) Light micrographs of the morphology of passaged and non-passaged PTELCs and visualization of selected proteins by immunocytochemical staining before and after passage. The antibodies against the different markers are visualized with FITC-coupled secondary antibodies, and the cell nuclei are stained with DAPI. The bars are 50 μm in size. (D) mRNA expression of epithelial markers (E-cadherin, collagen IV, ZO-1) and mesenchymal markers (fibronectin, N-cadherin, cadherin 11 Mmp-2, Licam) in passaged diffD9 cells compared to expression in unpassaged diffD9 cells, analyzed by quantitative RT-PCR. (E) Visualization and quantification of protein expression of E-cadherin and N-cadherin. (F) In the second approach displayed in Fig. 25A₂, qRT-PCR analysis of mRNA expression of EMT markers in diffD9 cells treated with IC₂₀ and IC₅₀ of cisplatin derived from diffD9 for 24 hours and cultured without differentiation factors for seven additional days with the indicated toxin concentrations compared to untreated diffD9 cells. Data from at least 3 independent experiments (qPCR also included 3 technical replicates) are expressed as mean + SD. *p≤0.5, **p<0.01, ***p<0.001 and ****p<0.0001 compared to non-passaged diffD9 cells (Student's t-test). Mmp-2: matrix metalloproteinase-2, ZO-1: zonula occludens-1, REGM = renal epithelial growth medium, ROCK = Rho-associated protein kinase, BMP = bone morphogenetic protein. diffD = differentiation day 0, 3 and 9. hiPSC = human induced pluripotent stem cells, PTELC= proximal tubular epithelial-like cells, EdU = 5-ethynyl-2'-deoxyuridine.

3.4.3.2. Impact of toxin treatment on the expression of EMT markers

The next question we wanted to address was whether treatment of terminally differentiated PTELCs during passage with the known nephrotoxins cisplatin and cyclosporin A affects the subsequent EMT-based dedifferentiation process of the surviving PTELCs fraction into terminally dedifferentiated PTELCs. To this end, mRNA expression of EMT markers in terminally dedifferentiated PTELCs (day 7: an appropriate time point when most of the EMT markers are most expressed based on preliminary work) was analyzed after 24 h treatment of dedifferentiating PTELCs (day 3) with IC_{20} and IC_{50} of cisplatin and CsA derived from differentiated PTELCs (**Fig. 25A**). As shown in **Fig. 26A**, treatment of the dedifferentiated PTELCs with IC_{20} and IC_{50} of cisplatin resulted in a dose-dependent decrease, significant for all genes in the higher dose samples except for vimentin, in the expression of all tested mesenchymal genes in the dedifferentiated PTELCs treated on day three compared to the untreated control. Conversely, treatment with cisplatin significantly increased the mRNA expression of the epithelial marker *ZO-1*. In contrast, the expression of *collagen IV* significantly decreased dose-dependently. The third epithelial marker, *E-cadherin*, on the other hand, was not significantly affected by treatment with cisplatin. Furthermore, like cisplatin, the IC_{20} and IC_{50} of CsA also led to a significant dose-dependent decrease in the expression of all tested mesenchymal phenotype genes in dedifferentiated PTELCs treated on day three compared to the untreated control (**Fig. 26B**). Apart from *ZO-1*, CsA also significantly reduced the expression of the epithelial markers *collagen IV* and *E-cadherin* in dedifferentiated PTELCs treated on day 3 with IC_{20} and IC_{50} compared to the untreated control.

To further validate our results, we conducted an additional experiment using a different approach (**Fig. 25A₂**). Since direct passage to examine the EMT phenotype in PTELCs is not physiological, we mimicked a toxic insult by treating the cells directly with toxic doses of cisplatin for 24 h after differentiation to induce injury. After six additional days of cultivation (day 7) with daily medium changes, we then checked for EMT markers. As shown in **Fig. 25F**, after seven days of cultivation, the cells demonstrated a significant upregulation of mesenchymal markers and downregulation of epithelial markers compared to the untreated differentiated PTELCs, confirming our earlier observations.

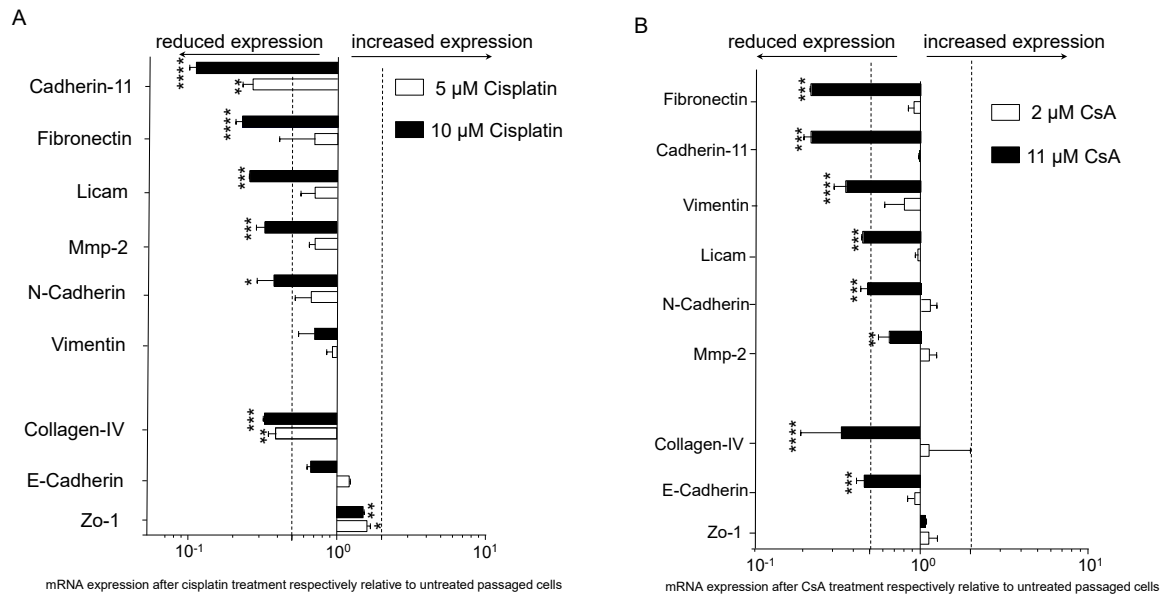


Figure 26: Effect of cisplatin and cyclosporin A on mRNA expression of EMT markers. Based on the treatment scheme shown in Fig. 25A₁, qRT-PCR analysis of mRNA expression of marker genes of untreated and treated passaged cells with the indicated concentrations of **(A)** cisplatin and **(B)** cyclosporin A on day 3 of the dedifferentiation process for 24 h. After daily medium changes, the mRNA expression of EMT markers was analyzed on day 7. Data from at least 2 independent experiments and 3 technical replicates are expressed as mean + SD. *p<0.05, **p<0.01, and ***p<0.001, and ****p<0.0001 compared with untreated passaged cells and unpassaged cells.

3.4.4. Discussion

An understanding of the tubular epithelial regenerative response after acute kidney injury (AKI) could shed light on the relationship between incomplete repair and the risk of future chronic kidney disease (CKD). While it is universally accepted that following AKI, tubular epithelial repair can result either from the differentiation of pre-existing intratubular stem cells or through the dedifferentiation of surviving tubular epithelial cells [94], there is a lack of information on the impact of AKI-inducing substances on these tubular epithelial regeneration processes, although it is known that some tubular epithelial cells resulting from these regeneration pathways lack full functionality [183, 184, 229]. Therefore, this study aims to build on our previous study by analysing the effect of nephrotoxic substances on tubular dedifferentiation to promote a comprehensive understanding of toxins on tubular epithelial repair capabilities. We utilized a previously modified one-step protocol to produce proximal tubule-like cells (PTELCs) from human induced pluripotent stem cells (hiPSCs). Subsequently, we induced dedifferentiation in these terminally differentiated cells through passaging and extensive cultivation. The PTELCs undergoing dedifferentiation were then exposed to IC₂₀ and IC₅₀ concentrations of cisplatin and CsA (diffD9), derived from a previous study [221]. We evaluated the impact of these toxins on the efficiency of PTELCs dedifferentiation by analysing EMT markers.

Interestingly, our results showed that passage of PTELCs after differentiation significantly increased their proliferative capacity compared to non-passaged PTELCs. Based on this result, we speculated that this increase in proliferation appears to be related to PTELCs entering the cell cycle again to initiate the dedifferentiation process. Consistent with this line of thinking, Vogtseder et al. [266] have already shown in rats using BrdU staining of rat kidney tissue that repair of injured areas results from the division of fully differentiated cells that are usually quiescent but dedifferentiate by increasing their proliferative behaviour [266]. Thus, an increase in proliferative capacity is an essential feature of PTECs dedifferentiation. Expectedly, the passage of differentiated PTELCs did not only increase their proliferate capacity but also changed their morphology from cobblestone-shaped to fibroblast-like. At the same time, changes in the actin cytoskeleton and expression of tight junction protein-1 were also observed within 7 days of passage, all of which are characteristic of an EMT phenotype. In line with these results, Chandrasekaran and colleagues also reported morphological changes in passaged iPSC-derived PTELCs generated from an utterly different

differentiation protocol [23]. Furthermore, their study could also show that the polarized cobblestone phenotype of the PTELCs could be maintained after passage in the presence of the GW788388 hydrate [23]. Thus, these results not only strongly emphasized the need to utilize GW788388 hydrate to prevent dedifferentiation in PTECs in culture but also provided additional evidence for the possible activation of an EMT phenotype during the dedifferentiation process since GW788388 hydrate is a selective inhibitor of TGF-beta, a key initiator of EMT and renal fibrosis [267]. Therefore, a central question that arises is whether the changes in morphology and the increase in proliferation during dedifferentiation in PTELCs imply a potential acquisition of an EMT phenotype. Indeed, our gene and protein expression data also indicate that 7 days after passaging, our PTELCs were undergoing a phenotypic transformation as evidenced by a phenotypic switch involving decreased expression of epithelial markers and increased expression of mesenchymal markers, demonstrating induction of an EMT phenotype compared to non-passaged cells. In agreement with this observation, Butt et al. [129] and Maeshima et al. [127] have reported that tubular epithelial cells undergo EMT and developed into proliferating mesenchymal cells that migrate into the denuded areas of the basement membrane. Thus, we speculate that our differentiated PTELCs acquired an EMT phenotype after passaging to dedifferentiate. Nevertheless, as passaging is not a normal physiological process, we also showed that exposing the cells immediately after differentiation to cisplatin-induced injury also induced an EMT phenotype after 7 days of cultivation, possibly to restore damaged areas. However, to address the question of whether toxicants can impair the EMT-induced dedifferentiation process of PTELCs, our data showed for the first time that cisplatin and CsA treatments selectively impaired the expression of EMT markers associated with PTELCs' dedifferentiation process, thus providing preliminary evidence for a possible alteration of PTELCs' dedifferentiation process by toxins. However, further experiments are necessary for a more precise understanding, as only the mRNA expression of specific markers of EMT was analyzed in this study.

In conclusion, this study confirms that terminally differentiated PTELCs undergo EMT one week after passage, and interestingly, this process can be interrupted by toxins such as cisplatin and CsA. Surprisingly, in addition to the passaged cells, differentiated PTELCs also undergo EMT immediately after cisplatin-induced injury. However, additional readouts are needed to confirm these findings and identify the most suitable physiological model for an in-depth understanding of the role of toxins in the EMT process in the kidney.

4. Overall discussion

Previous studies have shown that renal tubular epithelial function tends to decline after regeneration [127, 229, 230]. To understand the possible causes of this loss of renal epithelial cell function, it is crucial to investigate a possible role of toxins during the regeneration process. Therefore, we investigated the sensitivity and function of human induced pluripotent stem cells (hiPSC) during their differentiation into proximal tubular epithelial-like cells (PTELC) to known nephrotoxins and oxidative stress. We have shown for the first time that cells at different states of differentiation exhibit different sensitivities to the known nephrotoxic and oxidizing agents tested in this study, which the nature of the agents can partly explain. These substances also selectively altered the functionality and expression of proximal tubular epithelial cells (PTEC) genes during regeneration, which could have an unfavourable effect on the regeneration processes.

4.1. Differentiation of hiPSC generates cellular structures expressing markers of proximal tubular epithelial cells (PTELCs)

In principle, the human kidney stems from the intermediate mesoderm cells that differentiate into a nephron progenitor stage, the so-called metanephric mesenchyme, and eventually gives rise to proximal tubular cells and the glomerular podocytes [268]. In agreement with this concept, the protocol for differentiation of hiPSCs into PTELCs, adapted from Kandasamy et al., [22], utilizes bone morphogenetic proteins (BMP 2 and 7), a transforming growth factor of the TGF- β superfamily, which has been shown to promote growth of the intermediate mesoderm in developing kidney [269], supplemented in a renal epithelial growth medium from the second day of differentiation, recapitulated embryonic proximal tubular epithelial regeneration *in vitro* and produced hiPSC-derived PTELCs within 9 days [221]. When comparing hiPSC-derived PTELCs with hiPSCs, we observed that after the application of the one-step differentiation protocol, the morphology of the cells changed from the typical round morphology of hiPSCs to a more cuboidal, mononuclear renal epithelial cell-like morphology consisting of domes and tubular structures with a transepithelial resistance stabilized at 100 Ωcm^2 (**see SFig. 1**), which was also observed with a proximal tubular epithelial cell line RPTEC. This allowed initial conclusions to be drawn about the functional competence of the cells, as dome formation has been reported from polarized healthy tubular epithelial cells under *in vitro* culture conditions and indicates active trans-epithelial fluid transport and functional activity of the cells

[270]. Furthermore, the substantial decrease in proliferation over the time span of the differentiation process also emphasizes the pronounced degree of differentiation of the cells after 9 days. This finding is consistent with the results of Nadasdy et al. [98], who showed in 12 different intrinsic renal cell populations in 20 normal human kidneys that adult proximal tubule epithelial cells exhibit a slow proliferation rate.

In addition to displaying typical morphological structures that are characteristics of human proximal tubular epithelial cells (HPTEC), hiPSC-derived PTELCs after 9 days of differentiation also displayed PTEC marker gene expression patterns comparable to those of a commercially available RPTEC/Tert1 line while the significant downregulation of the *OCT3/4*, *NANOG*, and *SOX2* expression confirmed the loss of pluripotency. Noteworthy, in agreement with Kandasamy et al. [22], most of the markers analyzed in PTELCs, such as the pluripotent stem cell markers *OCT3/4*, *NANOG*, and *SOX2*, the epithelial markers E-cadherin and ZO-1, the PTEC markers *CAD-16* and *AQP-1*, and five out of nine transporters, showed a comparable change in the levels of mRNA expression. The post-differentiation expression levels are also consistent with the data of overlapping markers of PTELCs differentiated from hiPSC by another research group using an utterly different differentiation protocol [23]. Consistent with the mRNA data, *OCT-3/4* levels were also reduced at the protein level after differentiation, as demonstrated by immunocytochemistry, as also shown by Chandrasekaran et al. [23]. At the same time, the expression of epithelial and PTEC markers increased with the correct cellular localization, except *CD-13*, which is consistent with the corresponding markers studied by the other two groups [22, 23]. Moreover, more than 95% of PTELCs were positive for the HPTEC marker, aquaporin-1, after differentiation, as quantified by flow cytometry, indicating that the differentiation process was quite efficient, which was also observed by Kandasamy et al. [22]. Interestingly, the expression of *AQP-1* in the cells was also still significant, at least up to day 12 of differentiation, almost to the same extent as in the cells from day 9 (see **SFig. 1**), which indicates that the differentiation status of our PTELCs could be maintained over 72 h, which is essential for toxicity tests, especially for tests that go beyond an acute exposure of 24 h (repeated dose toxicity testing). Long-term stability is often a problem with iPSC-derived cells. Therefore, this protocol represents an improvement of the protocol previously reported by Kandasamy et al., [22] where direct differentiation of iPSCs into PTELCs lacked long-term stability, and the presence of proximal tubular specific markers was only detected 24 h after differentiation.

4.2. PTELCs Express PTEC transporters and recapitulate PTEC-specific transporters properties

Proximal tubular epithelial cells (PTECs) eliminate drugs, foreign substances and toxins, a task performed by apical and basolateral transporters [271]. These transporters are a unique feature of PTECs. They play an essential role in the movement of organic anions and cations, with elimination through the urine made possible by transport by PTECs, being an essential route in the detoxification process. Consistent with this concept, 9 of the 12 PTEC transporters studied were expressed at a similar level to the commercially available RPTEC/TERT1 line and exceeded the expression levels observed in hiPSCs. Transporters expressed at the physiological level include CTR-1 and -2, OAT-1 and -3, PEPT-1, PEPT-2, and OCTN-2, as well as megalin and cubilin, which are responsible for albumin uptake, an essential function of the proximal tubule [260]. However, the mRNA expression levels of other transporters studied, such as *OCT-2*, *MDR-1*, and *SGLT-2*, were decreased compared to hiPSCs. Interestingly, while *OCT-2*, a transporter involved in cisplatin uptake [197, 198], showed reduced mRNA expression, no substantial difference at the protein level was observed in PTELCs compared to hiPSCs. This discrepancy between mRNA and protein expression levels could be attributed to differences in stability, with proteins being more stable due to their long half-life compared to mRNA. Second, since the epithelialisation of cells seems to be crucial for obtaining pluripotent traits [195], additional epithelial cell-specific genes, in addition to the common epithelial markers currently being tested, might be expected to be already basally expressed in hiPSCs, e.g. transporters. Notably, studies have reported the expression of glucose transporter SGLT2 in pluripotent stem cells, which was found to be highly downregulated in our differentiated cells compared to hiPSCs [199, 200].

Besides showing essential expression of tubular transporters, the next question is whether these transporters are fully functional after differentiation. To this end, three functional assays were performed (**Fig. 12 and SFig 1**). The results showed that the differentiated PTELCs demonstrated megalin-dependent cubilin-mediated uptake of fluorescent albumin after 9 days of differentiation, which was also surprisingly maintained at least up to day 12 of differentiation, indicating sustained functionality post-differentiation. Similar albumin uptake activity was also observed with the tubular epithelial cell line LLC-PK1, which served as a positive control. In contrast, RPTEC/TERT1 cell line, used as a negative control, showed reduced albumin uptake, consistent with previous reports [23, 194]. The

presence of megalin and cubilin in the differentiated PTELCs supports their ability to transport albumin, as these receptors are essential for protein reabsorption, including albumin filtered into the glomeruli [260]. Furthermore, PTELCs exhibited uptake activity mediated by the organic anion transporter (OAT) after differentiation, as confirmed by inhibitory uptake assays with the OAT substrate 6-carboxyfluorescein (6-CF) and the inhibitor probenecid, confirming previous results in hiPSC-derived PTELC-containing organoids, an observation also previously reported in hiPSC-derived organoids containing PTELCs by Lawrence and colleagues [21].

In addition, functional transporters involved in the clearance of drugs or other substances from tubular epithelial cells are also another desirable, important feature for iPSC-derived PTELCs in the context of toxicity assay assessment. We also looked at the functional activity of the well-studied exporter transporter P-glycoprotein (Mdr-1). Due to its broad substrate affinity, Mdr-1 is one of the most studied efflux transporters in ADMET (absorption, distribution, metabolism, excretion, and toxicity) studies of pharmaceutical compounds. *MDR-1* was detected at a lower mRNA level in PTELCs, however, as has been observed for some other transporters, the expression of MDR-1 is not well represented by the mRNA levels [23, 272]. Using calcein acetoxymethyl ester (calcein-AM) as an Mdr-1 substrate and CsA as a potent substrate of Mdr-1 and a complementary inhibitor of calcein-AM, we were able to show that, despite low *MDR-1* mRNA levels, PTELCs showed increased efflux of calcein in the absence of CsA, demonstrating functional MDR-1 activity. In contrast, CsA-treated PTELCs showed increased CsA-inhibitable calcein accumulation (**see SFig. 1**). This observation was in line with previous studies conducted by Chandrasekaran et al. [23], who showed that hiPSC-derived PTELCs generated using a different differentiation protocol also showed Mdr-1 efflux activity after differentiation.

4.3. Sensitivity of hiPSC, hiPSC differentiating, and hiPSC differentiated into PTELCs towards known genotoxic and non-genotoxic nephrotoxins

Having shown that hiPSC can differentiate into PTELCs possessing many characteristics representative of PTECs, the primary aim of our work was to determine whether we will see specific differentiation-dependent sensitivity to different types of nephrotoxins, using this hiPSC-derived PTELC differentiation model as a case study. For this purpose, hiPSC, hiPSC differentiating into PTELC,

and hiPSC differentiated into PTELC were studied for their sensitivity to selected nephrotoxins. These included the genotoxic nephrotoxin cisplatin and the non-genotoxic nephrotoxin cyclosporine A. Our data showed for the first time that the defence system of the cells against cisplatin must have changed considerably with the differentiation process because undifferentiated hiPSC and differentiating hiPSC were the most sensitive to the genotoxin cisplatin, with an IC₅₀ of about 1 µM, although they showed different proliferation rates. Whereas fully differentiated PTELCs had the lowest proliferation rate and were not as sensitive, with an IC₅₀ of 18 µM almost 20 times higher. This was to be expected as cisplatin is a DNA-damaging agent known to interfere with DNA synthesis and replication in rapidly proliferating cells, such as stem cells [35]. However, to uncover the molecular mechanisms underlying the hypersensitivity of hiPSC and differentiating hiPSC to cisplatin, our findings revealed that the different cisplatin sensitivity of hiPSC and differentiating hiPSC compared with differentiated PTELCs may be due to variations in proliferation rates, as shown by the results of EdU incorporation measurements. Interestingly, cisplatin treatment had no significant effect on the proliferation itself of differentiating hiPSC compared to hiPSC despite their similar sensitivity to cisplatin. This suggests that the sensitivity of the differentiating cells to cisplatin may be linked to other cytotoxic effects of the drug. Intriguingly, we also showed that cisplatin and ionising radiation, used here as a positive control, induced the highest number of γ-H2AX foci in cells of this differentiation state compared with undifferentiated hiPSC and fully differentiated PTELCs, as measured by γ-H2AX immunofluorescence. In contrast, the expression of their basal DNA repair genes, which provide an indirect indication of the cell's repair capabilities, was significantly reduced when compared to undifferentiated hiPSC and fully differentiated PTELC. Saretzki and colleagues reported a similar observation, which showed that DNA damage levels increased during differentiation, whereas the expression of genes involved in different types of DNA repair decreased during the differentiation of human embryonic stem cells into different extraembryonic and embryonic differentiation stages [250]. These data thus suggested that DNA damage could significantly contribute to the increased sensitivity of differentiating cells to cisplatin.

Besides the induction of DNA damage, we also observed that all stages of differentiation, including hiPSCs and differentiated PTELCs, were susceptible to cisplatin-induced cell death rather than senescence. We speculated that DNA damage induced by cisplatin treatment could be the reason for this observed cell death. Consistent with these data, the co-treatment of cisplatin and the pan-

caspase inhibitor QVD, effectively restored cell viability. This observation suggests that the cell death induced by cisplatin is predominantly apoptotic. This result is somewhat unexpected because, in addition to apoptosis, cisplatin also induces other forms of cell death in cisplatin-treated cells, such as ferroptosis and necrosis [237-239].

In addition, renal tubular epithelial damage caused by xenobiotic-induced nephrotoxicity can lead to epithelial-mesenchymal transition (EMT) in renal tubular epithelial cells. Consistent with this notion, cisplatin-induced proximal renal tubular apoptosis was previously reported to be preceded by induction of an EMT phenotype involving actin cytoskeletal reorganisation associated with disruption of cell-matrix and cell-cell adhesion [243]. Similar to their observation, we found a downregulation in the expression of epithelial markers and an upregulation in the expression of mesenchymal markers at the RNA and protein levels, suggesting a phenotypic switch with EMT-induced features in our differentiated PTELCs following cisplatin-mediated injury.

Regarding the pattern of CsA toxicity in cells, we observed that the proliferation rate of undifferentiated hiPSCs and differentiated PTELCs was significantly reduced after CsA treatment. Confirming this finding, Lally et al. [244] and Seki et al. [245] also observed a decrease in proliferative capacity in cultured tubular epithelial and mesenchymal cells, respectively, but not in stem cells after CsA treatment. Our investigation into the potential activation of senescence mechanisms revealed that CsA preferentially induced early signs of premature senescence in undifferentiated hiPSCs but not in differentiated stem cells. This finding is in marked contrast to previous studies suggesting that CsA induces cellular senescence in human renal tubular epithelial cells [247]. We acknowledge that further experiments, such as senescence-associated β -galactosidase staining, telomere length determination, and cell cycle analysis, are necessary for clarification. However, our preliminary findings suggest that the sensitivity of hiPSCs and differentiated cells to CsA may not depend on senescence activation. Our research revealed that differentiating hiPSCs and differentiated PTELCs were particularly susceptible to CsA-induced cell death, predominantly through apoptotic mechanisms, in contrast to undifferentiated hiPSCs. This is in line with previous studies indicating that CsA induced apoptosis in renal proximal tubular cell lines [244, 248]. Furthermore, our study revealed that CsA-induced nephrotoxicity, like cisplatin, induced an EMT phenotype in renal PTELCs. This observation suggests that this EMT phenotype may represent an initial response to repair CsA-induced

damage in renal tubular epithelial cells or a prerequisite for renal fibrosis and death of damaged renal epithelial cells by apoptosis, an observation similar to that previously reported by McMorrow et al. [249] who showed that CsA directly induced EMT in renal tubular epithelial cells.

Treatment with cisplatin and cyclosporin A not only reduced cell viability by causing DNA damage, apoptosis, and phenotypic transformation but also selectively affected the expression of differentiation-related markers and transporter proteins, including the albumin transporters megalin and cubulin in differentiated progeny. Consequently, the function of albumin uptake in the cells was reduced drastically. Surprisingly, this effect was even more prominent in the treated PTELCs progenitor cells differentiated into PTELCs compared to PTELCs treated after differentiation. Thus, these data suggest that even an acute exposure of differentiating PTELC precursors to cisplatin and cyclosporin A might affect the differentiation and functionality of the surviving progeny. This finding could explain the observed loss of renal epithelial function after regeneration from AKI. However, further experiments are necessary for a more comprehensive understanding, as only mRNA expression of specific tubular differentiation markers and albumin uptake activity were analysed in this study.

4.4. Sensitivity of hiPSC, hiPSC differentiating, and hiPSC differentiated into PTELCs towards known oxidative stress inducing agents

Since damage to the proximal tubular epithelium is also caused by oxidative stress [73, 232, 253], we investigated not only the effects of known nephrotoxic drugs on tubular differentiation but also how oxidative stress affects the sensitivity of cells at different stages of the tubular differentiation process. Surprisingly, our study showed for the first time that differentiating hiPSCs were more susceptible to oxidants such as H₂O₂, menadione and TBHQ compared to undifferentiated hiPSCs and fully differentiated PTELCs. This result is of crucial importance from a toxicological point of view, as it suggests that stem cells differentiating into PTELCs are particularly susceptible to oxidative stress induced by oxidising agents. Moreover, we have shown that these oxidants induce oxidative stress in our cells at different stages of differentiation compared to the untreated control cells, as revealed by the increased expression of the surrogate oxidative stress marker 4-hydroxy-2-nonenal (4-HNE). Interestingly, this marker seems to be more expressed in the differentiating cells than in the other stages of differentiation (**see**

Fig S4). To explain this increased susceptibility of differentiating cells to oxidative stress, our gene expression data showed a significant decrease in antioxidant defences during cell differentiation, with major antioxidant genes downregulated in differentiating cells compared to fully differentiated cells. In agreement with this finding, Saretzki et al. [250] also observed a decrease in antioxidant defences during differentiation, highlighting the impact of differentiation on the antioxidant capacity of cells. Based on this low expression of redox genes in differentiating cells, we hypothesised that stem cells differentiating into PTELCs are likely to have significantly reduced redox properties on the third day of differentiation. Consequently, their antioxidant defence would be weakened, and the oxidative stress induced by the oxidants would increasingly exceed the buffering capacity of the cell, which would significantly impair viability. In addition, further experiments are needed to determine whether this increased sensitivity of differentiating cells to oxidants may be because the differentiating cells are also more vulnerable to the cytotoxic effects of oxidative stress induced by these substances, such as mitochondrial damage, oxidative DNA damage and direct activation of apoptosis [253]; and as also reviewed by [73].

Accordingly, to gain a more profound understanding of the molecular mechanisms behind the increased sensitivity of differentiating cells to oxidising agents, we focused on menadione and TBHQ, as they are stable and easy to handle in cells. Our research has shown that these substances not only inhibit proliferation but also induce apoptosis in differentiating cells. This practical application of our findings is of great importance as it provides insights into the specific effects of oxidising agents on cells at different stages of differentiation, potentially leading to future therapeutic strategies. Xiao and colleagues investigated the effect of H₂O₂-induced oxidative stress on bone marrow stem cells (MAPCs), their endothelial differentiation, and underlying mechanisms *in vitro* [252]. Contrary to our result, they observed a rather significant inhibition of proliferation and dose-dependent induction of apoptosis in the undifferentiated MAPCs [252]. Nevertheless, this study did not investigate the effect of H₂O₂ on MAPCs differentiating into endothelial cells and on MAPC-derived endothelial cells. In addition, Rhyu et al. and Wang et al. have shown that H₂O₂-induced oxidative stress induces EMT in the rat proximal tubular epithelial cell line NRK-52E [257, 258]. However, we did not observe a phenotype change characteristic of EMT induction in our differentiated PTELCs after menadione and TBHQ-induced injury, a result that was also observed in a human PTEC model after H₂O₂-induced injury by Khan et al. [253].

Exposure to menadione and TBHQ not only significantly reduced cell viability but also impaired the functionality of differentiated PTELCs and the expression of individual marker genes associated with tubular differentiation. Interestingly, menadione exposure reduced mRNA expression of the PTEC transporter megalin, possibly explaining the loss of albumin uptake capacity, while TBHQ, on the other hand, increased megalin expression, leading to a corresponding increase in albumin uptake in differentiated PTELCs. These contradictory effects observed here between these two oxidants may be because they activate different signaling pathways involved in megalin/cubilin endocytosis system and, therefore, the different effects. Despite these contradictory effects on megalin expression, previous studies have shown that H₂O₂-induced oxidative stress increases megalin expression in another cell line [259]. Although other substances that induce oxidative stress, such as cisplatin, are known to bind to megalin and interfere with its interaction with its ligands, including albumin, to our knowledge, there are no reports that this is the case with menadione or TBHQ. Further studies are needed to clarify how these oxidative stress inducers affect megalin expression in PTECs. In addition, we observed that both compounds significantly decreased the PTEC marker aquaporin 1 in the differentiated PTELCs. Although there is no evidence in the literature, it is noteworthy that mitochondrial oxidative stress induced by manganese (III)-tetrakis (4-benzoic acid) porphyrin chloride (MnTBAP) in obstructive kidney disease also leads to downregulation of aquaporins, including aquaporin 1 [261].

4.5. Differentiated PTELC dedifferentiated by acquiring an EMT phenotype and this phenotype is impaired by nephrotoxic substances

The regenerative response of proximal tubular epithelial cells (PTEC) to acute kidney injury (AKI) is not only due to the differentiation of the preexisting intratubular stem cell population into new PTEC but also largely due to the dedifferentiation of the surviving uninjured PTEC [94, 99]. Therefore, to gain a comprehensive understanding of the causes of the loss of renal functionality after regeneration, the impact of toxic substances on the PTEC dedifferentiation process was also investigated, in addition to the effects of toxins on the differentiation of PTEC from stem cells.

Dedifferentiation refers to the direct transformation of one differentiated cell type into another by acquiring intermediate tubular epithelial progenitor properties. It has been proposed as a central mechanism for proximal tubule repair and is

characterised by an intense proliferation of epithelial cells in the proximal tubule [273]. Analysis of the proliferation behaviour in the proximal tubule showed that the production of new epithelial cells in the proximal tubule largely results from the division of fully differentiated epithelial cells that are usually quiescent but dedifferentiated after injury [266]. After injury, all surviving fully differentiated tubule cells have an equal chance to rapidly enter the cell cycle to contribute to epithelial regeneration [101]. In agreement with this observation, our EdU incorporation measurements in a model where cells were injured by subculturing (which involves the use of the protease trypsin to cleave tight junction proteins and adherence molecules between the extracellular matrix of the cells, resulting in injury) showed that passaging the fully differentiated PTELCs significantly increased their proliferation capacities compared to the unpassaged PTELCs. This finding thus lends support to the previous hypothesis suggesting that terminally differentiated PTEC increase their proliferative capacity after injury to dedifferentiate and replace lost neighbouring tubular epithelial cells by proliferative self-duplication.

Moreover, the passage of PTELCs induced fibroblast-like morphology and led to a change in the orientation and location of the actin cytoskeleton and tight junction proteins, an observation also reported by Chandrasekaran and colleagues [23]. Therefore, the central question is whether the changes in morphology and the increase in proliferation capacity during dedifferentiation of PTELCs also involve a phenotypic switch characteristic of EMT induction, as previously reported by Bonventre [99] and Zhuang et al. [107]. Interestingly, our gene and protein expression data suggest that our differentiated PTELCs underwent EMT within 7 days of passage, as evidenced by the phenotypic switch that included a decrease in epithelial marker expression and an increase in mesenchyme marker expression, which is a hallmark of EMT induction compared to the non-passaged cells. Overall, we can surmise that our fully differentiated PTELCs acquired an EMT phenotype after passage to proliferate and dedifferentiate. However, although the passaging of PTELC did model the *in vivo* tubular regenerative model where PTEC undergo an EMT-induced dedifferentiation, as the passaging is not a normal physiological process, we have shown that direct exposure of the cells after differentiation to cisplatin-induced damage also initiated the induction of an EMT phenotype, possibly to restore damaged areas. However, additional experiments are required for further clarification, e.g., performing a scratch assay in which an injured area is created, and the extracellular matrix of the cell monolayer is destroyed to determine whether this scratched area can also be repaired by inducing an EMT phenotype.

Nevertheless, to address the question of whether toxicants can impair the EMT-induced dedifferentiation process of PTELCs, our data present a novel insight into the potential impairment of the dedifferentiation process of PTEC by toxins. For the first time, we have shown that treatment with cisplatin and cyclosporin A selectively impaired the expression of markers associated with the EMT phenotype during the dedifferentiation process of PTELCs. This finding sparks further curiosity and the need for more detailed experiments to fully understand the implications, as only the mRNA expression of specific EMT markers was analysed in this study.

5. Limitations and Outlook

Although PTELCs exhibit expression of several necessary transporters and features specific to renal proximal tubular cells, including organic anion transporter (OAT)-mediated uptake activity, P-glycoprotein efflux, and functional albumin transport (which the tubular epithelial cell line RPTEC/TERT1, for example, are not capable of), we recognise that they have limitations. While more than 95% of our hiPSC-derived PTELCs showed increased expression of the specific marker for proximal tubules such as aquaporin 1, we cannot claim at this point that our PTELCs represents a pure population. In this context, analyses of the expression of markers characteristic of neurons, endothelial cells, podocytes, cells of the loop of Henle, distal tubular cells and cells of the collecting duct must be performed in the future to exclude the existence of other cell types. To strengthen the *in vivo* relevance of our model, a detailed molecular and functional characterisation between our hiPSC-derived PTELCs and primary PTEC or tissues would be helpful. Moreover, more hiPSC lines, especially those of renal origin, should be included in the future, not only to compensate for the influence of possible epigenetic memory but also to address the inherent variability issues usually observed between hiPSC lines [165].

Furthermore, like most hiPSC-based cell models, our PTELCs still need to be fully mature compared to adult human kidney cells and may not express the entire constellation of proximal tubular-specific genes and xenobiotic metabolising enzymes. Therefore, adjustments to the culture conditions will be necessary to achieve better maturation. This could include using other small molecules, such as the glycogen synthase kinase 3-inhibitor CHIR99021 and the activator of retinoic acid receptors TTNPB [23], in addition to the growth factors BMP 2 and 7 to push the cells further into the renal tubule lineage. In addition, modifications of the

culture conditions, such as different extracellular matrix components, need to be utilised to mimic the 3D microenvironment present *in vivo*. Furthermore, different apical and basal media need to be tested in the future to expose the cells to toxins in a matrix more similar to primary urine. Maturation of the cells can also be achieved by coculture with other cell types in the kidney, such as endothelial cells, which has already been reported to improved structural and functional maturation of PTEC in a microfluidic model [274]. We do not claim that the model presented here can adequately represent PTEC differentiation *in vivo*. Instead, we propose it as a potentially useful *in vitro* tool to explore the effects of toxins during renal regeneration. In this regard, we have only addressed the acute 24-h toxicity of oxidative stress and known nephrotoxic drugs on the tubular regeneration process. However, as chronic renal damage is more problematic, this model will also be used in the future to investigate the effects of chronic toxicity on tubular regeneration by performing repeated dose toxicity tests using suboptimal doses, as the differentiation status of PTELCs could be maintained over several days.

6. Summary

In this study, we aimed to investigate the effects of nephrotoxins and oxidative stress on the differentiation and dedifferentiation of renal proximal tubular epithelial cells (PTEC). PTEC are constantly subjected to potentially harmful metabolites and oxidants during detoxification and excretion of foreign substances such as drugs and xenobiotics into the urine, which can lead to tubular epithelial damage and death, resulting in acute kidney injury. Nevertheless, the regenerative potential of the kidney allows the replacement of damaged cells either by local stem cell differentiation or by restoring the proliferative properties of surviving PTEC. However, it is known that kidney function still declines, suggesting that the damaged cells are not replaced by fully functional cells.

To fully understand the possible causes of this loss of renal cell function, it would be useful to understand the role of toxins during the tubular regeneration process. Therefore, we investigated the response of human induced pluripotent stem cells (hiPSCs) to known nephrotoxins and oxidising agents during their differentiation into proximal tubular epithelial-like cells (PTELCs). Our aim was to establish models of human induced pluripotent stem cells (hiPSCs) differentiating into proximal tubular epithelial-like cells (PTELCs) to recapitulate the two tubular epithelial regeneration pathways *in vitro* and to use these models to study the responses of the cells at different stages of regeneration to selected known toxins. These included the genotoxic nephrotoxin cisplatin, the non-genotoxic nephrotoxin cyclosporin A and the oxidising agents hydrogen peroxide (H₂O₂), menadione, and tert-butylhydroquinone (TBHQ).

In the first model used to recapitulate PTEC regeneration from stem cell differentiation, hiPSC differentiated into PTELC that exhibited a variety of typical morphological features, increased expression of prototypic markers and transporters of PTEC and were also capable of functional PTEC features such as megalin/cubulin and OAT-mediated transport and exhibited p-glycoprotein efflux function. Our hiPSC-derived PTELC model was used to analyse the response of undifferentiated hiPSC, differentiating hiPSC, and hiPSC differentiated from PTELC to the selected toxins. Our results showed that hiPSC and differentiating hiPSC exhibited the same sensitivity to the genotoxin cisplatin, with an IC₅₀ of about 1 µM, although they showed different proliferation rates. In addition, differentiated cells had the lowest proliferation rate and were not as sensitive, with almost twenty times higher IC₅₀. Concerning the non-genotoxic cyclosporin A, cells of all three differentiation stages showed similar sensitivity. Surprisingly,

differentiating hiPSCs were more susceptible to oxidative stress induced by all three oxidants tested than hiPSCs and PTELCs. When investigating the nature of toxicity, DNA repair and antioxidant defence genes were most downregulated in differentiating hiPSCs compared to hiPSCs and PTELCs. Accordingly, cisplatin and ionising radiation (used as a positive control) induced the highest amount of γ H2AX foci in cells of this differentiation state. Oxidising agents and cisplatin induced apoptosis at all differentiation stages, and cyclosporin A also induced senescence. EMT was most strongly induced by cyclosporin A, followed by cisplatin, while the oxidising agents did not upregulate EMT markers to a relevant extent. Overall, these results show the diverse reaction of cells at different differentiation states to substances with varying modes of action. While it is evident that a DNA-damaging substance like cisplatin has the highest impact on fast-growing proliferating cells, the deleterious effect of oxidants on differentiating cells was unexpected.

In the second model used to recapitulate tubular epithelial dedifferentiation, we demonstrated that our differentiated PTELCs could dedifferentiate after passage by increasing their proliferative capacity, an essential feature of proximal tubular dedifferentiation. Moreover, analysis of the passaged PTELCs showed that they exhibited fibroblast-like morphology and upregulated EMT-associated markers. This suggests that the cells adopted an EMT phenotype, enabling their re-entry into the cell cycle to proliferate and dedifferentiate, thus contributing to tubular epithelial regeneration. Interestingly, this EMT-based dedifferentiation process was significantly disrupted by treatment with cisplatin and cyclosporin A, as shown by the change in expression of EMT-associated genes. Together, these data provided further evidence, thus supporting our hypothesis that nephrotoxic substances and oxidative stress can impede tubular epithelial regeneration. Our results indicate a high sensitivity of the differentiating cells to toxins, which could have an unfavourable effect on the regeneration processes. Therefore, our model of hiPSCs differentiating into cells that recapitulate proximal tubular epithelial cells not only morphologically but also in their mRNA and protein expression patterns and functions appears suitable to investigate toxins' influence on kidney regeneration processes in more detail in the future.

7. References

1. Al-Awqati, Q. and J.A. Oliver, *Stem cells in the kidney*. *Kidney Int*, 2002. **61**(2): p. 387-95.
2. Faria, J., S. Ahmed, K.G.F. Gerritsen, et al., *Kidney-based in vitro models for drug-induced toxicity testing*. *Arch Toxicol*, 2019. **93**(12): p. 3397-3418.
3. Choudhury, D. and Z. Ahmed, *Drug-associated renal dysfunction and injury*. *Nat Clin Pract Nephrol*, 2006. **2**(2): p. 80-91.
4. Vaidya, V.S., M.A. Ferguson, and J.V. Bonventre, *Biomarkers of acute kidney injury*. *Annu Rev Pharmacol Toxicol*, 2008. **48**: p. 463-93.
5. Tiong, H.Y., P. Huang, S. Xiong, et al., *Drug-induced nephrotoxicity: clinical impact and preclinical in vitro models*. *Mol Pharm*, 2014. **11**(7): p. 1933-48.
6. Lote, C.J., *Essential anatomy of the kidney principles of renal physiology*. Springer, New York, 2012: p. 21–32.
7. Adhipandito, C.C., SH.; Lin, Y.H.; Wu, S.H. , *Atypical Renal Clearance of Nanoparticles Larger Than the Kidney Filtration Threshold*. *Int J Mol Sci*, 2021. **22**(20): p. 11182.
8. Quaggin, S.E. and J.A. Kreidberg, *Development of the renal glomerulus: good neighbors and good fences*. *Development*, 2008. **135**(4): p. 609-20.
9. Suh, J.H. and J.H. Miner, *The glomerular basement membrane as a barrier to albumin*. *Nature Reviews Nephrology*, 2013. **9**(8): p. 470-477.
10. Ballermann, B.J.S., R.V., *Resolved: capillary endothelium is a major contributor to the glomerular filtration barrier*. *J Am Soc Nephrol.*, 2007. **18**(9): p. 2432-8.
11. Maunsbach, A.B., *Observations on the segmentation of the proximal tubule in the rat kidney. Comparison of results from phase contrast, fluorescence and electron microscopy*. *J Ultrastruct Res*, 1966. **16**(3): p. 239-58.
12. Wang, K. and B. Kestenbaum, *Proximal Tubular Secretory Clearance: A Neglected Partner of Kidney Function*. *Clin J Am Soc Nephrol*, 2018. **13**(8): p. 1291-1296.
13. International Transporter, C., K.M. Giacomini, S.M. Huang, et al., *Membrane transporters in drug development*. *Nat Rev Drug Discov*, 2010. **9**(3): p. 215-36.
14. Nigam, S.K., W. Wu, K.T. Bush, et al., *Handling of Drugs, Metabolites, and Uremic Toxins by Kidney Proximal Tubule Drug Transporters*. *Clin J Am Soc Nephrol*, 2015. **10**(11): p. 2039-49.
15. S.K., N., *The SLC22 Transporter Family: A Paradigm for the Impact of Drug Transporters on Metabolic Pathways, Signaling, and Disease*. *Annu Rev Pharmacol Toxicol*, 2018. **58**: p. 663-687.
16. Nielsen, R., H. Birn, S.K. Moestrup, et al., *Characterization of a kidney proximal tubule cell line, LLC-PK1, expressing endocytotic active megalin*. *J Am Soc Nephrol*, 1998. **9**(10): p. 1767-76.
17. Maunsbach, A.B., D. Marples, E. Chin, et al., *Aquaporin-1 water channel expression in human kidney*. *J Am Soc Nephrol*, 1997. **8**(1): p. 1-14.
18. Eshbach, M.L. and O.A. Weisz, *Receptor-Mediated Endocytosis in the Proximal Tubule*. *Annu Rev Physiol*, 2017. **79**: p. 425-448.
19. Eirin, A., A. Lerman, and L.O. Lerman, *The Emerging Role of Mitochondrial Targeting in Kidney Disease*. *Handb Exp Pharmacol*, 2017. **240**: p. 229-250.
20. Naughton, C.A., *Drug-induced nephrotoxicity*. *Am Fam Physician*, 2008. **78**(6): p. 743-50.
21. Lawrence ML, E.M., Morlock M, Liu W, Liu S, Palakkan A, Seidl LF, Hohenstein P, Sjögren AK, Davies JA. , *Human iPSC-derived renal organoids engineered to report oxidative stress can predict drug-induced toxicity*. *iScience*, 2022. **25**(3): p. 103884.
22. Kandasamy, K., J.K. Chuah, R. Su, et al., *Prediction of drug-induced nephrotoxicity and injury mechanisms with human induced pluripotent stem cell-derived cells and machine learning methods*. *Sci Rep*, 2015. **5**: p. 12337.

23. Chandrasekaran, V., G. Carta, D. da Costa Pereira, et al., *Generation and characterization of iPSC-derived renal proximal tubule-like cells with extended stability*. Sci Rep, 2021. **11**(1): p. 11575.
24. Liang, Y., S. Li, and L. Chen, *The physiological role of drug transporters*. Protein Cell, 2015. **6**(5): p. 334-50.
25. Ferguson, M.A., V.S. Vaidya, and J.V. Bonventre, *Biomarkers of nephrotoxic acute kidney injury*. Toxicology, 2008. **245**(3): p. 182-93.
26. OpenStax, ed. *Anatomy & Physiology*.: 1st ed. Physiology of Urine Formation: Glomerular Filtration, ed. L.M.B.S.B.S.D.A.H.R.H.J.K.M.L.P.M.K.M.-G.K.O.D.Q.J. Runyeon; OSU OERU; and OpenStax. 2019, Creative Commons Attribution ShareAlike.
27. Lameire, N., W. Van Biesen, and R. Vanholder, *Acute renal failure*. Lancet, 2005. **365**(9457): p. 417-30.
28. Kleinknecht, D., P. Landais, and B. Goldfarb, *Drug-associated acute renal failure. A prospective collaborative study of 81 biopsied patients*. Adv Exp Med Biol, 1987. **212**: p. 125-8.
29. Chawla LS, E.P., Star RA, Kimmel PL. , *Acute kidney injury and chronic kidney disease as interconnected syndromes*. N Engl J Med, 2014. **371** (1): p. 58-66.
30. Coca, S.G., S. Singanamala, and C.R. Parikh, *Chronic kidney disease after acute kidney injury: a systematic review and meta-analysis*. Kidney Int, 2012. **81**(5): p. 442-8.
31. Chertow, G.M., E. Burdick, M. Honour, et al., *Acute kidney injury, mortality, length of stay, and costs in hospitalized patients*. J Am Soc Nephrol, 2005. **16**(11): p. 3365-70.
32. Webster, A.C., E.V. Nagler, R.L. Morton, et al., *Chronic Kidney Disease*. Lancet, 2017. **389**(10075): p. 1238-1252.
33. Barnett, L.M.A. and B.S. Cummings, *Nephrotoxicity and Renal Pathophysiology: A Contemporary Perspective*. Toxicol Sci, 2018. **164**(2): p. 379-390.
34. Cepeda, V., M.A. Fuertes, J. Castilla, et al., *Biochemical mechanisms of cisplatin cytotoxicity*. Anticancer Agents Med Chem, 2007. **7**(1): p. 3-18.
35. Wang, D. and S.J. Lippard, *Cellular processing of platinum anticancer drugs*. Nat Rev Drug Discov, 2005. **4**(4): p. 307-20.
36. Siddik, Z.H., *Cisplatin: mode of cytotoxic action and molecular basis of resistance*. Oncogene, 2003. **22**(47): p. 7265-79.
37. Fink, D., Howell, S.B. , *How Does Cisplatin Kill Cells?*, in *Platinum-Based Drugs in Cancer Therapy. Cancer Drug Discovery and Development*, L.R. In: Kelland, Farrell, N.P. (eds), Editor. 2000, Humana Press: Totowa, NJ.
38. Sastry, J. and S.J. Kellie, *Severe neurotoxicity, ototoxicity and nephrotoxicity following high-dose cisplatin and amifostine*. Pediatr Hematol Oncol, 2005. **22**(5): p. 441-5.
39. Arany, I. and R.L. Safirstein, *Cisplatin nephrotoxicity*. Semin Nephrol, 2003. **23**(5): p. 460-4.
40. El-Gerbed, M.s.A., *Ameliorative effect of fish oil on the cisplatin induced hepatotoxicity and nephrotoxicity in rats*. Research Journal of Pharmaceutical, Biological and Chemical Sciences, 2013. **4**: p. 479-491.
41. Ozkok, A. and C.L. Edelstein, *Pathophysiology of cisplatin-induced acute kidney injury*. Biomed Res Int, 2014. **2014**: p. 967826.
42. Pabla, N. and Z. Dong, *Cisplatin nephrotoxicity: mechanisms and renoprotective strategies*. Kidney Int, 2008. **73**(9): p. 994-1007.
43. Miller, R.P., R.K. Tadagavadi, G. Ramesh, et al., *Mechanisms of Cisplatin nephrotoxicity*. Toxins (Basel), 2010. **2**(11): p. 2490-518.
44. Ciarimboli, G., *Membrane transporters as mediators of cisplatin side-effects*. Anticancer Res, 2014. **34**(1): p. 547-550.
45. Faubel, S.L., E.; Reznikov, L.; Ljubanović, D.; Hoke, T.S.; Somerset, H.; Oh, D.; Lu, L.; Klein, C.; Dinarello, C.; Edelstein, C. , *Cisplatin-Induced Acute Renal Failure Is Associated with an Increase in the Cytokines Interleukin (IL)-1 β , IL-18,*

- IL-6, and Neutrophil Infiltration in the Kidney*. J Pharmacol Exp Ther., 2007. **322**: p. 8–15.
46. Akcay, A., Q. Nguyen, and C.L. Edelstein, *Mediators of inflammation in acute kidney injury*. Mediators Inflamm, 2009. **2009**: p. 137072.
 47. Basu, A. and S. Krishnamurthy, *Cellular responses to Cisplatin-induced DNA damage*. J Nucleic Acids, 2010. **2010**.
 48. Jiang, M., X. Yi, S. Hsu, et al., *Role of p53 in cisplatin-induced tubular cell apoptosis: dependence on p53 transcriptional activity*. Am J Physiol Renal Physiol, 2004. **287**(6): p. F1140-7.
 49. Cummings, B.S. and R.G. Schnellmann, *Cisplatin-induced renal cell apoptosis: caspase 3-dependent and -independent pathways*. J Pharmacol Exp Ther, 2002. **302**(1): p. 8-17.
 50. Ciccia A, E.S., *The DNA damage response: making it safe to play with knives*. . Mol Cell., 2010. **40**(2): p. 179-204.
 51. Roos WP, T.A., Kaina B. , *DNA damage and the balance between survival and death in cancer biology*. Nat Rev Cancer, 2016. **16**(1): p. 20-33.
 52. Harper, J.W. and S.J. Elledge, *The DNA damage response: ten years after*. Mol Cell, 2007. **28**(5): p. 739-45.
 53. Shiloh, Y., *ATM and ATR: networking cellular responses to DNA damage*. Curr Opin Genet Dev, 2001. **11**(1): p. 71-7.
 54. Levine, A.J., *p53: 800 million years of evolution and 40 years of discovery*. Nat Rev Cancer, 2020. **20**(8): p. 471-480.
 55. Vousden K.H, P.C.C., *Blinded by the Light: The Growing Complexity of p53*. Cell, 2009. **137**(3): p. 413-431.
 56. Pabla, N., Z. Ma, M.A. McIlhatton, et al., *hMSH2 recruits ATR to DNA damage sites for activation during DNA damage-induced apoptosis*. J Biol Chem, 2011. **286**(12): p. 10411-8.
 57. Wang, J., N. Pabla, C.Y. Wang, et al., *Caspase-mediated cleavage of ATM during cisplatin-induced tubular cell apoptosis: inactivation of its kinase activity toward p53*. Am J Physiol Renal Physiol, 2006. **291**(6): p. F1300-7.
 58. Kim YJ, K.T., Park SR, Kim HT, Ryu SY, Jung JY. , *Expression of the Mre11-Rad50-Nbs1 complex in cisplatin nephrotoxicity*. Environ Toxicol Pharmacol, 2015. **40**(1): p. 12–17.
 59. Borel, J.F., C. Feurer, C. Magnee, et al., *Effects of the new anti-lymphocytic peptide cyclosporin A in animals*. Immunology, 1977. **32**(6): p. 1017-25.
 60. Cecka, J.M. and P.I. Terasaki, *The UNOS Scientific Renal Transplant Registry--1991*. Clin Transpl, 1991: p. 1-11.
 61. Wu, Q., X. Wang, E. Nepovimova, et al., *Mechanism of cyclosporine A nephrotoxicity: Oxidative stress, autophagy, and signalings*. Food Chem Toxicol, 2018. **118**: p. 889-907.
 62. BF., E., *Do we know the site of action of cyclosporin?* Immunology Today, 1992. **13**(12): p. 487-490.
 63. Busauschina, A., P. Schnuelle, and F.J. van der Woude, *Cyclosporine nephrotoxicity*. Transplant Proc, 2004. **36**(2 Suppl): p. 229S-233S.
 64. Maia, R.C., M.K. Carrico, C.E. Klumb, et al., *Clinical approach to circumvention of multidrug resistance in refractory leukemic patients: association of cyclosporin A with etoposide*. J Exp Clin Cancer Res, 1997. **16**(4): p. 419-24.
 65. da Silva, J.B., M.H. de Melo Lima, and S.R. Secoli, *Influence of cyclosporine on the occurrence of nephrotoxicity after allogeneic hematopoietic stem cell transplantation: a systematic review*. Rev Bras Hematol Hemoter, 2014. **36**(5): p. 363-8.
 66. Hows, J.M., P.M. Chipping, S. Fairhead, et al., *Nephrotoxicity in bone marrow transplant recipients treated with cyclosporin A*. Br J Haematol, 1983. **54**(1): p. 69-78.
 67. Naesens, M., D.R. Kuypers, and M. Sarwal, *Calcineurin inhibitor nephrotoxicity*. Clin J Am Soc Nephrol, 2009. **4**(2): p. 481-508.

68. Lassila, M., P. Finckenberg, A.K. Pere, et al., *Comparison of enalapril and valsartan in cyclosporine A-induced hypertension and nephrotoxicity in spontaneously hypertensive rats on high-sodium diet*. Br J Pharmacol, 2000. **130**(6): p. 1339-47.
69. Liu, Q.F., J.M. Ye, L.X. Yu, et al., *Klotho mitigates cyclosporine A (CsA)-induced epithelial-mesenchymal transition (EMT) and renal fibrosis in rats*. Int Urol Nephrol, 2017. **49**(2): p. 345-352.
70. Bruck, K., V.S. Stel, G. Gambaro, et al., *CKD Prevalence Varies across the European General Population*. J Am Soc Nephrol, 2016. **27**(7): p. 2135-47.
71. Basile, D.P., M.D. Anderson, and T.A. Sutton, *Pathophysiology of acute kidney injury*. Compr Physiol, 2012. **2**(2): p. 1303-53.
72. Bhargava, P. and R.G. Schnellmann, *Mitochondrial energetics in the kidney*. Nat Rev Nephrol, 2017. **13**(10): p. 629-646.
73. Daenen, K., A. Andries, D. Mekahli, et al., *Oxidative stress in chronic kidney disease*. Pediatr Nephrol, 2019. **34**(6): p. 975-991.
74. Verma, S., P. Singh, S. Khurana, et al., *Implications of oxidative stress in chronic kidney disease: a review on current concepts and therapies*. Kidney Res Clin Pract, 2021. **40**(2): p. 183-193.
75. Sies, H., *Oxidative stress: oxidants and antioxidants*. Exp Physiol, 1997. **82**(2): p. 291-5.
76. Jha, J.C., C. Banal, B.S. Chow, et al., *Diabetes and Kidney Disease: Role of Oxidative Stress*. Antioxid Redox Signal, 2016. **25**(12): p. 657-684.
77. Droge, W., *Free radicals in the physiological control of cell function*. Physiol Rev, 2002. **82**(1): p. 47-95.
78. Birben, E., U.M. Sahiner, C. Sackesen, et al., *Oxidative stress and antioxidant defense*. World Allergy Organ J, 2012. **5**(1): p. 9-19.
79. Beckman, K.B. and B.N. Ames, *Oxidative decay of DNA*. J Biol Chem, 1997. **272**(32): p. 19633-6.
80. Descamps-Latscha, B., T. Druke, and V. Witko-Sarsat, *Dialysis-induced oxidative stress: biological aspects, clinical consequences, and therapy*. Semin Dial, 2001. **14**(3): p. 193-9.
81. Kwon, G., M.J. Uddin, G. Lee, et al., *A novel pan-Nox inhibitor, APX-115, protects kidney injury in streptozotocin-induced diabetic mice: possible role of peroxisomal and mitochondrial biogenesis*. Oncotarget, 2017. **8**(43): p. 74217-74232.
82. Granata, S., G. Zaza, S. Simone, et al., *Mitochondrial dysregulation and oxidative stress in patients with chronic kidney disease*. BMC Genomics, 2009. **10**: p. 388.
83. Baliga, R., N. Ueda, P.D. Walker, et al., *Oxidant mechanisms in toxic acute renal failure*. Drug Metab Rev, 1999. **31**(4): p. 971-97.
84. Wang, L., K. Matsushita, I. Araki, et al., *Inhibition of c-Jun N-terminal kinase ameliorates apoptosis induced by hydrogen peroxide in the kidney tubule epithelial cells (NRK-52E)*. Nephron, 2002. **91**(1): p. 142-7.
85. Nowak, G., G.L. Clifton, M.L. Godwin, et al., *Activation of ERK1/2 pathway mediates oxidant-induced decreases in mitochondrial function in renal cells*. Am J Physiol Renal Physiol, 2006. **291**(4): p. F840-55.
86. Pozdzik, A.A., I.J. Salmon, F.D. DeBelle, et al., *Aristolochic acid induces proximal tubule apoptosis and epithelial to mesenchymal transformation*. Kidney Int, 2008. **73**(5): p. 595-607.
87. Zorov, D.B., *Amelioration of aminoglycoside nephrotoxicity requires protection of renal mitochondria*. Kidney Int, 2010. **77**(10): p. 841-3.
88. Morales, A.I., D. Detaille, M. Prieto, et al., *Metformin prevents experimental gentamicin-induced nephropathy by a mitochondria-dependent pathway*. Kidney Int, 2010. **77**(10): p. 861-9.
89. Randjelovic, P., S. Veljkovic, N. Stojiljkovic, et al., *Protective effect of selenium on gentamicin-induced oxidative stress and nephrotoxicity in rats*. Drug Chem Toxicol, 2012. **35**(2): p. 141-8.

90. Kawai, Y., T. Nakao, N. Kunimura, et al., *Relationship of intracellular calcium and oxygen radicals to Cisplatin-related renal cell injury*. J Pharmacol Sci, 2006. **100**(1): p. 65-72.
91. Pan, H., P. Mukhopadhyay, M. Rajesh, et al., *Cannabidiol attenuates cisplatin-induced nephrotoxicity by decreasing oxidative/nitrosative stress, inflammation, and cell death*. J Pharmacol Exp Ther, 2009. **328**(3): p. 708-14.
92. Kumar, S., *Cellular and molecular pathways of renal repair after acute kidney injury*. Kidney Int, 2018. **93**(1): p. 27-40.
93. Castrop, H., *The Role of Renal Interstitial Cells in Proximal Tubular Regeneration*. Nephron, 2019. **141**(4): p. 265-272.
94. Berger, K. and M.J. Moeller, *Mechanisms of epithelial repair and regeneration after acute kidney injury*. Semin Nephrol, 2014. **34**(4): p. 394-403.
95. Chou, Y.-H., S.-Y. Pan, C.-H. Yang, et al., *Stem cells and kidney regeneration*. Journal of the Formosan Medical Association, 2014. **113**(4): p. 201-209.
96. Diep, C.Q., D. Ma, R.C. Deo, et al., *Identification of adult nephron progenitors capable of kidney regeneration in zebrafish*. Nature, 2011. **470**(7332): p. 95-100.
97. Romagnani, P., L. Lasagni, and G. Remuzzi, *Renal progenitors: an evolutionary conserved strategy for kidney regeneration*. Nat Rev Nephrol, 2013. **9**(3): p. 137-46.
98. Nadasdy, T., Z. Laszik, K.E. Blick, et al., *Proliferative activity of intrinsic cell populations in the normal human kidney*. J Am Soc Nephrol, 1994. **4**(12): p. 2032-9.
99. Bonventre, J.V., *Dedifferentiation and proliferation of surviving epithelial cells in acute renal failure*. J Am Soc Nephrol, 2003. **14 Suppl 1**: p. S55-61.
100. Humphreys, B.D., M.T. Valerius, A. Kobayashi, et al., *Intrinsic epithelial cells repair the kidney after injury*. Cell Stem Cell, 2008. **2**(3): p. 284-91.
101. Vogetseder, A., N. Picard, A. Gaspert, et al., *Proliferation capacity of the renal proximal tubule involves the bulk of differentiated epithelial cells*. Am J Physiol Cell Physiol, 2008. **294**(1): p. C22-8.
102. Kramann, R., T. Kusaba, and B.D. Humphreys, *Who regenerates the kidney tubule? Nephrol Dial Transplant*, 2015. **30**(6): p. 903-10.
103. Schiessl, I.M., A. Grill, K. Fremter, et al., *Renal Interstitial Platelet-Derived Growth Factor Receptor-beta Cells Support Proximal Tubular Regeneration*. J Am Soc Nephrol, 2018. **29**(5): p. 1383-1396.
104. Kusaba, T. and B.D. Humphreys, *Controversies on the origin of proliferating epithelial cells after kidney injury*. Pediatr Nephrol, 2014. **29**(4): p. 673-9.
105. Hallman MA, Z.S., Schnellmann RG. , *Regulation of dedifferentiation and redifferentiation in renal proximal tubular cells by the epidermal growth factor receptor*. J Pharmacol Exp Ther. , 2008. **325**(2) p. 520-8.
106. Li Y, Y.J., Luo JH, Dedhar S, Liu Y. , *Tubular epithelial cell dedifferentiation is driven by the helix-loop-helix transcriptional inhibitor Id1*. J Am Soc Nephrol. , 2007. **18**(2): p. 449-60.
107. Zhuang S, Y.Y., Han J, Schnellmann RG. , *p38 kinase-mediated transactivation of the epidermal growth factor receptor is required for dedifferentiation of renal epithelial cells after oxidant injury*. J Biol Chem. , 2005. **280**(22): p. 21036-42.
108. Chang-Panesso, M. and B.D. Humphreys, *Cellular plasticity in kidney injury and repair*. Nat Rev Nephrol, 2017. **13**(1): p. 39-46.
109. Jiang, Y.S., T. Jiang, B. Huang, et al., *Epithelial–mesenchymal transition of renal tubules: Divergent processes of repairing in acute or chronic injury? Medical Hypotheses*, 2013. **81**(1): p. 73-75.
110. Thiery, J.P., H. Acloque, R.Y. Huang, et al., *Epithelial-mesenchymal transitions in development and disease*. Cell, 2009. **139**(5): p. 871-90.
111. Kalluri R, W.R., *The basics of epithelial-mesenchymal transition*. J Clin Invest., 2009. **119**(6): p. 1420-1428.

112. Thompson, E.W., D.F. Newgreen, and D. Tarin, *Carcinoma invasion and metastasis: a role for epithelial-mesenchymal transition?* *Cancer Res*, 2005. **65**(14): p. 5991-5; discussion 5995.
113. Soltermann, A., V. Tischler, S. Arbogast, et al., *Prognostic significance of epithelial-mesenchymal and mesenchymal-epithelial transition protein expression in non-small cell lung cancer.* *Clin Cancer Res*, 2008. **14**(22): p. 7430-7.
114. Rasheed, Z.A.Y., J.; Wang, Q.; Kowalski, J.; Freed, I.; Murter, C.; Hong, S.M.; Koorstra, J.B.; Rajeshkumar, N.V.; He, X.; Goggins, M.; Iacobuzio-Donahue, C.; Berman, D.M.; Laheru, D.; Jimeno, A.; Hidalgo, M.; Maitra, A.; Matsui, W. , *Prognostic significance of tumorigenic cells with mesenchymal features in pancreatic adenocarcinoma.* *J. Natl. Cancer Inst.*, 2010. **102**(5) p. 340-351.
115. Kalluri, R. and E.G. Neilson, *Epithelial-mesenchymal transition and its implications for fibrosis.* *J Clin Invest*, 2003. **112**(12): p. 1776-84.
116. Shook, D. and R. Keller, *Mechanisms, mechanics and function of epithelial-mesenchymal transitions in early development.* *Mech Dev*, 2003. **120**(11): p. 1351-83.
117. Nieto, M.A., R.Y. Huang, R.A. Jackson, et al., *Emt: 2016.* *Cell*, 2016. **166**(1): p. 21-45.
118. Taube JH, H.J., Komurov K, Zhou AY, Gupta S, Yang J, Hartwell K, Onder TT, Gupta PB, Evans KW, Hollier BG, Ram PT, Lander ES, Rosen JM, Weinberg RA, Mani SA. , *Core epithelial-to-mesenchymal transition interactome gene-expression signature is associated with claudin-low and metaplastic breast cancer subtypes.* *Proc Natl Acad Sci U S A.* , 2010. **107**(35): p. 15449-54.
119. Yilmaz, M. and G. Christofori, *EMT, the cytoskeleton, and cancer cell invasion.* *Cancer Metastasis Rev*, 2009. **28**(1-2): p. 15-33.
120. De Craene B, B.G., *Regulatory networks defining EMT during cancer initiation and progression.* *Nat Rev Cancer.*, 2013. **13**(2) p. 97-110.
121. Diaz-Lopez, A., G. Moreno-Bueno, and A. Cano, *Role of microRNA in epithelial to mesenchymal transition and metastasis and clinical perspectives.* *Cancer Manag Res*, 2014. **6**: p. 205-16.
122. Gabbert, H., R. Wagner, R. Moll, et al., *Tumor dedifferentiation: an important step in tumor invasion.* *Clin Exp Metastasis*, 1985. **3**(4): p. 257-79.
123. Aghdassi A, S.M., Guenther A, Mayerle J, Behn CO, Heidecke CD, Friess H, Büchler M, Evert M, Lerch MM, Weiss FU. . , *Recruitment of histone deacetylases HDAC1 and HDAC2 by the transcriptional repressor ZEB1 downregulates E-cadherin expression in pancreatic cancer.* *Gut.* , 2012. **61**(3): p. 439-48.
124. Liu, Y., *Epithelial to mesenchymal transition in renal fibrogenesis: pathologic significance, molecular mechanism, and therapeutic intervention.* *J Am Soc Nephrol*, 2004. **15**(1): p. 1-12.
125. Pawar, S., S. Kartha, and F.G. Toback, *Differential gene expression in migrating renal epithelial cells after wounding.* *J Cell Physiol*, 1995. **165**(3): p. 556-65.
126. Imgrund, M., E. Grone, H.J. Grone, et al., *Re-expression of the developmental gene Pax-2 during experimental acute tubular necrosis in mice 1.* *Kidney Int*, 1999. **56**(4): p. 1423-31.
127. Maeshima A, Y.S., Nojima Y. , *Identification of renal progenitor-like tubular cells that participate in the regeneration processes of the kidney.* *J Am Soc Nephrol.* , 2003. **14**(12): p. 3138-46.
128. AM., E.-N., *Plasticity of kidney cells: role in kidney remodeling and scarring.* *Kidney Int.* , 2003. **64**(5): p. 1553-63.
129. Butt, M.J., A.F. Tarantal, D.F. Jimenez, et al., *Collecting duct epithelial-mesenchymal transition in fetal urinary tract obstruction.* *Kidney Int*, 2007. **72**(8): p. 936-44.
130. Kim K, L.Z., Hay ED. , *Direct evidence for a role of beta-catenin/LEF-1 signaling pathway in induction of EMT.* *Cell Biol Int.*, 2002. **26**(5): p. 463-76.

131. Zeisberg, M. and R. Kalluri, *The role of epithelial-to-mesenchymal transition in renal fibrosis*. J Mol Med (Berl), 2004. **82**(3): p. 175-81.
132. Neilson, E.G., *Setting a trap for tissue fibrosis*. Nat Med, 2005. **11**(4): p. 373-4.
133. Zeisberg, M., J. Hanai, H. Sugimoto, et al., *BMP-7 counteracts TGF-beta1-induced epithelial-to-mesenchymal transition and reverses chronic renal injury*. Nat Med, 2003. **9**(7): p. 964-8.
134. Lombardi D, B.F., Romagnani P. , *How much can the tubule regenerate and who does it? An open question*. Nephrol Dial Transplant., 2016. **31**(8): p. 1243-50.
135. Bussolati, B., S. Bruno, C. Grange, et al., *Isolation of renal progenitor cells from adult human kidney*. Am J Pathol, 2005. **166**(2): p. 545-55.
136. Lindgren, D., A.K. Bostrom, K. Nilsson, et al., *Isolation and characterization of progenitor-like cells from human renal proximal tubules*. Am J Pathol, 2011. **178**(2): p. 828-37.
137. Angelotti ML, R.E., Ballerini L, Peired A, Mazzinghi B, Sagrinati C, Parente E, Gacci M, Carini M, Rotondi M, Fogo AB, Lazzeri E, Lasagni L, Romagnani P. , *Characterization of renal progenitors committed toward tubular lineage and their regenerative potential in renal tubular injury*. Stem Cells. 2012. **30**(8) p. 1714-25.
138. Chambers, B.E. and R.A. Wingert, *Renal progenitors: Roles in kidney disease and regeneration*. World J Stem Cells, 2016. **8**(11): p. 367-375.
139. Bond AM, M.G., Song H. , *Adult Mammalian Neural Stem Cells and Neurogenesis: Five Decades Later*. Cell Stem Cell., 2015. **17**(4) p. 385-95.
140. Hagege, A.A., C. Carrion, P. Menasche, et al., *Viability and differentiation of autologous skeletal myoblast grafts in ischaemic cardiomyopathy*. Lancet, 2003. **361**(9356): p. 491-2.
141. Reinecke H, P.V., Murry CE. , *Skeletal muscle stem cells do not transdifferentiate into cardiomyocytes after cardiac grafting*. J Mol Cell Cardiol., 2002. **34**(2): p. 241-9.
142. Morrison SJ, S.A., *Stem cells and niches: mechanisms that promote stem cell maintenance throughout life*. Cell, 2008. **132**(4) p. 598-611.
143. Li Z, L.L., *Understanding hematopoietic stem-cell microenvironments*. Trends Biochem Sci., 2006. **31**(10) p. 589-95.
144. Raaijmakers, M.H. and D.T. Scadden, *Evolving concepts on the microenvironmental niche for hematopoietic stem cells*. Curr Opin Hematol, 2008. **15**(4): p. 301-6.
145. Gurusamy, N., A. Alsayari, S. Rajasingh, et al., *Adult Stem Cells for Regenerative Therapy*. Prog Mol Biol Transl Sci, 2018. **160**: p. 1-22.
146. Gavrillov, S., V.E. Papaioannou, and D.W. Landry, *Alternative strategies for the derivation of human embryonic stem cell lines and the role of dead embryos*. Curr Stem Cell Res Ther, 2009. **4**(1): p. 81-6.
147. Kraushaar U, M.T., Hess D, Gepstein L, Mummery CL, Braam SR, Guenther E. , *Cardiac safety pharmacology: from human ether-a-gogo related gene channel block towards induced pluripotent stem cell based disease models*. Expert Opin Drug Saf., 2012. **11**(2) p. 285-98.
148. Suter-Dick, L., P.M. Alves, B.J. Blaauboer, et al., *Stem cell-derived systems in toxicology assessment*. Stem Cells Dev, 2015. **24**(11): p. 1284-96.
149. Takayama, K. and H. Mizuguchi, *Generation of human pluripotent stem cell-derived hepatocyte-like cells for drug toxicity screening*. Drug Metab Pharmacokinet, 2017. **32**(1): p. 12-20.
150. Odawara, A., N. Matsuda, Y. Ishibashi, et al., *Toxicological evaluation of convulsant and anticonvulsant drugs in human induced pluripotent stem cell-derived cortical neuronal networks using an MEA system*. Sci Rep, 2018. **8**(1): p. 10416.
151. Takahashi, K. and S. Yamanaka, *Induction of pluripotent stem cells from mouse embryonic and adult fibroblast cultures by defined factors*. Cell, 2006. **126**(4): p. 663-76.

152. Orford KW, S.D., *Deconstructing stem cell self-renewal: genetic insights into cell-cycle regulation*. Nat Rev Genet., 2008. **9(2)**: p. 115-28.
153. Zhang H, W.Z., *Mechanisms that mediate stem cell self-renewal and differentiation*. J Cell Biochem, 2008. **103(3)** p. 709-18.
154. Thomson, J.A., J. Itskovitz-Eldor, S.S. Shapiro, et al., *Embryonic stem cell lines derived from human blastocysts*. Science, 1998. **282(5391)**: p. 1145-7.
155. Bishop, A.E., L.D. Buttery, and J.M. Polak, *Embryonic stem cells*. J Pathol, 2002. **197(4)**: p. 424-9.
156. Andorno, R., *Biomedicine and international human rights law: in search of a global consensus*. Bull World Health Organ, 2002. **80(12)**: p. 959-63.
157. de Wert G, M.C., *Human embryonic stem cells: research, ethics and policy*. Hum Reprod., 2003. **18(4)**: p. 672-82.
158. J., G., *Harveian Oration 2014: Stem cells and cell replacement prospects*. Clin Med (Lond), 2015. **15(2)**: p. 160-7.
159. Takahashi, K., K. Tanabe, M. Ohnuki, et al., *Induction of pluripotent stem cells from adult human fibroblasts by defined factors*. Cell, 2007. **131(5)**: p. 861-72.
160. Yu, J.V., M.A; Smuga-Otto, K; Antosiewicz-Bourget, J; Frane, J.L; Tian, S; Nie, J; Jonsdottir, G.L; Ruotti, V; Stewart, R; Slukvin, I.I; Thomson, J.A. , Science, 2007. **318(5858)**: p. 1917-20.
161. Lowry, W.E., L. Richter, R. Yachechko, et al., *Generation of human induced pluripotent stem cells from dermal fibroblasts*. Proc Natl Acad Sci U S A, 2008. **105(8)**: p. 2883-8.
162. Saxena, A., J.E. Fish, M.D. White, et al., *Stromal Cell-Derived Factor-1 α Is Cardioprotective After Myocardial Infarction*. Circulation, 2008. **117(17)**: p. 2224-2231.
163. Salazar, K.D.L., S.M.; Brody, A.R. , *Mesenchymal stem cells produce Wnt isoforms and TGF- β 1 that mediate proliferation and procollagen expression by lung fibroblasts*. Am. J. Physiol. Lung Cell. Mol. Physiol., 2009. **297**: p. L1002–L1011.
164. Kumada, Y. and S. Zhang, *Significant Type I and Type III Collagen Production from Human Periodontal Ligament Fibroblasts in 3D Peptide Scaffolds without Extra Growth Factors*. PLoS ONE, 2010. **5(4)**: p. e10305.
165. Nath, S.C., L. Menendez, and I. Friedrich Ben-Nun, *Overcoming the Variability of iPSCs in the Manufacturing of Cell-Based Therapies*. Int J Mol Sci, 2023. **24(23)**.
166. Loh, Y.H., S. Agarwal, I.H. Park, et al., *Generation of induced pluripotent stem cells from human blood*. Blood, 2009. **113(22)**: p. 5476-9.
167. Zhou, T., C. Benda, S. Duzinger, et al., *Generation of induced pluripotent stem cells from urine*. J Am Soc Nephrol, 2011. **22(7)**: p. 1221-8.
168. Aasen, T., A. Raya, M.J. Barrero, et al., *Efficient and rapid generation of induced pluripotent stem cells from human keratinocytes*. Nat Biotechnol, 2008. **26(11)**: p. 1276-84.
169. Raab S, K.M., Liebau S, Linta L. , *A Comparative View on Human Somatic Cell Sources for iPSC Generation*. Stem Cells Int., 2014: p. 2014:768391.
170. Al Abbar, A., S.C. Ngai, N. Nograles, et al., *Induced Pluripotent Stem Cells: Reprogramming Platforms and Applications in Cell Replacement Therapy*. Biores Open Access, 2020. **9(1)**: p. 121-136.
171. Malik, N. and M.S. Rao, *A review of the methods for human iPSC derivation*. Methods Mol Biol, 2013. **997**: p. 23-33.
172. Lai, M.I., W.Y. Wendy-Yeo, R. Ramasamy, et al., *Advancements in reprogramming strategies for the generation of induced pluripotent stem cells*. J Assist Reprod Genet, 2011. **28(4)**: p. 291-301.
173. Morizane, R., A.Q. Lam, B.S. Freedman, et al., *Nephron organoids derived from human pluripotent stem cells model kidney development and injury*. Nat Biotechnol, 2015. **33(11)**: p. 1193-200.

174. Freedman, B.S., C.R. Brooks, A.Q. Lam, et al., *Modelling kidney disease with CRISPR-mutant kidney organoids derived from human pluripotent epiblast spheroids*. Nat Commun, 2015. **6**: p. 8715.
175. Taguchi, A., Y. Kaku, T. Ohmori, et al., *Redefining the in vivo origin of metanephric nephron progenitors enables generation of complex kidney structures from pluripotent stem cells*. Cell Stem Cell, 2014. **14**(1): p. 53-67.
176. Takasato, M., P.X. Er, H.S. Chiu, et al., *Kidney organoids from human iPS cells contain multiple lineages and model human nephrogenesis*. Nature, 2015. **526**(7574): p. 564-8.
177. Takasato, M., P.X. Er, H.S. Chiu, et al., *Generation of kidney organoids from human pluripotent stem cells*. Nat Protoc, 2016. **11**(9): p. 1681-92.
178. Bonventre, J.V., *Kidney organoids-a new tool for kidney therapeutic development*. Kidney Int, 2018. **94**(6): p. 1040-1042.
179. Lam AQ, F.B., Morizane R, Lerou PH, Valerius MT, Bonventre JV. , *Rapid and efficient differentiation of human pluripotent stem cells into intermediate mesoderm that forms tubules expressing kidney proximal tubular markers*. J Am Soc Nephrol., 2014. **25**(6): p. 1211-25.
180. Ngo TTT, R.B., Sébastien I, Neubauer JC, Kurtz A, Hariharan K. . , *Functional differentiation and scalable production of renal proximal tubular epithelial cells from human pluripotent stem cells in a dynamic culture system*. Cell Prolif., 2022. **55**(3): p. e13190.
181. Narayanan, K.S., K.M; Tasnim, F; Kandasamy, K.; Schumacher, A.; Ni, M.; Goa, S.; Gopalan, B.; Zink, D.; Ying, Y.J. , *Human embryonic stem cells differentiate into functional renal proximal tubular-like cells*. Kidney Int. , 2013. **83**(4) p. 593-603.
182. Nieskens, T.T.G. and A.K. Sjogren, *Emerging In Vitro Systems to Screen and Predict Drug-Induced Kidney Toxicity*. Semin Nephrol, 2019. **39**(2): p. 215-226.
183. Rangaswamy, D. and K. Sud, *Acute kidney injury and disease: Long-term consequences and management*. Nephrology (Carlton), 2018. **23**(11): p. 969-980.
184. Goldstein, S.L., B.L. Jaber, S. Faubel, et al., *AKI transition of care: a potential opportunity to detect and prevent CKD*. Clin J Am Soc Nephrol, 2013. **8**(3): p. 476-83.
185. Zink, D., J.K.C. Chuah, and J.Y. Ying, *Assessing Toxicity with Human Cell-Based In Vitro Methods*. Trends Mol Med, 2020. **26**(6): p. 570-582.
186. Vinken, M., E. Benfenati, F. Busquet, et al., *Safer chemicals using less animals: kick-off of the European ONTOX project*. Toxicology, 2021. **458**: p. 152846.
187. Chu, X., K. Bleasby, and R. Evers, *Species differences in drug transporters and implications for translating preclinical findings to humans*. Expert Opin Drug Metab Toxicol, 2013. **9**(3): p. 237-52.
188. Zou, L., A. Stecula, A. Gupta, et al., *Molecular Mechanisms for Species Differences in Organic Anion Transporter 1, OAT1: Implications for Renal Drug Toxicity*. Molecular Pharmacology, 2018. **94**(1): p. 689-699.
189. Morizane, R., T. Miyoshi, and J.V. Bonventre, *Concise Review: Kidney Generation with Human Pluripotent Stem Cells*. Stem Cells, 2017. **35**(11): p. 2209-2217.
190. Bajaj, P., A.D. Rodrigues, C.M. Stepan, et al., *Human Pluripotent Stem Cell-Derived Kidney Model for Nephrotoxicity Studies*. Drug Metabolism and Disposition, 2018. **46**(11): p. 1703-1711.
191. Secker, P.F., N. Schlichenmaier, M. Beilmann, et al., *Functional transepithelial transport measurements to detect nephrotoxicity in vitro using the RPTEC/TERT1 cell line*. Archives of Toxicology, 2019. **93**(7): p. 1965-1978.
192. O'Brien, J., I. Wilson, T. Orton, et al., *Investigation of the Alamar Blue (resazurin) fluorescent dye for the assessment of mammalian cell cytotoxicity*. European Journal of Biochemistry, 2000. **267**(17): p. 5421-5426.

193. Valentich, J.D., R. Tchao, and J. Leighton, *Hemicyst formation stimulated by cyclic AMP in dog kidney cell line MDCK*. Journal of Cellular Physiology, 1979. **100**(2): p. 291-304.
194. Wieser, M., Stadler, G., Jennings, P., Streubel, B., Pfaller, W., Ambros, P., Riedl, C., Katinger, H., Grillari, J., & Grillari-Voglauer, R. , *HTERT alone immortalizes epithelial cells of renal proximal tubules without changing their functional characteristics*. American Journal of Physiology-Renal Physiology, 2008. **295**: p. F1365–F1375.
195. Yang, Y., H. Liu, F. Liu, et al., *Mitochondrial dysregulation and protection in cisplatin nephrotoxicity*. Archives of Toxicology, 2014. **88**(6): p. 1249-1256.
196. Fukusumi, H., Y. Handa, T. Shofuda, et al., *Evaluation of the susceptibility of neurons and neural stem/progenitor cells derived from human induced pluripotent stem cells to anticancer drugs*. J Pharmacol Sci, 2019. **140**(4): p. 331-336.
197. Pešková, L., V. Vinarský, T. Bárta, et al., *Human Embryonic Stem Cells Acquire Responsiveness to TRAIL upon Exposure to Cisplatin*. Stem Cells Int, 2019. **2019**: p. 4279481.
198. Upadhyaya, P., A. Di Serafino, L. Sorino, et al., *Genetic and epigenetic modifications induced by chemotherapeutic drugs: human amniotic fluid stem cells as an in-vitro model*. BMC Med Genomics, 2019. **12**(1): p. 146.
199. Wing, C., M. Komatsu, S.M. Delaney, et al., *Application of stem cell derived neuronal cells to evaluate neurotoxic chemotherapy*. Stem Cell Res, 2017. **22**: p. 79-88.
200. Wang, M., Wang, J., Tsui, A. Y., Li, Z., Zhang, Y., Zhao, Q., Xing, H., & Wang, X. , *Mechanisms of peripheral neurotoxicity associated with four chemotherapy drugs using human induced pluripotent stem cell-derived peripheral neurons*. Toxicology in Vitro, 2021. **77**: p. 105233.
201. Guo, H., N. Deng, L. Dou, et al., *3-D Human Renal Tubular Organoids Generated from Urine-Derived Stem Cells for Nephrotoxicity Screening*. ACS Biomaterials Science & Engineering, 2020. **6**(12): p. 6701-6709.
202. Antonios, J.P.F., G.J.; Cleary, D.R.; Martin, J.R.; Ciacci, J.D.; Pham, M.H., *Immunosuppressive mechanisms for stem cell transplant survival in spinal cord injury*. Neurosurg. Focus 2019. **49**: p. E9.
203. Wellens, S., Dehouck, L., Chandrasekaran, V., Singh, P., Loiola, R. A., Sevin, E., Exner, T., Jennings, P., Gosselet, F., & Culot, M. , *Evaluation of a human iPSC-derived BBB model for repeated dose toxicity testing with cyclosporine A as model compound*. Toxicology in Vitro, 2021. **73** p. 105112.
204. Schultze, N., Wanka, H., Zwicker, P., Lindequist, U., & Haertel, B. (2017). , *Mitochondrial functions of THP-1 monocytes following the exposure to selected natural compounds*. Toxicology, 2017. **377** p. 57-63.
205. De Arriba, G., De Hornedo, J. P., Rubio, S. R., Fernández, M. C., Martínez, S. B., Camarero, M. M., & Cid, T. P. , *Vitamin E protects against the mitochondrial damage caused by cyclosporin A in LLC-PK1 cells*. Toxicology and Applied Pharmacology,, 2009. **239**(3) p. 241-250.
206. Nagavally, R.R., S. Sunilkumar, M. Akhtar, et al., *Chrysin Ameliorates Cyclosporine-A-Induced Renal Fibrosis by Inhibiting TGF-β(1)-Induced Epithelial-Mesenchymal Transition*. Int J Mol Sci, 2021. **22**(19).
207. Lv, Z., G. Xie, H. Cui, et al., *Cyclosporin-A reduced the cytotoxicity of propranolol in HUVECs via p38 MAPK signaling*. Medicine (Baltimore), 2022. **101**(4): p. e28329.
208. Wang, T., N. Li, L. Jin, et al., *The calcium pump PMCA4 prevents epithelial-mesenchymal transition by inhibiting NFATc1-ZEB1 pathway in gastric cancer*. Biochim Biophys Acta Mol Cell Res, 2020. **1867**(12): p. 118833.
209. Hori, Y., N. Aoki, S. Kuwahara, et al., *Megalín Blockade with Cilastatin Suppresses Drug-Induced Nephrotoxicity*. J Am Soc Nephrol, 2017. **28**(6): p. 1783-1791.

210. Mahadevappa, R., Nielsen, R., Christensen, E. I., & Birn, H. (2014). , *Megalyn in acute kidney injury: Foe and friend*. American Journal of Physiology-Renal Physiology, 2014. **306**: p. F147–F154.
211. Arjumand, W., A. Seth, and S. Sultana, *Rutin attenuates cisplatin induced renal inflammation and apoptosis by reducing NFkB, TNF- α and caspase-3 expression in wistar rats*. Food Chem Toxicol, 2011. **49**(9): p. 2013-21.
212. Kishore, B.K., Krane, C. M., Di Iulio, D., Menon, A. G., & Cacini, W. , *Expression of renal aquaporins 1, 2, and 3 in a rat model of cisplatin-induced polyuria*. Kidney International, 2000. **58**(2) p. 701-711.
213. Afjal, M.A., Goswami, P., Ahmad, S., Dabeer, S., Akhter, J., Salman, M., Raisuddin, S. , *Tempol (4-hydroxy tempo) protects mice from cisplatin-induced acute kidney injury via modulation of expression of aquaporins and kidney injury molecule-1*. Drug and Chemical Toxicology, 2020. **45**(3) p. 1355–1363.
214. Shitara, Y., T. Itoh, H. Sato, et al., *Inhibition of Transporter-Mediated Hepatic Uptake as a Mechanism for Drug-Drug Interaction between Cerivastatin and Cyclosporin A*. Journal of Pharmacology and Experimental Therapeutics, 2003. **304**(2): p. 610-616.
215. Nascimento, C.R., F. Braga, L.S. Capella, et al., *Comparative Study on the Effects of Cyclosporin A in Renal Cells in Culture*. Nephron Experimental Nephrology, 2005. **99**(3): p. e77-e86.
216. Motohashi, H., T. Katsura, H. Saito, et al., *Pharmaceutical Research*, 2001. **18**(5): p. 713-717.
217. Shitara, Y., K. Takeuchi, Y. Nagamatsu, et al., *Long-lasting inhibitory effects of cyclosporin A, but not tacrolimus, on OATP1B1- and OATP1B3-mediated uptake*. Drug Metab Pharmacokinet, 2012. **27**(4): p. 368-78.
218. Lim, S.W., K.O. Ahn, M.R. Sheen, et al., *Downregulation of renal sodium transporters and tonicity-responsive enhancer binding protein by long-term treatment with cyclosporin A*. J Am Soc Nephrol, 2007. **18**(2): p. 421-9.
219. Edemir, B., S. Reuter, R. Borgulya, et al., *Acute rejection modulates gene expression in the collecting duct*. J Am Soc Nephrol, 2008. **19**(3): p. 538-46.
220. Capolongo, G., S. Damiano, Y. Suzumoto, et al., *Cyclosporin-induced hypertension is associated with the up-regulation of Na⁺-K⁺-2Cl⁻ cotransporter (NKCC2)*. Nephrol Dial Transplant, 2024. **39**(2): p. 297-304.
221. Mboni-Johnston, I.M., N.M.Z. Kouidrat, C. Hirsch, et al., *Sensitivity of Human Induced Pluripotent Stem Cells and Thereof Differentiated Kidney Proximal Tubular Cells towards Selected Nephrotoxins*. Int J Mol Sci, 2023. **25**(1).
222. Sedelnikova, O.A., E.P. Rogakou, I.G. Panyutin, et al., *Quantitative detection of (125)IdU-induced DNA double-strand breaks with gamma-H2AX antibody*. Radiat Res, 2002. **158**(4): p. 486-92.
223. Mah, L.J., A. El-Osta, and T.C. Karagiannis, *γ H2AX: a sensitive molecular marker of DNA damage and repair*. Leukemia, 2010. **24**(4): p. 679-686.
224. Wood, R.D., *Nucleotide excision repair in mammalian cells*. J Biol Chem, 1997. **272**(38): p. 23465-8.
225. Köberle, B., J.R.W. Masters, J.A. Hartley, et al., *Defective repair of cisplatin-induced DNA damage caused by reduced XPA protein in testicular germ cell tumours*. Current Biology, 1999. **9**(5): p. 273-278.
226. Sakai, W., E.M. Swisher, B.Y. Karlan, et al., *Secondary mutations as a mechanism of cisplatin resistance in BRCA2-mutated cancers*. Nature, 2008. **451**(7182): p. 1116-1120.
227. Szeto, C.C. and K.M. Chow, *Nephrotoxicity related to new therapeutic compounds*. Ren Fail, 2005. **27**(3): p. 329-33.
228. Ameku T, T.D., Sone M, Numata T, Nakamura M, Shiota F, Toyoda T, Matsui S, Araoka T, Yasuno T, Mae S, Kobayashi H, Kondo N, Kitaoka F, Amano N, Arai S, Ichisaka T, Matsuura N, Inoue S, Yamamoto T, Takahashi K, Asaka I, Yamada Y, Ubara Y, Muso E, Fukatsu A, Watanabe A, Sato Y, Nakahata T, Mori Y, Koizumi A, Nakao K, Yamanaka S, Osafune K. , *Identification of MMP1 as a*

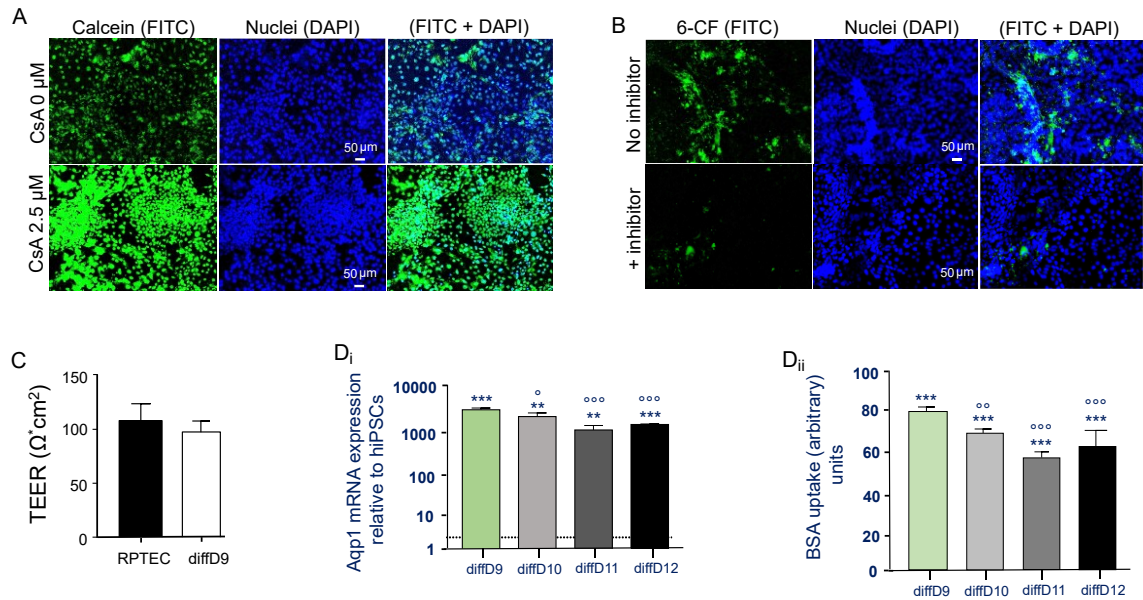
- novel risk factor for intracranial aneurysms in ADPKD using iPSC models.* Sci Rep, 2016. **6**: p. 30013.
229. Venkatachalam, M.A., J.M. Weinberg, W. Kriz, et al., *Failed Tubule Recovery, AKI-CKD Transition, and Kidney Disease Progression.* J Am Soc Nephrol, 2015. **26**(8): p. 1765-76.
 230. Venkatachalam, M.A., H. Geng, R. Lan, et al., *14.08 - Maladaptive Repair and AKI to CKD Transition, in Comprehensive Toxicology (Third Edition),* C.A. McQueen, Editor. 2018, Elsevier: Oxford. p. 164-188.
 231. Mehta, R.L., M.T. Pascual, S. Soroko, et al., *Spectrum of acute renal failure in the intensive care unit: The PICARD experience.* Kidney International, 2004. **66**(4): p. 1613-1621.
 232. Honda, T., Y. Hirakawa, and M. Nangaku, *The role of oxidative stress and hypoxia in renal disease.* Kidney Research and Clinical Practice, 2019. **38**(4): p. 414-426.
 233. Percy, C.J., D. Power, and G.C. Gobe, *Renal ageing: Changes in the cellular mechanism of energy metabolism and oxidant handling (Review Article).* Nephrology, 2008. **13**(2): p. 147-152.
 234. Doss, M.X. and A. Sachinidis, *Current Challenges of iPSC-Based Disease Modeling and Therapeutic Implications.* Cells, 2019. **8**(5): p. 403.
 235. Yu, J., M.A. Vodyanik, K. Smuga-Otto, et al., *Induced Pluripotent Stem Cell Lines Derived from Human Somatic Cells.* Science, 2007. **318**(5858): p. 1917-1920.
 236. Gavrieli, Y., Y. Sherman, and S.A. Ben-Sasson, *Identification of programmed cell death in situ via specific labeling of nuclear DNA fragmentation.* J Cell Biol, 1992. **119**(3): p. 493-501.
 237. Ikeda, Y., H. Hamano, Y. Horinouchi, et al., *Role of ferroptosis in cisplatin-induced acute nephrotoxicity in mice.* J Trace Elem Med Biol, 2021. **67**: p. 126798.
 238. Lieberthal, W., V. Triaca, and J. Levine, *Mechanisms of death induced by cisplatin in proximal tubular epithelial cells: apoptosis vs. necrosis.* Am J Physiol, 1996. **270**(4 Pt 2): p. F700-8.
 239. Lee, R.H., J.M. Song, M.Y. Park, et al., *Cisplatin-induced apoptosis by translocation of endogenous Bax in mouse collecting duct cells.* Biochem Pharmacol, 2001. **62**(8): p. 1013-23.
 240. Ciarimboli, G., *Membrane transporters as mediators of cisplatin side-effects.* Anticancer Res, 2014. **34**(1): p. 547-50.
 241. Qi, R., & Yang, C. , *Renal tubular epithelial cells: The neglected mediator of tubulointerstitial fibrosis after injury.* Cell Death & Disease, 2018. **9**(11): p. 1-11.
 242. Cao, Y., J. Xu, D. Cui, et al., *Protective effect of carnosine on hydrogen peroxide-induced oxidative stress in human kidney tubular epithelial cells.* Biochem Biophys Res Commun, 2021. **534**: p. 576-582.
 243. Benedetti, G., M. Fokkelman, K. Yan, et al., *The nuclear factor kappaB family member RelB facilitates apoptosis of renal epithelial cells caused by cisplatin/tumor necrosis factor alpha synergy by suppressing an epithelial to mesenchymal transition-like phenotypic switch.* Mol Pharmacol, 2013. **84**(1): p. 128-38.
 244. Lally, C., E. Healy, and M.P. Ryan, *Cyclosporine A-induced cell cycle arrest and cell death in renal epithelial cells.* Kidney Int, 1999. **56**(4): p. 1254-7.
 245. Seki, Y., K. Toba, I. Fuse, et al., *In vitro effect of cyclosporin A, mitomycin C and prednisolone on cell kinetics in cultured human umbilical vein endothelial cells.* Thromb Res, 2005. **115**(3): p. 219-28.
 246. Sun, J. and Y. Wang, *Effects of cyclosporin A on proliferation of cultured rat mesangial cells.* J Tongji Med Univ, 1997. **17**(2): p. 115-7.
 247. Jennings, P., C. Koppelstaetter, S. Aydin, et al., *Cyclosporine A induces senescence in renal tubular epithelial cells.* Am J Physiol Renal Physiol, 2007. **293**(3): p. F831-8.

248. Healy, E., M. Dempsey, C. Lally, et al., *Apoptosis and necrosis: mechanisms of cell death induced by cyclosporine A in a renal proximal tubular cell line*. *Kidney Int*, 1998. **54**(6): p. 1955-66.
249. McMorrow, T., M.M. Gaffney, C. Slattery, et al., *Cyclosporine A induced epithelial–mesenchymal transition in human renal proximal tubular epithelial cells*. *Nephrology Dialysis Transplantation*, 2005. **20**(10): p. 2215-2225.
250. Saretzki, G., T. Walter, S. Atkinson, et al., *Downregulation of multiple stress defense mechanisms during differentiation of human embryonic stem cells*. *Stem Cells*, 2008. **26**(2): p. 455-64.
251. Eltutan, B.I., C. Kiser, İ. Ercan, et al., *In vitro effects of H2O2 on neural stem cell differentiation*. *In Vitro Cellular & Developmental Biology - Animal*, 2022. **58**(9): p. 810-816.
252. Xiao, Y., X. Li, Y. Cui, et al., *Hydrogen peroxide inhibits proliferation and endothelial differentiation of bone marrow stem cells partially via reactive oxygen species generation*. *Life Sci*, 2014. **112**(1-2): p. 33-40.
253. Khan, M.A., X. Wang, K.T.K. Giuliani, et al., *Underlying Histopathology Determines Response to Oxidative Stress in Cultured Human Primary Proximal Tubular Epithelial Cells*. *Int J Mol Sci*, 2020. **21**(2).
254. Karimi, Z., M. Ghaffari, J. Ezzati Nazhad Dolatabadi, et al., *The protective effect of thymoquinone on tert-butylhydroquinone induced cytotoxicity in human umbilical vein endothelial cells*. *Toxicol Res (Camb)*, 2019. **8**(6): p. 1050-1056.
255. Jin, X.L., K. Wang, L. Liu, et al., *Nuclear factor-like factor 2-antioxidant response element signaling activation by tert-butylhydroquinone attenuates acute heat stress in bovine mammary epithelial cells*. *Journal of Dairy Science*, 2016. **99**(11): p. 9094-9103.
256. Chen, Q. and A.I. Cederbaum, *Menadione cytotoxicity to Hep G2 cells and protection by activation of nuclear factor-kappaB*. *Mol Pharmacol*, 1997. **52**(4): p. 648-57.
257. Rhyu, D.Y., Y. Yang, H. Ha, et al., *Role of reactive oxygen species in TGF-beta1-induced mitogen-activated protein kinase activation and epithelial-mesenchymal transition in renal tubular epithelial cells*. *J Am Soc Nephrol*, 2005. **16**(3): p. 667-75.
258. Wang, Y., L. Pang, Y. Zhang, et al., *Fenofibrate Improved Interstitial Fibrosis of Renal Allograft through Inhibited Epithelial-Mesenchymal Transition Induced by Oxidative Stress*. *Oxid Med Cell Longev*, 2019. **2019**: p. 8936856.
259. Kurosaki, Y., A. Imoto, F. Kawakami, et al., *Oxidative stress increases megalin expression in the renal proximal tubules during the normoalbuminuric stage of diabetes mellitus*. *Am J Physiol Renal Physiol*, 2018. **314**(3): p. F462-F470.
260. Nielsen, R., E.I. Christensen, and H. Birn, *Megalyn and cubilin in proximal tubule protein reabsorption: from experimental models to human disease*. *Kidney Int*, 2016. **89**(1): p. 58-67.
261. Liu, M., Y. Sun, M. Xu, et al., *Role of mitochondrial oxidative stress in modulating the expressions of aquaporins in obstructive kidney disease*. *Am J Physiol Renal Physiol*, 2018. **314**(4): p. F658-F666.
262. Palevsky, P.M.Z., J.H.; O'Connor, T.Z.; Chertow, G.M.; Crowley, S.T.; Choudhury, D.; Finkel, K.; Kellum, J.A.; Paganini, E.; Schein, R.M.H.; Smith, M.W.; Swanson, K.M. , *Intensity of renal support in critically ill patients with acute kidney injury*. *N Engl J Med.*, 2008. **359** p. 7–20.
263. Guo, X. and C. Nzerue, *How to prevent, recognize, and treat drug-induced nephrotoxicity*. *Cleve Clin J Med*, 2002. **69**(4): p. 289-90, 293-4, 296-7 passim.
264. Thadhani, R., M. Pascual, and J.V. Bonventre, *Acute renal failure*. *N Engl J Med*, 1996. **334**(22): p. 1448-60.
265. Makris, K. and L. Spanou, *Acute Kidney Injury: Definition, Pathophysiology and Clinical Phenotypes*. *Clin Biochem Rev*, 2016. **37**(2): p. 85-98.
266. Vogetseder, A., A. Karadeniz, B. Kaissling, et al., *Tubular cell proliferation in the healthy rat kidney*. *Histochemistry and Cell Biology*, 2005. **124**(2): p. 97-104.

267. Petersen, M., M. Thorikay, M. Deckers, et al., *Oral administration of GW788388, an inhibitor of TGF-beta type I and II receptor kinases, decreases renal fibrosis*. *Kidney Int*, 2008. **73**(6): p. 705-15.
268. Little, M.H. and A.P. McMahon, *Mammalian Kidney Development: Principles, Progress, and Projections*. Cold Spring Harbor Perspectives in Biology, 2012. **4**(5): p. a008300-a008300.
269. James, R.G., & Schultheiss, T. M., *Bmp signaling promotes intermediate mesoderm gene expression in a dose-dependent, cell-autonomous and translation-dependent manner*. *Developmental Biology*, 2005. **288**(1): p. 113-125.
270. Valentich, J.D., R. Tchao, and J. Leighton, *Hemicyst formation stimulated by cyclic AMP in dog kidney cell line MDCK*. *J Cell Physiol*, 1979. **100**(2): p. 291-304.
271. Inui, K.I., S. Masuda, and H. Saito, *Cellular and molecular aspects of drug transport in the kidney*. *Kidney Int*, 2000. **58**(3): p. 944-58.
272. Kosztyu, P., P. Dolezel, R. Vaclavikova, et al., *Can the assessment of ABCB1 gene expression predict its function in vitro?* *Eur J Haematol*, 2015. **95**(2): p. 150-9.
273. Terada, Y., H. Tanaka, T. Okado, et al., *Expression and function of the developmental gene Wnt-4 during experimental acute renal failure in rats*. *J Am Soc Nephrol*, 2003. **14**(5): p. 1223-33.
274. Vedula, E.M., J.L. Alonso, M.A. Arnaout, et al., *A microfluidic renal proximal tubule with active reabsorptive function*. *PLoS One*, 2017. **12**(10): p. e0184330.
275. Zalata, Lammertijn, Christophe, et al., *The correlates and alleged biochemical background of the resazurin reduction test in semen*. *International Journal of Andrology*, 1998. **21**(5): p. 289-294.
276. Riss, T.L., R.A. Moravec, A.L. Niles, et al., *Cell Viability Assays*, in *Assay Guidance Manual*, S. Markossian, et al., Editors. 2004, Eli Lilly & Company and the National Center for Advancing Translational Sciences: Bethesda (MD).
277. Ligasová, A. and K. Koberna, *DNA Replication: From Radioisotopes to Click Chemistry*. *Molecules*, 2018. **23**(11).
278. Holló, Z., L. Homolya, C.W. Davis, et al., *Calcein accumulation as a fluorometric functional assay of the multidrug transporter*. *Biochim Biophys Acta*, 1994. **1191**(2): p. 384-8.

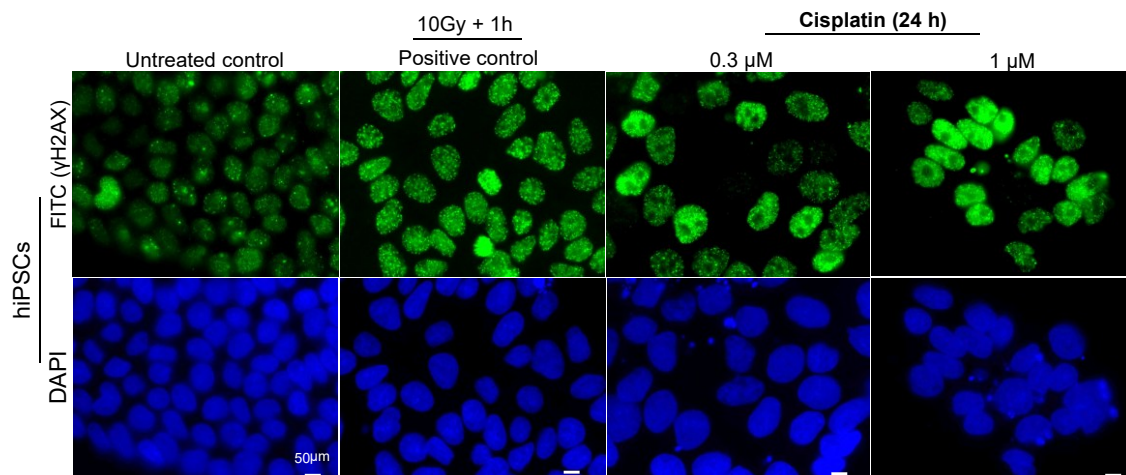
8. Appendix

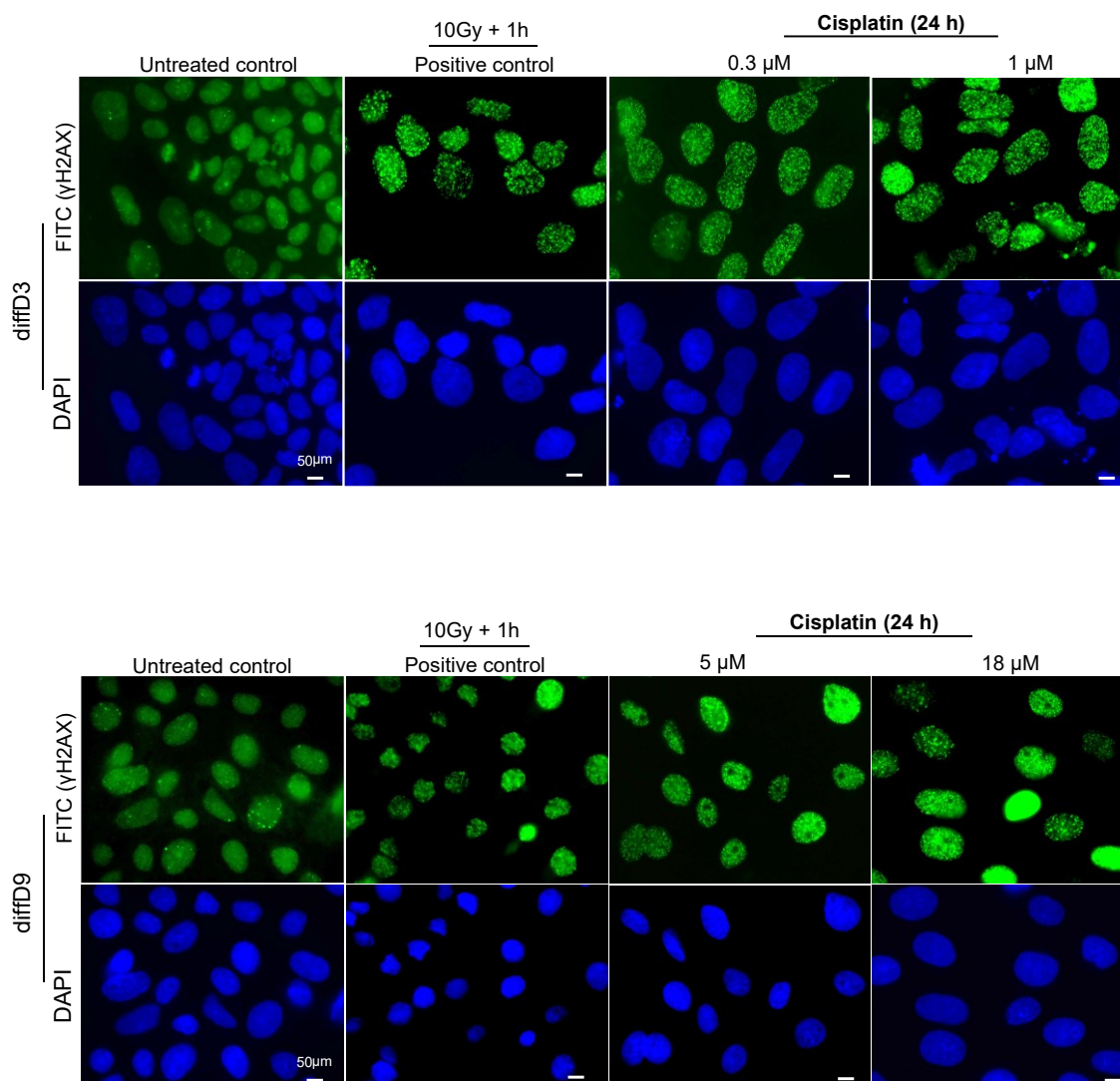
8.1. Differentiated PTELCs displayed renal functions



Supplementary Figure 1: Differentiated PTELCs display renal functions and maintain their differentiation status over three days after differentiation. (A) Representative images of calcein accumulation in differentiated PTELCs in the presence and absence of the complete inhibitor cyclosporin A. Nuclei were counterstained with DAPI (blue) and calcein-colored green FITC. (B) Specific tubular uptake of the fluorescent anion 6-CF (green) in PTECLs either with or without the anion transporter inhibitor probenecid. The scale bar represents 50 μ m. (C) Transepithelial electrical resistance (TEER) measurements of differentiated PTELCs and RPTEC/TERT1 cells. PTECs and RPTEC/TERT1 cells were seeded on membrane filter inserts at 100% confluence, and TEER was measured. (D) Time-dependent quantification of Aqp-1 and albumin uptake of differentiated PTELCs by qRT-PCR (i) and FACS (ii), respectively. Data from at least 3 independent experiments (qPCR also included 3 technical replicates) are expressed as mean + SD. ** $p < 0.01$, *** $p < 0.001$ vs. hiPSC, $^{\circ}p \leq 0.05$, $^{\circ\circ}p < 0.01$, $^{\circ\circ\circ}p < 0.001$ vs. diffD9; Aqp-1 = aquaporin 1, diffD=differentiation day, hiPSC = human induced pluripotent stem cells, PTELC = proximal tubule epithelial-like cell, 6-CF = Carboxyfluorescein.

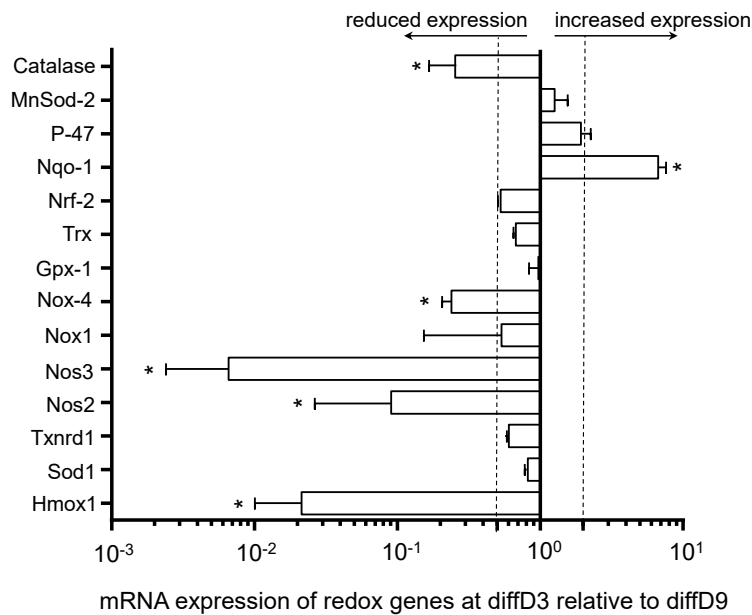
8.2. Incidence of γ -H2AX foci in cells at different differentiation stages



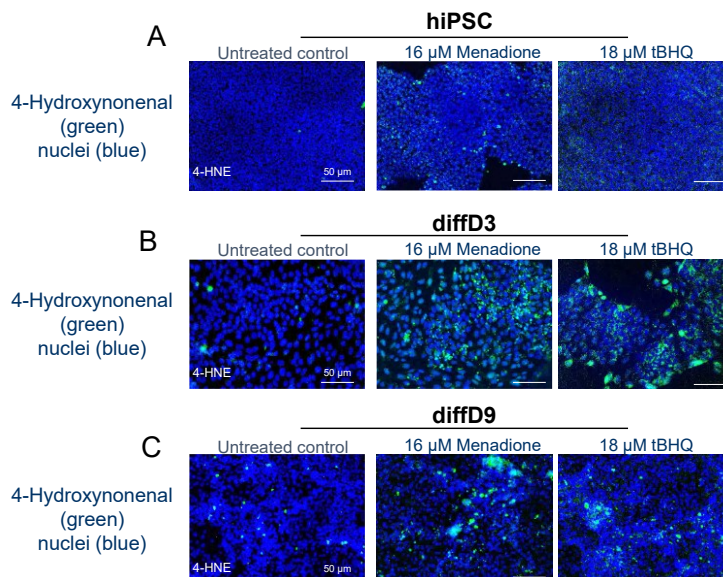


Supplementary Figure 2: γ -H2AX analysis during differentiation of PTELCs from hiPSCs. Antibody detection of DNA double-strand breaks (via the surrogate marker γ -H2AX) in hiPSC, differentiating and differentiated PTELCs after treatment with cisplatin and ionising radiation at the indicated doses. Representative images of the localisation of γ -H2AX foci (green fluorescence (FITC)) and DAPI-stained nuclei (blue fluorescence) are shown, taken at 40x magnification.

8.3. Expression of redox genes and induction of oxidative by oxidants in cells at different stages of differentiation



Supplementary Figure 3: Changes in the expression of redox genes during the differentiation of PTELCs from F4-hiPSC. The mRNA expression in differentiated (diffD3) relative to the expression in differentiated (diffD9) was analyzed by quantitative RT-PCR. The relative mRNA expression of diffD9 was set to 1.0. Data represents the mean + SD of three independent experiments performed in three technical replicates. Student's test, * $p \leq 0.05$ vs. diffD9. diffD3 = differentiation day 3, diffD9 = differentiation day 9, Gpx-1 = Glutathione peroxidase 1, Hmox-1 = Heme oxygenase (decycling) 1, Nos = Nitric oxide synthase 2/3, Nox = NADPH oxidase 1/4, Sod-1 = Superoxide dismutase 1, Txnrd-1 = Thioredoxin reductase 1, Trx = Thioredoxin, Nrf-2 = Nuclear factor erythroid 2-related factor 2, Nqo-1 = NAD(P)H dehydrogenase 1, MnSod-2 = manganese-dependent superoxide dismutase.



Supplementary Figure 4: Menadione and TBHQ induce oxidative stress in cells at different stages of differentiation. Undifferentiated hiPSC, differentiated cells (diffD3) and fully differentiated cells (diffD9) were treated with IC50 of menadione (16 μ M) and TBHQ (18 μ M) for 24 hours and then stained with antibodies against 4-HNE (green) and DAPI (blue). Representative images of 4-HNE-positive cells from (A) undifferentiated hiPSC, (B) differentiating cells (diffD3) and (C) fully differentiated cells (diffD9) are shown at 20x magnification. 4-HNE = 4-hydroxynonenal, diffD3 = differentiation day 3, diffD9 = differentiation day 9, hiPSC = human induced pluripotent stem cells, TBHQ = tertbutylhydroquinone.

8.4. Full description of the Materials and Methods used

8.4.1. Materials

The human induced pluripotent stem cell line Foreskin-4 (F4) (from now on referred to as hiPSCs) was purchased from WiCell Stem Cell Bank (Madison, USA). Human embryonic stem cell qualified Matrigel and Reduced Growth Factor Basement Membrane Matrix are from Corning (New York, USA). mTeSR1 medium was from StemCell Technologies (Vancouver, Canada), while renal epithelial growth medium (REGM) containing various growth factors and supplements (REGM BulletKit) was from Lonza (Basel, Switzerland). Y-27632 dihydrochloride and BMP-2 were from Sigma-Aldrich (St. Louis, USA), and BMP-7 was supplied by Thermo Fisher Scientific (Waltham, USA). All chemicals and other supplies were purchased from Teva (Petach Tikva, Israel), Enzo Life Sciences (Farmingdale, NY, USA), Sigma-Aldrich (St. Louis, USA), Baseclick (Tutzingen, Germany), Miltenyi Biotec (Bergisch Gladbach, Germany), Qiagen (Venlo, Netherlands), Biotec (Luckenwalde, Germany) Tecan (Männedorf, Switzerland), Olympus (Shinjuku, Tokyo, Japan), Biometra (Jena, Germany), GE Healthcare Life Sciences (Buckinghamshire, UK), Bio-Rad Laboratories (Hercules, CA, USA), BD biosciences (Franklin Lakes, NJ, USA), Zeiss (Oberkochen, Germany), Binder (Tuttlingen, Germany), Greiner Bio-One, Austria, TPP, Switzerland, Life Technologies, USA, VWR, USA, Sarstedt, Germany, Bio-Rad Laboratories (Hercules, CA, USA), BD biosciences (Franklin Lakes, NJ, USA), Wayne Rasband, NIH (Bethesda, MD, USA). The primers were purchased from Eurofins Genomics (Val Fleuri, Luxembourg), while antibodies were purchased from Abcam (Cambridge, UK) and BD Bioscience (Heidelberg, Germany), Cell Signaling (Beverly, Massachusetts, USA), Thermo Scientific (Waltham, USA), Biozol (Eching, Germany), Santa Cruz Biotec (California, USA), Invitrogen, Sigma-Aldrich (St. Louis, USA), and the fluorophore-conjugated secondary antibody Alexa Fluor 488 was purchased from Life Technologies (Carlsbad, California, USA). The primers and antibodies used in this project are listed in Tables 10 and 11, respectively.

8.4.1. 1. Table 1: Primer sequences used for real-time PCR

Gene	Forward	Reverse
TXNRD1	AGCATGTCATGTGAGGACGG	CCAATTCGAGAGCGTTCTCT
P47	GGGCGCGGATTATAGCAGT	CCCCAGTCACTCACGTTTCC
NRF2	CAGCTTTTGGCGCAGACATT	AGTGACTGAAACGTAGCCGA
BRAC2	AACATTCCTTCCTAAGTCTA	AACAACAATTACGAACCAA
CHECK2	CTCTGCTGGCTGAGGCTG	GAGACATCACGACCGCGT
GPX1	CCGGGACTACACCCAGATGA	TTGGCGTTCTCCTGATGCC
HMOX1	CTGCTCAACATCCAGCTCTTTG	CTTGGTGTGATGGGTCAGCA
IL-8	TTGGCAGCCTTCTGATTCTT	GGGTGAAAGGTTTGGAGTATG
P-21	AGTCAGTTCCTTGTGGAGCC	GACATGGCGCCTCCTCTG
β-Gal	TGCGCAATGCCACCCA	CAGGGCACATACGTCTGGAT
TRX	GATGGTCAAGAGCCCAACCA	CCGGGAAGTATCTCGGTGTG
MNSOD2	GCTTTCTCGTCTTCAGCACC	AGATACCCCAAAACCGGAGC
CATALASE	CAAAATGCTTCAGGGCCGC	GAGCACGGTAGGGACAGTTC
NQO1	ACCTTGTGATATTCCAGTTCCCC	GAACACTCGCTCAAACCAGC
NOS2	CTCCACATTGTTGTTGAT	AATCCAGATAAGTGACATAAG
NOS3	TGGAGTCTTGTGTAGGATA	CAAGGAGACGAAGAGAAC
NOX1	AATGTCACATACTCCACTG	CTCTCCAGCCTATCTCAT
SOD1	GCCTCATAATAAGTGCCATA	TCTGTTTCAATGACCTGTATT
MSH2	ATCATTCTCCTTGGATGCCTTAT	CTTCTTCTGGTTCGTCAGTATAGA
LIG1	CTTTGGAGGTCTTTAGGG	GAAGTGGCAACAGAGAAG
LIG3	GGAATAGGCACAGTCTT	GCTATATGTCTTTGGCTTTC
MGMT	AATCACTTCTCCGAATTTTAC	CTCTTCACCATCCCCTTT
PARP1	CACTTGCTGCTTGTGAA	GAACGACCTGATCTGGAA
POLE	AATCATCATAATCTGGTCTGT	TTTGGCATTGACATTGAG
RAD51	TGAAGTAGTTTGTCAAGC	AATTAGTTCCAATGGGTTT
REV3	TGTAGGAGGTAGGGAATA	AGTGTCTATTAGTATCAGGAA
SELE	ATTCCAATCCAGTAATAAC	GCTATGACTTATGATGAG
TOPO2α	AAGCGAGCCTGATTATTC	ACGGTGTGGATATTCTAAG
TOPO2β	GGCAATTTCTTTCCATTA	ATAACATTCCAACCAGAT
XPA	ACACGCTGCTTCTTACTG	AAGGAAGTCCGACAGGAA
XPC	TAAATAGCAAATCTCCTTTCC	ACACCTACTACCTCTCAA
XRCC1	ATTTAGGTCTCTTGGGAA	GAGGAAGTTGGATTTGAA
XRCC3	CTCCTTTACCGATTTACG	CATTGTTCTGTCTTTCT
MRE11A	GGTTGCCATCTTGATAGTT	GCCTGTCCAGTTTGAAT
ERCC1	TGTGTAGATCGGAATAAG	AGGAAGAAATTTGTGATAC
LIG4	CAGTAGGAGAAGCACCAA	TGAGCACATTGAGAAGGA
XRCC4	CTTCTCATTGACACCAAGAT	TGCCTGGACACCATTACA
OGG1	GATGTTGTTGTTGGAGGAA	AAGAGGTGGCTCAGAAAT
RPL32	GTTACGACCCATCAGCCCTTG	CATGATGCCGAGAAGGAGATGG
SGLT2	CAGTCTCCGGCATAGCAAGG	GGCCTGGGGCTCATTATC
SOX2	AGGATAAGTACACGCTGCC	TAAGTGTCCATGCGCTGGTT
ZO1	GAGAGGATTTGTCCGCTCAG	AGGCCTCAGAAATCCAGCTT
COLLAGEN IV	GTCAAAGTCTGTTCTGTGGGG	CCGCCTCCAACCTTGCGG
FIBRONECTIN	CCGGTTCAGGCCAGTAATA	CCACCACACCAATTCCTTG

Gene	Forward	Reverse
ACTB	GAGCACAGAGCCTCGCC	TCATCATCCATGGTGAGCTGG
AQP1	CATCCTCTCAGGCATCACCTC	CACACCATCAGCCAGGTCATTG
CAD16	AGCACGTGTGAAGTCGAAGT	ACTGAGGTTCTGGGAAGTGATG
CD13	TGGCCACTACACAGATGCAG	CTGGGACCTTTGGGAAGCAT
CTR1	TGATGCCTATGACCTTCTAC	GAATGCTGACTTGTGACTTAC
CTR2	CTGTACTGTATGAAGGCATC	AAAGTGACACAAATACCACC
CUBN	TAGCTTCGTGAAGGTGTGGG	GACTGGAAGACGGCAGTGAA
ECAD	CAGGACCAGGACTTTGACTT	AGATACCGGGGACACTCAT
GLUT5	GCCAAAGTGCACCCAGAATG	GTCAGCCTCCCTTCTTCAT
MDR1	AGTCGGAGTATCTTCTTC	TTGAATAGCGAAACATTGA
MEG	GCCAGTGGCCAAGAATGTGA	TCCGCGTCATCTGAACAGTC
NANOG	ACCTCAGCTACAAACAGGTGAA	AAAGGCTGGGGTAGGTAGGT
NCAD	AGGCTTCTGGTAAAATCGCA	GCAGTTGCTAAACTTCACATTGAG
OAT1	AGTATGGAGGTACTCCGGGC	GCATGGAGAGGCAGAGGAAG
OAT3	CTTTGTGCCCTTGGACTTGC	GGAAGAGGCAGCTGAAGGAG
OCT2	GAAGCCGAAAATATGCAAAG	TGCAGGGATTCTACTTTTG
OCT3/4	ACCCACACTGCAGCAGATCA	CCACACTCGGACCACATCCT
OCTN2	CACCATTGTGACCGAGCAAG	AGCAGGCTTCTTTCCCATCC
PEPT1	CAAGTGCATCGGTTTTGCCA	CTCTTTAGCCCAGTCCAGCC
PEPT2	CTGGGAGGACAAGTGGTACA	AGTCCGTTCTCTGCATGTT
CAD 11	CACGTCCCCAGTTAGCTTCTTC	GGCCCTGTGACATTCTTTCG
LICAM	CTTCGGCGAGTACAGGTCC	CCAAAGGCCTTCTCCTCGTT
VIMENTIN	GGTCAAGACGTGCCAGAGAA	TGCGGCTGCGAGAAAAATTG
APEX1	GCTGGTAGTTTGTCTCTG	AGGATTAGATTGGGTAAGGA
ATM	TGAGGAAGATAGTAAGAG	CAAGATGTTATAGAGTT
DDB2	CTACTAGCAGACACATCC	TTTAACCCTCTCAATACCA

ACTB = β -actin, AQP1 = aquaporin-1, CAD16 = cadherin 16, CD13 = alanyl aminopeptidase, CTR1/2 = copper transporter 1/2, CUBN = cubilin, ECAD = E-cadherin, CAD = cadherin 11, GLUT5 = glucose transporter 5, MDR1 = multidrug resistance protein 1, MEG = megalin, NANOG = homeobox protein, NCAD = N-cadherin, OAT1/3 = organic anion transporter 1, OCT 2 = organic cation transporter 2, OCT3/4 = octamer-binding transcription factor 3/4, OCTN2 = organic cation/carnitine transporter 2, PEPT1/2 = peptide transporter 1/2, RPL32 = ribosomal protein L32, SGLT2 = sodium/glucose cotransporter 2, SOX2 = sex determining region Y-box 2, ZO1 = zonula occludens 1, Gpx1 = glutathione peroxidase 1, CHECK1 = Checkpoint kinase 1 homolog, DDB2 = Damage specific DNA binding protein 2, ERCC1 = Excision repair cross-complementing rodent repair deficiency, HMOX1 = Heme oxygenase 1, XRCC1/3/4 = X-ray repair complementing defective repair in Chinese hamster 4, XPC = Xeroderma pigmentosum, complementation group C, XPA = Xeroderma pigmentosum, complementation group A, TXNRD1 = Thioredoxin reductase 1, TOPO II α/β = Topoisomerase (DNA) II α/β , SOD1 = Superoxide dismutase 1, SELE = Selectin, POLE = Polymerase (DNA directed), epsilon, PARP1 = Poly (ADP-ribose) polymerase 1, OGG1 = 8-oxoguanine DNA-glycosylase 1, NOX1 = NADPH oxidase 1, NOS2/3 = Nitric oxide synthase 2/3, MSH2 = MutS homolog 2, MRE11A = Meiotic recombination 11 homolog A, MGMT = O-6-methylguanine-DNA methyltransferase, LIG1/3/4 = Ligase I/III/IV, IL8 = Interleukin 8, β -GAL = beta galactosidase, ATM = Ataxia telangiectasia mutated homolog, APEX1 = Apurinic/apyrimidinic endonuclease 1, BRCA2 = Breast cancer 2, NRF2 = Nuclear factor erythroid 2-related factor 2, NQO1, quinone oxidoreductase 1, TRX = Thioredoxin, MNSO4 = manganese-dependent superoxide dismutase, REV3 = Protein reversionless 3-like.

8.4.1.2. Table 2: Antibodies used

Protein	Order Number	Company	Dilution
AQP1	AB9566	Abcam	1:250
CD13	AB108310	Abcam	1:500
GAPDH	2118S	Cell Signalling	1:4000
ECAD	610181	BD	1:1000
FIBRO	AB2413	Abcam	1:500
CTR1	AB129067	Abcam	1:25
CTR2	PA5-53246	Thermo Scientific	1:1000
MEG	AB236244	Abcam	1:500
OCT2	MB59600162	Biozol	1:500
OCT4	AB183900	Abcam	1:100
URO10	SC-58889	Santa Cruz Biotech	1:1000
ZO1	61-7300	Thermo Scientific	1:1000
NCAD	AB18203	Abcam	1:100
Phalloidin-Alexa Fluor 488	R37110	Invitrogen	1:200
Calcein-AM	C1430	Sigma-Aldrich	1:1000

AQP1 = aquaporin-1, CD13 = alanyl aminopeptidase, CTR1/2 = copper transporter 1/2, ECAD = E-cadherin, GAPDH = Glyceraldehyde 3-phosphate dehydrogenase, MEG = megalin, OCT2 = organic cation transporter 2, OCT4 = octamer-binding transcription factor 4, URO-10 = urothelial glycoprotein, ZO1 = zonula occludens 1, FIBRO = fibronectin, NCAD, N-cadherin, Calcein-AM = Calcein acetoxymethyl ester.

8.4.2. Methods

8.4.2.1. Cell biological methods

8.4.2.1.1. Cultivation of RPTEC and LLC-PK1 Cells

Human proximal tubule epithelial cells (RPTEC/TERT1) and porcine proximal tubule epithelial cells (LLC-PK1) were cultured in 75 cm² cell culture flasks containing 10 ml of the respective culture medium (**Section 2.9.2**). For proper maintenance of the cells, the cultures were passaged at a ratio of 1:3 (LLC-PK1) and 1:10 (RPTEC) once a week or whenever the cultured cells showed 70-90 % confluence. For this purpose, cells were detached by incubation in 5 ml trypsin/EDTA solution at 37 °C for 10 min. The proteolytic effect of trypsin/EDTA was stopped by adding 5 ml of prewarmed culture medium (LLP-PK1) or 5 ml of trypsin inhibitor (RPTEC). The cell suspension was then transferred to a 50 ml tube and centrifuged at 400 x g for 10 min at room temperature (RT). The supernatant was then removed, and the cells were resuspended in 10 ml of their respective

medium, diluted at a specific ratio (1:3 to 1:10) depending on the confluence, and transferred to the culture flasks. All cell cultures were performed under sterile conditions and incubated at 37 °C, 5 % CO₂, and 86 % humidity.

8.4.2.1.2. Cultivation of human induced pluripotent stem cells (hiPSCs)

The human induced pluripotent stem cells (F4-hiPSCs) used in this study were routinely cultured on six-well plates with a cell⁺ growth surface coated with human embryonic stem cell (hESC) qualified Matrigel in mTeSR1 medium (**section 2.3.2**). For this purpose, aliquots (6 well format) of hESC qualified Matrigel was dissolved in 6 ml cold DMEM with high glucose but without supplements, and 1 ml of this mixture was used to cover the bottom of each well of a 6-well plate. Matrigel-coated plates were either stored at 4 °C for one week or directly incubated for one hour at RT. After incubation, DMEM was aspirated from the Matrigel-coated wells and 1.85 ml of mTeSR1 medium supplemented with 1 µl (10 µM) ROCK inhibitor was added into each well and prewarmed at 37 °C in an incubator.

In vitro cultivation of hiPSC lines took place on this Matrigel-coated 6-well cell culture plate in mTeSRTM1 medium, allowing cell aggregates to grow at the bottom of the plate. For maintenance and expansion, cultures were split at a ratio of 1:6 twice a week when cultures reached a confluency of 70 – 90 %. For this purpose, medium was removed from the confluent hiPSCs, stored and the cells were washed once with 1 ml DPBS. Gentle dissociation of the adherent cells was achieved by incubation with 1 ml DPBS for 5 min. Using a cell spatula, the cells were completely scraped off the bottom and the reaction stopped with the previously removed medium. Subsequently, the cell suspension was transferred into a 15 ml tube and cells were sedimented *via* centrifugation for 2 min at 38 g at RT. Afterwards, the supernatant was then aspirated, and the cell pellet resuspended in mTeSR depending on the desired cell density. 150 µl of the cell suspension could now be seeded onto the prepared Matrigel-coated plates. Medium changed was perform daily until the next passage. Both hiPSC lines were cultured for maintenance, expansion, and experiments at 37 °C, 5 % CO₂ and 86 % humidity.

8.4.2.1.3. Cryopreservation and thawing of hiPSCs.

For cryopreservation, hiPSCs were detached from the bottom of the cell culture plate, centrifuged, and pelleted as described in section 3.1.2. Subsequently, 1 ml of Cryo Brew (StemMACSTM iPS-Brew XF) was placed in a labelled 2 ml Cryo.sTM freezing vessel and the cell pellet resuspended in 900 µl Cryo Brew. The 900 µl

cell suspension was then transferred to the freezing tube and frozen at $-80\text{ }^{\circ}\text{C}$ in a CoolCell insulated container. After 24 h, the frozen cells stored at $-80\text{ }^{\circ}\text{C}$ was then transferred into a tank of liquid nitrogen for long term storage. To thaw hiPSCs, 2 wells of a 6-well cell culture plate were coated with Matrigel and 1.5 ml of mTeSR medium supplemented with $2\text{ }\mu\text{l}$ ($10\text{ }\mu\text{M}$) ROCK inhibitor as described in 3.1.2. Subsequently, the frozen tubes containing the cells were removed from a liquid nitrogen tank and disinfected with 80 % ethanol. The cells were warmed in a water bath until only a small ice-crystal was visible. The cell suspension in the tube was transferred to a 50 ml falcon, and 5 ml of pre-warmed DMEM without additives was added dropwise to the cell suspension with careful swirling, followed by sedimentation at $200\times g$ for 5 min at RT. The supernatant was aspirated, and 1 ml mTeSR was used to carefully resuspend the cell pellet. Subsequently, 0.5 ml of cell suspension was seeded into each well of a Matrigel-coated plate and cultured at $37\text{ }^{\circ}\text{C}$, 5 % CO_2 , and 86 % humidity in an incubator. The cell culture medium was changed daily until the next passage.

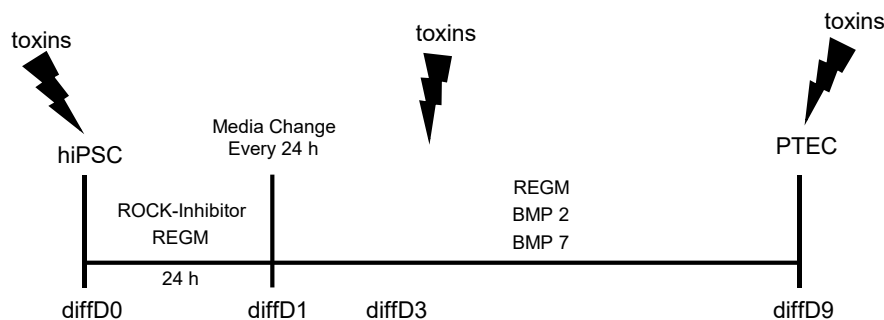
8.4.2.1.4. Differentiation of hiPSCs into proximal tubular epithelial-like cells

Confluent hiPSCs on wells coated with Matrigel were differentiated into proximal tubular-like cells (PTELCs) according to the one-step protocol developed by Kandasamy et al. with slight modifications. For this purpose, 12-well culture plates were coated with growth factor-reduced Matrigel (GFR) for one hour at RT according to the manufacturer's instructions, and 1 ml of renal epithelial growth medium (REGM) containing $0.5\text{ }\mu\text{l/well}$ ($10\text{ }\mu\text{M}$) ROCK inhibitor was added and stored in the incubator until seeding. Confluent hiPSCs were washed with DPBS and then detached from the plate by incubation with StemPro™ Accutase™ at $37\text{ }^{\circ}\text{C}$ for approximately 5 min. The proteolytic reaction was stopped by carefully resuspending the cells with a fresh medium. Cell counting was then performed using $20\text{ }\mu\text{l}$ of the cell suspension mixed with $20\text{ }\mu\text{l}$ of a 0.4 % trypan blue solution, and cell viability was determined using a Neubauer counting chamber. In parallel, the remaining cell suspension was sedimented by centrifugation at $200\times g$ for 5 min at RT. Afterward, the cell aggregates were resuspended with fresh REGM to obtain 1000 000 cells/ml. Then, $30\text{ }\mu\text{l}$ of this cell suspension, containing 3000 cells, was seeded per well into the Matrigel-coated plate and incubated overnight. After 24 h, the cells were transferred to REGM differentiation medium without ROCK inhibitor but with $0.1\text{ }\mu\text{l/ml}$ bone morphogenetic protein-2 (BMP-2) and $0.025\text{ }\mu\text{l/ml}$ BMP-7 and cultured under these conditions for 9 days with a daily medium change to induce differentiation towards PTELC. hiPSC-derived PTELCs were treated

directly with nephrotoxic substances or harvested for further experiments on day 9.

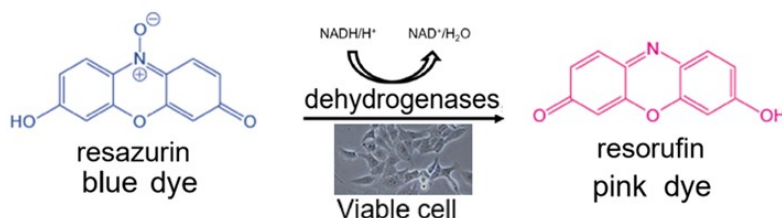
8.4.2.1.5. Drug treatment and cytotoxicity assay

To investigate the effect of toxins on the renal developmental and regeneration processes, hiPSCs, hiPSC in the process of differentiating into PTELC on differentiation day three (diffD3) and hiPSC after nine days of differentiation (diffD9) were treated with different concentrations of the model compounds cisplatin, a genotoxic nephrotoxin and cyclosporin A, a non-genotoxic nephrotoxin, and as well as some known oxidative stress-inducing agents such as hydrogen peroxide (H₂O₂), menadione, and tert-butylhydroquinone (tBHQ). Specifically, 3000 cells from the same hiPSC batch were seeded into a Matrigel-coated 24-well cell⁺ culture plate as described in Section 3.1.5. After 0, 3, and 9 days of differentiation, cells were treated in triplicate for 24 h with different concentrations of the various compounds and their respective vehicle controls (DMSO or basal medium), except for H₂O₂, where cells were treated for only 30 min. The nephrotoxicity of these compounds was measured using the Alamar Blue assay. The Alamar Blue Assay is a colorimetric assay for measuring cells' metabolic activity as a cell viability marker. In principle, dehydrogenase in metabolically active cells can reduce resazurin, a membrane-permeable, non-fluorescent blue dye, to resorufin upon entry into the cells, resulting in a pink dye that fluoresces at 590 nm. The pink dye can, therefore, be used to indicate the presence of metabolically active enzymes and, thus, cell viability. This principle can be illustrated in **Fig. 4**. The fluorescence intensity of resorufin can therefore be measured using a microplate reader at an emission wavelength of 590 nm and an excitation wavelength of 535 nm [192].



Supplementary Figure 4: Protocol for the differentiation of hiPSC to PTELCs, adapted from Kandasamy et al. [22]. Schematic representation of the protocol for differentiating hiPSCs into PTELC and for the treatment time points during the differentiation process. The seeding of singularized hiPSCs on day 0 was conducted with REGM supplemented with 5 μ M ROCK inhibitor. From day 1, the medium was changed daily with REGM without ROCK inhibitor but with BMP-2 and BMP-7 to drive the cells towards proximal tubular cells within 9 days of differentiation.

After treatment with the various agents and vehicle controls, the medium was aspirated and the cells and blank controls were incubated at 37 $^{\circ}$ C and 5 % CO_2 for 4 hours in the dark with 500 μ l of freshly prepared resazurin working solution, as described in Table 3. The optical density (OD) was measured in quadruplicates at 535 nm and 590 nm using a microplate reader (Tecan infinite 200). Relative cell viability values were normalized to the respective vehicle controls and expressed as percentages using the formular:



Supplementary Figure 5: Structure of the blue resazurin substrate and the pink, fluorescent resorufin product resulting from reduction by diaphorase enzymes in viable cells [275]. Figure modified from Riss *et al.*[276].

Table 3: Preparation of Resazurin working solution

Components	Compositions
Resazurin stock solution (440 mM)	40 mM Na-Resazurin in dimethylformamide
NaCl/Pi buffer	150 mM NaCl, 3.77 mM Na_2HPO_4 1.06 mM KH_2PO_4
Resazurin – Pi buffer solution (440 μ M)	Resazurin stock solution (1: 1000) with NaCl-Pi
Resazurin working solution (44 mM)	Resazurin-NaCl/Pi (1:10) with DMEM (no phenol red)

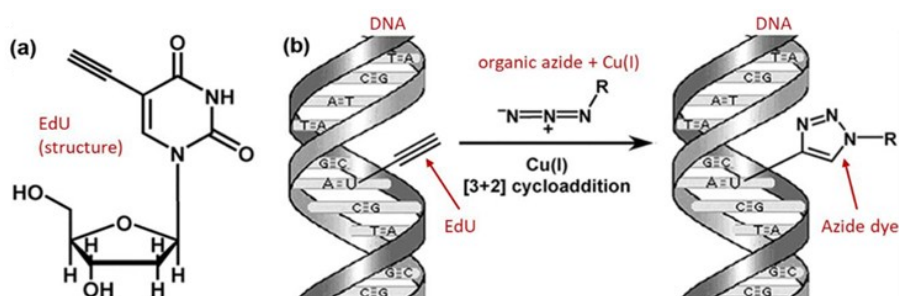
8.4.2.1.6. Immunobiological methods

8.4.2.1.6.1. Immunofluorescence analysis

Immunofluorescence staining was performed to monitor the expression of prototypical proximal tubule-related proteins in hiPSC-derived PTELCs. This technique allows visualization of a specific protein in a cell population or compartment where the protein is expressed. It is based on primary antibodies specific for the protein of interest and secondary antibodies that bind to the primary antibodies. The secondary antibodies are conjugated to a fluorophore or an enzyme that catalyzes a visible reaction after adding a chromogenic substrate. For this approach, coverslip-coated hiPSC-derived PTELCs and RPTEC were fixed with 1 ml of 4 % cold formaldehyde/PBS for 15 min at RT in a fume cupboard. Afterward, the fixed cells were washed three times for 5 min with PBS and permeabilized with 0.3 % Triton in PBS for 10 min at RT. After that, the cells were rinsed thrice with PBS for 5 min and incubated with blocking buffer (5 % BSA/PBS) for one hour at RT in a humidified chamber to prevent unspecific binding of the primary antibody. After blocking, incubation with primary antibodies in the dilution indicated in Table 2 were performed at 4 °C overnight in a humid chamber. After thorough washing with PBS to remove the unbound primary antibody, a fluorescence-labeled secondary antibody (Alexa Fluor 488/550 goat polyclonal to mouse or rabbit) was added and incubated in the dark (1:1000; 2 hours). Nuclear DNA was stained with Vectashield containing DAPI (4',6-diamidino-2-phenylindole). Coverslip-containing slides were sealed with nail polish and examined with an Olympus Bx43 fluorescence microscope.

8.4.2.1.6.2. Analysis of cell proliferation by measuring EdU incorporation

To monitor the proliferation rate during the differentiation of hiPSCs into PTECs, the incorporation of fluorescent 5-ethynyl-2'-deoxyuridine (EdU) into S-phase cells was analyzed using the EdU-Click-488 proliferation assay kit according to the manufacturer's instructions. This assay is based on the finding that the thymidine analog EdU is incorporated into DNA during DNA synthesis in proliferating cells. This EdU incorporation can, therefore, be visualized using click chemistry, which involves the reaction between the terminal alkyne group of EdU in the major groove of DNA with an organic 6-FAM azide dye in the presence of catalytic amounts of copper(I) ions. The 6-FAM azide dye excites at 496 nm and emits at 516 nm (**Fig. 6**), as previously shown by Ligasova *et al.* [277].



Supplementary Figure 6: Schematic representation of EdU (a) structure and its reaction with the azide dye in DNA (b). EdU is a thymidine analog with a terminal alkyne group in the 5-position. This molecule is incorporated into cellular DNA during replication in place of the standard thymidine nucleotide. Its incorporation is detected when the terminal alkyne group in the major grooves of the DNA double helix reacts with organic azides by Cu(I)-catalyzed cycloaddition—adapted from Ligasova *et al.* [277].

In brief, 3000 cells from the same hiPSC batch were seeded into a Matrigel-coated 12-well cell⁺ culture plate with 18 mm glass coverslips. After 0, 3, and 9 days of differentiation, the coverslip-coated cells were incubated with 1 ml DMEM without phenol red supplemented with 1 μ l (10 μ M) EdU for 2 hours at 37 °C. Afterward, the cells were washed thrice with 1 ml of 3% BSA/PBS and fixed in 1 ml of cold 4 % formaldehyde/PBS for 15 minutes at RT in a fume hood. Subsequently, the cells were washed twice with 1 ml of 3 % BSA/PBS and incubated with 1 ml of 0.5 % Triton-X/PBS for 20 minutes at RT. During this incubation period, the click-it cocktails containing 379 μ l of distilled water (dH₂O), 50 μ l of 10x reaction buffer, 20 μ l of catalyst solution, 1 μ l of 10 mM 6-FAM azide, and 50 μ l of 10x buffer supplement was mixed in this exact order. After incubation, 50 μ l of the Alexa Fluor 488 conjugated dye reaction- cocktail was added (30 minutes, RT in the dark), followed by washing three times with 3 % BSA/PBS and counterstaining the nuclei with 6 μ l DAPI. Finally, slides were sealed with nail polish, and at least 200 cells were captured in dual-channel images (DAPI and FITC) using an Olympus Bx43 fluorescence microscope. The percentage of EdU-positive cells was determined using ImageJ version 1.51j8.

8.4.2.1.6.3. Flow cytometry-based analysis

Intracellular and cell surface proteins were also detected in hiPSC-derived PTELCs at the single-cell level using flow cytometric analysis. Flow cytometry allows cells to be molecularly characterized and quantified based on their size, granularity, and fluorescence intensity by optical measurement with a laser beam. For this purpose, the cells are diluted in a flow cell in suspension using an envelope flow, hydrodynamically focused on the process, and thus successively passed an optical

measuring point. The measurement principle is based on scattered light and fluorescence, which are detected when the cells pass the laser beam arranged at right angles to them. The size of the cells is determined by forward scattering (FSC) and granularity by side scattering (SSC). Therefore, by incubating cells with Fluorescently labelled antibodies against surface proteins or intracellular structures, fluorescent light can be emitted after excitation by a suitable laser, detected by photomultipliers, and converted into electrical signals. Based on this understanding, flow cytometric analysis was performed to quantitatively detect the proximal tubular markers aquaporin 1 (Aqp-1) and urothelial glycoprotein 10 (Uro-10). For this purpose, after trypsinization, at least one million cells were pelleted in four different 1.5 ml Eppendorf tubes by centrifugation (400 \times g, 4 minutes, 4 $^{\circ}$ C) and treated with 0.5 % Tween 20 in PBS at RT for 15 minutes. After centrifugation, cells were resuspended in 3 % BSA in PBS for 15 minutes at RT and centrifuged again at 400 \times g, 4 min, 4 $^{\circ}$ C. After aspiration of the supernatant, 100 μ l of the primary antibody against Aqp-1 (1:250; in 3 % BSA/PBS) and Uro-10 (1:1000; in 3% BSA/PBS) were added to each of the two tubes and incubated overnight at 4 $^{\circ}$ C. To determine the autofluorescence of the cells, one tube was incubated with 100 μ l 3 % BSA/PBS overnight at 4 $^{\circ}$ C as a negative control without antibody. The other tube containing cells was also incubated with 100 μ l 3 % BSA/PBS overnight at 4 $^{\circ}$ C and served as a second antibody control to determine non-specific binding. Afterward, the cell pellets were washed twice with 1 ml PBS and centrifuged at 400 \times g for 4 minutes. The supernatant of the cell pellets was removed, and 100 μ l of the second antibody diluted 1:1000 in 3 % BSA/PBS was added to the tube containing the cells with the first antibody treatment and to the tube containing the second antibody control. Meanwhile, 100 μ l of 3 % BSA/PBS was added to the tube containing the negative control. All four tubes were incubated for 2 hours in the dark at RT. After incubation, the cell pellets were resuspended twice with 1 ml of PBS and centrifuged at 400 \times g for 4 minutes. After aspiration of the supernatant, the cell pellets were resuspended in 300 μ l PBS, transferred to a 2 ml Eppendorf tube, and placed on ice until measurement with the BD Accuri™ C6 plus flow cytometer. The stained cell suspension flow was performed at an average flow rate, measuring at least 10,000 events (P1) per sample. Firstly, a scatter plot of the negative control was created, in which the two parameters, FSC (cell size) and SSC (cell granularity), are plotted against each other. Each cell or event is plotted as a separate point in the scatter plot. A specific region called gate was selected within the plot that excluded events too small to be intact cells, thereby excluding most cell debris and contamination for analysis. Secondly, another graph,

(histogram) was created using the events in the gate, which shows the fluorescence intensity in the FITC channel on the horizontal axis compared to the number of events in the gate on the vertical axis. In this histogram, a vertical threshold marker was placed at the boundary of the negative cell population so that only 5 % of the negative events were to the right of the marker. All events that exceeded this threshold were classified as positive. The histograms of the other samples showed the number of cells that exceeded this fluorescence threshold. To determine the percentage of Aqp-1 and Uro-10 positive cells, the background fluorescence of the second antibody control was subtracted from the percentage of cells that exceeded the fluorescence threshold.

8.4.2.1.6.4. TUNEL assay

To verify whether the nephrotoxic compounds cisplatin and cyclosporin A induce apoptosis in cells at different stages of differentiation, the TUNEL assay was performed using the In Situ Cell Death Detection Assay Kit, which can label apoptotic cells. The TUNEL (terminal deoxynucleotidyl transferase-mediated dUTP-fluorescein nick-end labelling) assay can detect cells undergoing apoptosis. In principle, the cell's DNA is fragmented during apoptosis, resulting in free hydroxyl groups within the DNA strand breaks. These free hydroxyl groups can be visualized by labelling with modified nucleotides through an enzymatic reaction [236]. Therefore, this assay kit contains the enzyme TdT, which catalyses the modified nucleotide fluorescein deoxyuridine triphosphate (dUTP) polymerization to the free hydroxyl groups. The modified nucleotide can be visualized under the microscope. For this purpose, coverslip-coated cells at different stages of differentiation with or without drug exposure were washed with PBS and fixed with 3.7 % PFA for 15 min at RT. After washing three times with PBS, cells were incubated with 0.5 % Triton-X/PBS for 10 min at RT and then blocked with 3 % BSA/PBS for 1 h at RT. After washing with PBS, one coverslip of each cell type was incubated with 150 U/ml DNase for 10 min at RT as a positive control. Subsequently, all coverslips were treated with labelling solution (5 µl enzyme solution + 45 µl labelling solution per coverslip) for one hour in the dark at 37 °C, and apoptotic cells were labelled with TdT and fluorescein-dUTP. After another washing step, coverslips were mounted with VECTASHIELD® Antifade Mounting Medium containing DAPI and sealed with nail polish. Fluorescence images were acquired using an Olympus BX43 fluorescence microscope at 20X magnification and analysed using ImageJ. TUNEL-positive cells were referenced to the total number of cells and normalized to the untreated control.

8.4.2.1.7. Transport assays and barrier function analysis

8.4.2.1.7.1. Albumin uptake assay

To investigate whether hiPSC-derived PTELCs exhibited transport properties typical of proximal tubules, cellular endocytosis of albumin as a surrogate marker of functionality was assessed by adding different concentrations of fluorescence labelled bovine serum albumin (BSA-FITC). For this purpose, hiPSCs, hiPSC-derived PTELCs, and the positive and negative control cell lines (LLC-PK1 and RPTEC, respectively) were incubated with serum-free medium with/without 12.5 µg/ml, 25 µg/ml, 50 µg/ml, 100 µg/ml, and 200 µg/ml BSA-FITC for 2 h at 37 °C. Afterward, the BSA-FITC uptake was stopped by washing the cells thrice at 5 min interval with ice-cold PBS. At this point, cells were either detached with 0.5 ml trypsin/EDTA for 5 min, fixed with 0.5 % cold formaldehyde in PBS (15 min, RT) and analyzed by flow cytometry as described in section 3.3.3 or fixed with 0.5 % cold formaldehyde in PBS (15 min, RT) followed by counterstaining of cell nuclei with DAPI and visualization with the Olympus Bx43 fluorescence microscope.

8.4.2.1.7.2. Organic anion uptake assay

To investigate organic anion transport by the basolateral organic anion transporters OAT-1 and OAT-3 in the cells after differentiation, an assay was performed using the fluorescent anion 6-Carboxyfluorescein (6-CF), a known substrate for the OATs as described previously by Lawrence and Colleagues [21]. For this purpose, diffD9 cells and RPTECs (positive control) on coverslips were incubated with 3 µM 6-CF at 37 °C for 40 minutes in the presence or absence of 50 µM OAT inhibitor (Probenecid). After incubation, the reaction was stopped by washing the coverslip-coated cells four times with ice cold HBSS. Subsequently, the cells were fixed with cold formaldehyde in PBS (15 minutes, RT), followed by counterstaining of cell nuclei with DAPI. Uptake of 6-CF was visualization with the Olympus Bx43 fluorescence microscope.

8.4.2.1.7.3. Calcein-AM assay (P-glycoprotein efflux assay)

The calcein accumulation assay was performed to detect the functional activity of the ABC transporter permeability (P)-glycoprotein (P-gp) in cells after 9 days of differentiation. During the assay, cells exposed to calcein acetoxymethyl ester (calcein-AM) become fluorescent after cleavage of calcein-AM by intracellular esterases that generate a fluorescent derivative calcein. P-gp actively extrudes calcein-AM but not fluorescent calcein, resulting in decreased cell fluorescence and

indicating functional P-gp presence [278]. Thus, PTELCs derived from hiPSC and the positive control cell line RPTECs grown on coverslips were incubated in 1 ml HBSS at 37 °C for 1 hour with and without cyclosporine A (CsA), a potent P-gp inhibitor. After incubation, coverslip-coated cells were washed once with 1 ml HBSS, followed by another 2-hour incubation with or without calcein and CsA. Hereafter, cells were washed twice with HBSS, fixed with 0.5 ml cold formaldehyde in PBS (15 min, RT), and nuclei counterstained with DAPI. Calcein retention was visualized using an Olympus Bx43 fluorescence microscope.

8.4.2.1.7.4. Analysis of Barrier function

The proximal tubule is usually characterized by a high epithelial tightness, essential for the cells' reabsorption and secretion function. Therefore, cultivation on transwell membrane filter inserts is considered the gold standard for renal proximal tubule cells, as it allows for basolateral-apical functional organization of the cells. The integrity of the renal proximal epithelial-like monolayer on membrane filters can be quantified by its insulating property as transepithelial electrical resistance (TEER). For this purpose, the TEER of matured hiPSC-derived PTELCs and RPTEC (positive control) was measured manually using an EVOM² ohmmeter according to the manufacturer's instructions. diffD9 cells on Matrigel-coated wells and RPTEC were harvested and plated on 6-transwell inserts at a density of 2.5×10^5 cells per insert. Both cell types were seeded on 6-transwell inserts without coating. However, diffD9 cells were cultured in REGM medium supplemented with the 1 μ M TGF-beta type 1 receptor inhibitor GW788388 hydrate to maintain their polarity and differentiation status. After 72 hours of seeding, epithelial resistance was measured, and the TEER value in $\Omega \cdot \text{cm}^2$ was determined by subtracting the resistance of the blank (inset with medium only) from the measured resistance (inset with media plus cells) and then multiplying by the surface area of the insert according to the following scheme:

$$\text{TEER value } (\Omega \cdot \text{cm}^2) = \text{TEER}_{\text{sample}} - \text{TEER}_{\text{blank}} * \text{surface area of insert } (4.5 \text{ cm}^2)$$

8.4.2.1.8. Molecular biological methods

8.4.2.1.8.1. RNA isolation and quantification

RNA was isolated from hiPSCs, diffD3, diffD9, and RPTEC either manually or with the help of the QIAcube automated machine using the RNeasy Mini Kit and RNase-free DNase kit from Qiagen according to the manufacturer's instructions. Briefly, adherent cells (hiPSCs diffD3, diffD9, and RPTEC) were detached by incubation with StemPro Accutase for 5 min at 37°C, and the effect of Accutase was stopped by adding pre-warmed medium (DMEM). The cell suspension was then transferred to a 15 ml falcon, and the cells were centrifuged at 200 g for 5 min at 4 °C. The supernatant was then aspirated, and the cells were resuspended in 1 ml DPBS, transferred to a labelled 1.5 ml tube, and centrifuged again at 200 g for 5 minutes at 4 °C. After centrifugation, the supernatant was aspirated, and the pellets were either frozen directly at -80 °C for storage or immediately subjected to RNA isolation. In the latter case, cell pellets were resuspended in 350 µl RLT buffer and thoroughly vortexed, and lysates were transferred to a DNA removal column. After centrifugation at 17.000 g for 2 min at RT, 350 µl of 70 % ethanol was added to the flow-through and homogenized by pipetting up and down several times. The lysate was then transferred to a RNeasy column and centrifuged at 8.000 g for 15 seconds. The flow-through with all impurities was then discarded, and 350 µl of RNA wash buffer I (RW1) was added to the column containing bound RNA. Centrifugation was repeated at 8.000 g for 15 seconds, and the flow-through was discarded. After that, 80 µl DNase-1 mixture consisting of 10 µl DNase 1 and 70 µl RDD buffer was added to the centre of the column and incubated for 15 minutes to denature the DNA. After incubation, 350 µl RW1 buffer was added to the RNeasy column and centrifuged at 8.000 g for 15 seconds. The flow-through was discarded, and 500 µl of RPE buffer was added and centrifuged at 800 g for 15 seconds. After discarding the supernatant, the RNeasy column was centrifuged at 8.000 g for 2 minutes after adding 500 µl of RPE buffer. The flow-through was discarded, and the column was transferred to a 2-mL safe-lock tube and centrifuged at 17.000 g for 1 minute. Finally, 30 to 50 µl of RNase-free water was pipetted onto the RNA binding column in a labelled 1.5 ml Eppendorf tube and the RNA was eluted from the column by centrifugation for 1 min at 8.000-g. The RNA concentrations were determined using the Nano Vue Plus spectrophotometer and were either stored at -80 °C or used immediately for cDNA synthesis.

8.4.2.1.8.2. Complementary DNA synthesis

Complementary DNA (cDNA) was synthesized from the isolated 2000 ng RNA in a reaction volume of 20 µl to obtain 100 ng/µl cDNA. For this purpose, the High-

Capacity RNA-to-cDNA Reverse Transcription Kit was used in combination with RiboLock Rnase Inhibitor according to the manufacturer's instructions. Briefly, 10 μ l of RNA mixture (RNA + RNase-free water) containing 2000 ng of RNA template was added to a PCR tube, and 10 μ l of the prepared master mix (Table 5) was added. The PCR tubes containing the reaction mixture were placed in the thermal cycler. The cDNA synthesis process was initiated with a pre- incubation phase at 25 °C for 10 minutes, followed by reverse transcription of RNA into cDNA by the reverse transcriptase enzyme at 37 °C for 120 minutes. The reaction was stopped by denaturing all enzymes at 85 °C for 5 minutes. The resulting cDNA was stored at – 20 °C or used directly for RT-qPCR.

Table 4: Master Mix composition for cDNA synthesis from mRNA templates

Components	Amount (μl) per sample
10 x Buffer	2.0
25 x dNTP-Mix (10 mM)	0.8
10 x Random Primers	2.0
Riboblock Rnase Inhibitor (40u/ μ l)	0.5
MultiScribe Reverse Transcriptase	1.0
Rnase free water	3.7
2000 ng RNA in Rnase free water	10.0
Total	20.0

8.4.2.1.8.3. Quantitative real-time polymerase chain reaction

Quantitative real-time polymerase chain reaction (qPCR) was performed to relatively quantify the expression of differentiation-associated markers, EMT-related markers, and DNA repair and redox genes in hiPSC-derived cells and RPTEC using the SensiMix SYBR Hi-ROX kit. For this purpose, an appropriate amount of the synthesized cDNA was mixed with SYBR® Green (Master mix 1), and 10.2 μ l of this mixture was pipetted into the wells of a 96-well PCR plate to detect deviations due to pipetting. Subsequently, 9.8 μ l of the respective primer dilutions in high-purity PCR water (Master mix 2) were added to each well. The PCR plate was then covered with MicroAmp transparent film, briefly centrifuged to allow the two master mixes (Table 11) to mix appropriately, and then inserted into

the CFX96 Touch Real-Time PCR Detection System for amplification according to table 7.

Table 5: Master Mix composition for quantitative real-time polymerase chain reaction from cDNA templates

Components	Concentration per well
cDNA	20 ng
SensiMix™ SYBR® Hi-ROX (2x)	1 x
Forward Primers	0.25 µM
Reverse Primers	0.25 µM

Table 6: Real-time quantitative PCR program

Steps	Temperature (°C)	Duration (min:sec)	
Initial denaturation	95	10.00	
Denaturation	95	0.8	X 44 cycles
Primer hybridization	55	2.0	
Elongation	72	0.5	

After completion of RT-qPCR, the PCR plate was discarded, and data were analysed using CFX Manager software according to the manufacturer's instructions. The Cq values obtained for the genes of interest were first normalized to the mean Cq values of the housekeeping genes Act-β and Rpl-32 and then to the control samples and expressed as a fold of this mean. Changes in ≤0.5- and ≥2-fold gene expression were considered biologically relevant. The gene-specific primer pairs used for amplification in this study (Table 12) were designed using NCBI (<https://www.ncbi.nlm.nih.gov/nucore/>). These primer sets were validated for specificity in qPCR with different cDNA concentrations.

8.4.2.1.9. Biochemical methods

8.4.2.1.9.1. Isolation and quantification of proteins

To further characterize the differentiation of hiPSCs into PTELCs, the expression of specific markers and transporters of proximal tubule was also analysed at the protein level by Western blotting, which involves preparation of whole cell lysates, determination of protein content followed by SDS-PAGE and Western blotting. For this purpose, cells were harvested as described in Section 3.5.1, and 100-150 μ l of freshly prepared radioimmunoprecipitation assay (RIPA) buffer containing 1x protease inhibitor cocktail, 1x phosphatase inhibitor cocktail, and 1 mM phenylmethylsulfonyl fluoride (PMSF) was added to the cell pellets to lyse the cells. After a 20 minutes incubation at RT, the cell lysates were treated with a sonicator (5x 35 % amplitude, 2 seconds pulse, 1 second pause, 5 shocks, RT) to ensure solubilization of proteins by degradation of the cells. The resulting cell debris was pelleted by centrifugation at 10,000 g for 15 minutes at 4 °C, and the proteinaceous supernatant was carefully transferred to a labelled 1.5 ml Eppendorf tube. The protein-containing supernatant was frozen at -80 °C or immediately subjected to protein determination and Western blotting. In the latter case, the protein concentration of the supernatant was determined by the DC™ protein assay using the Bradford method according to the manufacturer's instructions. For this purpose, a BSA standard concentration of 1 mg/ml was prepared, from which a dilution of 0.8 μ g/ml, 0.6 μ g/ml, 0.8 μ g/ml, 0.4 μ g/ml, 0.2 μ g/ml, 0.1 μ g/ml, and 0.05 μ g/ml was made and used for calibration. In addition, samples were prepared containing only ddH₂O (standard blank) and RIPA buffer (sample blank). Then, 5 μ l of the protein samples (1:5) and BSA standards in technical duplicates were pipetted into the wells of a transparent 96-well flat-bottom plate. Then 25 μ l of a 1:50 dilution of Reagent S in Reagent A was added to each well, followed by another 200 μ l of Reagent B. The reaction was incubated in the dark at RT for 15 minutes before light absorbance was measured at 750 nm using a Tecan Infinite 200 pro spectrophotometer. Protein concentrations were calculated using the resulting linear regression formula for the BSA standard curve. Subsequently, 50 μ g of the protein lysate was mixed with Roti loading buffer, and the protein samples were denatured in a heating block at 95 °C for 5 minutes. The sodium dodecyl sulfate (SDS) contained in the buffer, in combination with heat, serves as a denaturant, causing the three-dimensional structures of the proteins to dissolve. In addition, the β -mercaptoethanol contained in the Roti loading buffer cleaves the disulfide bridges between the peptides. The negatively charged SDS also forms complexes with the proteins, thus overriding the intrinsic charge of the proteins.

The proteins, therefore, exhibit a constant negative charge in relation to their molecular weight.

8.4.2.1.9.2. Sodium dodecyl sulfate polyacrylamide gel electrophoresis

The proteins isolated and denatured in **3.6.1** were separated according to their molecular weight by discontinuous sodium dodecyl sulfate-polyacrylamide gel electrophoresis (SDS-PAGE). By applying an electric field, the negatively charge proteins migrate to the anode and are separated by size through the pores of an acrylamide gel. The acrylamide gels used consisted of 5 % collection gel followed by a 10-12 % separation gel (**section 2.2**). In the collection gel, proteins were first concentrated at the boundary of the separation gel. Meanwhile, the proteins were separated according to their molecular weight in the separation gel. Proteins were separated in a running buffer at a 10-30 mA voltage. Gel electrophoresis was performed using the MINI-Protean Tetra Cell Electrophoresis system, and the PageRuler™ Plus Prestained Protein Ladder was used to determine the size of the proteins.

8.4.2.1.9.3. Western blotting

The proteins separated in SDS-PAGE were then wet-blotted onto a nitrocellulose membrane using the Mini Trans-Blot® Cell System. The wet blot was performed in a blotting buffer at 300 mA for 90 minutes. After blotting, the nitrocellulose membrane was temporarily stained with Ponceau S solution to demonstrate successful protein transfer. After that, the membrane was incubated in 5 % skim milk powder/Tris-buffered saline with Tween 20 (TBST) for 1 h to block nonspecific antibody binding. It was then incubated overnight at 4 °C with the primary antibody. After washing the membrane in TBST, incubation with HRP-coupled secondary antibody (1:2000 in 5 % milk powder/TBST) was performed for 2 hours at RT. After washing again with TBST, the membrane was incubated with a luminol-containing chemiluminescence solution of the BM Chemiluminescence Blotting Substrate (POD) kit for 1 minute at RT. The chemiluminescence intensity was photographed using the ChemiDoc™ Touch Imaging System and quantified using Image Lab™ software.

8.4.2.1. 9.3. Statistical analysis

Statistical analysis was performed using GraphPad Prism version 6 (GraphPad Software, San Diego, CA). Data are presented as the mean and standard deviation of three independent experiments ($n = 3$). The normal distribution was checked using Kolmogorov-Smirnov tests with Dallal-Wilkinson-Lilie for p-values. The multiple comparisons two-tailed unpaired Student's t-test was performed to compare two-sample groups comprising parametric distributed datasets. For non-normally distributed values, the Mann-Whitney U-test was used. Parametric data, including multiple groups, were tested by one-way analysis of variance (one-way ANOVA) for statistical significance with Tukey's and Dunnett's post hoc test. Non-parametrical datasets of multiple groups were analyzed with Kruskal-Wallis one-way ANOVA on ranks test. Statistically significant differences between the groups were assumed at a p-value <0.05 .

Curriculum vitae**School Education**

1996 – 2003	Primary Education: First School Leaving Certificate Kumba, Southwest Region, Cameroon
2003 – 2007	Secondary School: Ordinary Level Kumba, Southwest Region, Cameroon
2007 – 2009	University Entrance Certificate: Advanced Level Kumba, Southwest Region, Cameroon

University Education

2010 – 2013	Bachelor's Degree Programme in Biochemistry Bachelor's thesis at the Department of Biochemistry and Molecular Biology, University of Buea, Cameroon
2013 – 2016	Master's Degree Programme in Molecular Diagnostic Sciences. Master's thesis at the Department of Biochemistry and Molecular Biology, University of Buea, Cameroon
2018 – 2020	Master's Degree Programme in Medical Life Sciences Master's thesis at the Institute of Experimental Tumour Research, University of Kiel, Germany
2021 – 2024	Graduate Study Programme under the Research Training Group 2578 and Ph.D. thesis in Pharmacy at the Institute of Toxicology, Heinrich-Heine University of Düsseldorf, Germany

Publications and conference paper

1. Published

Mboni-Johnston, I.M.; Kouidrat, N.M.Z.; Hirsch, C.; Weber, A.G.; Meißner, A.; Adjaye, J.; Schupp, N. Sensitivity of Human Induced Pluripotent Stem Cells and Thereof Differentiated Kidney Proximal Tubular Cells towards Selected Nephrotoxins. *Int. J. Mol. Sci.* 2023, 25, 81. Doi.org/10.3390/ijms25010081.

2. Unpublished

Mboni-Johnston I.M.; Hartmann, S.; Kroll, C.; Berndt, C.; Adjaye, J.; Schupp, N. (2024). Impact of nephrotoxins and oxidants on survival and transport function of hiPSC-derived renal proximal tubular cells. *Biorxiv (preprint)*. Doi.org/10.1101/2025.02.17.638605.

Conference papers

- Mboni-Johnston, IM. & Schupp, N. (2022, October 03). *Effect of DNA damage cause by nephrotoxins and oxidative stress on the differentiation and dedifferentiation processes in the Kidney* [Oral presentation]. 2022 GUM Young Scientist Workshop, Institute for Pharmacology and Toxicology, University of Würzburg.
- Mboni-Johnston, IM. & Schupp, N. (2022, October 04 - 07). *Effect of DNA damage cause by nephrotoxins and oxidative stress on the differentiation and dedifferentiation processes in the Kidney* [Oral presentation]. 2022 conference of the 33rd Society of the Environmental Mutation Research (GUM)/GUM Conference, Institute for Pharmacology and Toxicology, University of Würzburg.
- Mboni-Johnston, IM. & Schupp, N. (2022, September 13 - 16). *hiPSCs and hiPSCs-derived renal proximal tubular cells showed different response to nephrotoxic compounds* [Poster presentation]. 2022 Conference of the 10th German Stem Cell Network (GSCN 2022), Münster, Messe and Center Halle Münsterland.

- Mboni-Johnston, IM. & Schupp, N. (2022, November 21 - 25). *hiPSCs and hiPSCs-derived renal proximal tubular cells showed different response to nephrotoxic compounds* [Poster session]. 21st International Congress of the European Society of Toxicology In Vitro (ESTIV 2022), Sitges, Barcelona, Spain.
- Mboni-Johnston, IM. & Schupp, N. (2022, March 07 - 10). *hiPSCs and hiPSCs-derived renal proximal tubular cells showed different response to nephrotoxic compounds* [Poster session]. 2022 virtual conference of the 7th German Society for Experimental and Clinical Pharmacology and Toxicology.
- Mboni-Johnston, IM. & Schupp, N. (2023, March 06 - 09). *hiPSCs and hiPSCs-derived renal proximal tubular cells showed different response to nephrotoxic compounds* [Poster session]. 2023 Conference of the 8th German Pharm-Tox Submit of the German Society for Experimental and Clinical Pharmacology and Toxicology., at Ulm University, Ulm, Baden-Wurtemberg, Germany.
- Mboni-Johnston, IM. & Schupp, N. (2024, March 13 - 15). Influence of Nephrotoxins on the Differentiation and Dedifferentiation Processes of Human Induced Pluripotent Stem Cells to Kidney Cells [Poster presentation]. 2024 Conference of the 9th German Pharm-Tox Submit of the German Society for Experimental and Clinical Pharmacology and Toxicology., at Munich, Germany.

Acknowledgements

I am infinitely grateful to several people for completing this work. First and foremost, I would like to thank my doctoral supervisor, Prof Dr Nicole Schupp and my institute director, Prof Dr Gerhard Fritz, for the opportunity to conduct my doctoral project on this exciting and challenging topic at the Institute of Toxicology. Thank you, Nicole, for the conception and dedicated supervision during the realisation of this thesis. Your always open door and quick feedback, even with your tight schedule, will stay with me forever. Furthermore, I cannot thank you enough for the incredible trust you have placed in me, as well as for your numerous advice on a professional and friendly level. You are indeed a person to emulate. I would also like to thank Prof Dr Rainer Kalscheuer from the Institute of Pharmaceutical Biology and Biotechnology for his willingness to supervise my thesis as a mentor. Many thanks to Prof. Dr James Adjaye from the Institute of Stem Cell Research and Regenerative Medicine for his incredible support, professional advice and excellent collaboration. I want to mention Prof Dr Anja Wilmes from the Department of Molecular and Computational Toxicology at the Vrije Universiteit Amsterdam, who allowed me to complete an internship.

A special thank you also goes to the Research Training Group 2578 and all the principal investigators. Your platform has catalysed the realisation of academic and professional dreams, and I am deeply grateful for this opportunity. I also extend my thanks to the DFG for providing the necessary funds to bring this project to life. I would also like to thank all Toxi's for the wonderful years at the institute. Many thanks for the enjoyable working environment and the help with all theoretical and practical questions during our seminars.

Apart from the people already mentioned, I would like to express my deepest gratefulness to my parents, Mr Mboni Johnston Njonji and Mrs Babienne Hellen Mende. Your memory remains a blessing in my life, and I am increasingly grateful for the reasons that become more apparent with each passing day. I cannot thank enough my brothers and sisters who have always supported me unconditionally. May God continue to bless them. And finally, to Almighty God, who has been my constant companion throughout my studies, I am eternally grateful for your guidance during difficult moments and for the gift of good health.

Declaration on oath

I, Mboni Johnston (born on 15 June 1989 in Konye), at this moment, declare on oath that I have written this academic thesis entitled:

Effect of genotoxic and non-genotoxic nephrotoxins on differentiation and dedifferentiation processes of renal proximal tubular epithelial cells

independently in accordance with the rules of good scientific practice and have not used any aids or sources other than those stated. I have not received any help besides scientific advice from my doctoral supervisor, Prof Dr Nicole Schupp, and the mentioned cooperation partners. This thesis has not been submitted as part of an examination procedure, nor has an academic degree been withdrawn. Parts of this thesis have already been published and are labelled accordingly in this thesis.

Düsseldorf, August 2024

Mboni Johnston